

Development of RNA aptamers binding environmental and food contaminants

**Vom Fachbereich Biologie
der Technischen Universität Darmstadt**

zur Erlangung des akademischen Grades
Doctor rerum naturalium
(Dr. rer. nat.)

**Dissertation
von Janice Kramat**

Erstgutachterin: Prof. Dr. Beatrix Süß
Zweitgutachter: Prof. Dr. Dominik Niopek

Darmstadt 2023

Kramat, Janice: Development of RNA aptamers binding environmental and food contaminants
Darmstadt, Technische Universität Darmstadt,
Jahr der Veröffentlichung der Dissertation auf TUprints: 2023
URN: urn:nbn:de:tuda-tuprints-244847
Tag der mündlichen Prüfung: 30.08.2023

Veröffentlicht unter CC BY-SA 4.0 International
<https://creativecommons.org/licenses/>

Research is formalised curiosity. It is poking and prying with a purpose.

- Zora Neale Hurston -

Table of contents

Summary	1
Zusammenfassung	3
1 Introduction	5
1.1 New methods are needed to detect harmful substances in the environment and in food	5
1.1.1 Biosensors	5
1.2 RNA aptamers	6
1.2.1 Selection of aptamers	7
1.2.2 Aptamers in biosensors	9
1.3 Target molecules with potentially harmful effects on environment or organisms	11
1.3.1 Sweeteners	11
1.3.2 Bisphenols	13
1.3.3 Antibiotics	15
1.4 Aim of this thesis	17
2 Results	19
2.1 Set-up of the Capture-SELEX method	19
2.2 Targeting synthetic sweeteners	20
2.3 Targeting bisphenols	22
2.3.1 Optimisation of the selection against bisphenol A	25
2.3.2 Investigating the enrichment of the bisphenol A selection	26
2.3.3 Development of RNA aptamers binding monohydric alcohols	27
2.3.3.1 Selection against monohydric alcohols	28
2.3.3.2 Cloning and sequencing of single selection rounds	30
2.3.3.3 Testing the specificity of potential aptamers	32
2.4 Targeting antibiotics	37
2.4.1 <i>In vitro</i> selection against kanamycin A	37
2.4.2 Development of the levofloxacin-binding aptamer trLXC	39
2.4.2.1 Next Generation Sequencing of the <i>in vitro</i> selection	40
2.4.2.2 Testing the specificity of potential aptamers	44
2.4.2.3 Determination of the dissociation constant of the aptamer LXC by isothermal titration calorimetry	45
2.4.2.4 Truncation and mutation study using ITC	46
2.4.2.5 In-line probing	51
2.5 Summary of the results	55

3	Discussion	57
3.1	Design of the RNA library for <i>in vitro</i> selection	57
3.2	Testing and assessing the selection conditions	58
3.2.1	The number of selection rounds depends on the target molecule and increases in stringency	59
3.2.2	Why is enrichment not achieved in every SELEX?	60
3.2.3	Suitability of small compounds as target molecules for Capture-SELEX	62
3.2.4	Assessing the elution of RNA molecules by monohydric alcohols	64
3.3	Development of the levofloxacin-binding aptamer trLXC	67
3.3.1	The method of selection monitoring can be based on the pool affinity or its enrichment	67
3.3.2	Evaluating the selection process and identify potential aptamers using Next Generation Sequencing	68
3.3.3	Characterising the aptamer trLXC enabled secondary structure elucidation and provided insights into aptamer-ligand binding	69
3.3.4	Using the levofloxacin-binding aptamer as a receptor in a biosensor	71
4	Material	73
5	Methods	83
5.1	Capture-SELEX	83
5.1.1	Pool preparation	83
5.1.2	<i>In vitro</i> selection	84
5.1.3	Evaluation of the elution of potential aptamers (specificity assay)	87
5.2	Analysis of enriched RNA pools or complete selection processes	88
5.2.1	Cloning and Sanger sequencing	88
5.2.2	Next Generation Sequencing	88
5.3	Preparation of DNA templates for <i>in vitro</i> transcription	89
5.3.1	PCR and overhang filling PCR	89
5.3.2	Cloning with pHDV	90
5.3.3	Hybridisation	91
5.4	<i>In vitro</i> transcription and purification	92
5.4.1	Gel purification	92
5.4.2	Purification using molecular weight cut-off columns	93
5.5	Isothermal titration calorimetry	95
5.5.1	Determination of the dissociation constant	95
5.5.2	Mutation and truncation study	95
5.6	In-line probing	96

6	Bibliography	99
7	Appendices	115
7.1	List of figures	115
7.2	List of tables	116
7.3	Abbreviations	117
7.4	Supplementary data	118
	Curriculum Vitae	119
	Ehrenwörtliche Erklärung	121
	Danksagung	123

Summary

The pollution of the environment by various substances is a central issue of our time. Humans introduce a wide variety of pollutants into nature through industrial processes, the use of certain substances in agriculture and the application of pharmaceuticals in factory farming. These contaminants can exert negative effects on the environment and living organisms due to their presence or specific effect and return to humans through various pathways. The detection of such substances in environmental samples or food is therefore essential for uncovering their entry routes and distribution. Analytical methods such as high-performance liquid chromatography (HPLC) or mass spectrometry (MS) are already used for this purpose. Both methods offer precise analysis and can detect even the smallest traces of various substances. However, this requires specially qualified staff, extensive laboratory equipment and very expensive instruments. In addition, the analyses take a certain amount of time and cannot be used flexibly or portably. Detection methods that do not have these disadvantages are based on sensor technology using biological elements. They represent rapid, simple, comparatively inexpensive analysis platforms that can be used on site. These are so-called biosensors and are based on a harmonised interplay of different components. The basis for the recognition of an analyte is provided by the bioreceptors. These can consist of whole microorganisms, isolated proteins such as enzymes or antibodies, or even short DNA or RNA molecules. They are responsible for the sensing of the analyte and enable the generation of a signal. This is subsequently converted into a visible or measurable signal by a transducer. Finally, a third component can be used to amplify and process this signal. Thus, biosensors provide not only a qualitative but also a quantitative evaluation of a wide variety of analytes. Based on the problems caused by environmental as well as food contamination, the aim of this study has been the development of short, single-stranded RNA sequences as suitable bioreceptors. These are also called aptamers and their application as recognition elements in biosensors make them aptasensors. Aptamers are able to bind a variety of different ligands. These include whole cells, proteins, but also ions or small compounds. In this work, the latter were selected as target molecules for RNA aptamers. The substance classes of artificial sweeteners as sugar substitutes, bisphenols, which are necessary to produce synthetic materials, as well as antibiotics used in human medicine and factory farming were chosen in particular. The individual representatives of these classes were acesulfame K, cyclamate, saccharin and sucralose as sweeteners, the bisphenols A, F, S and 4-hydroxyacetophenone, a degradation product of bisphenol A, as well as the antibiotics kanamycin A and levofloxacin. Some of these substances can already be detected in the environment and partially cause damage to nature and living organisms or are suspected of doing so. Therefore, they represent interesting analytes for aptamer-based biosensors. The origin of the development of aptamers involved different *in vitro* selections of ligand-binding RNA molecules from an extensive sequence library. The method used for this was derived from SELEX (systematic evolution of ligands by exponential enrichment), which was developed in 1990. It is called Capture-SELEX and is based on an iterative process. This always includes the immobilisation of RNA molecules, elution of these through interaction with the chosen ligand, amplification of the selected sequences and their preparation to be used as a new RNA pool for the next selection round. This led to an enrichment of potential aptamers for the target molecules bisphenol A, kanamycin A as well as levofloxacin. The selection against bisphenol A revealed that binding did not occur to the ligand itself but to ethanol, which was required for the solubility of the bisphenol in aqueous solution. Based on this discovery, further steps in the development of an RNA aptamer were focused on monohydric alcohols as ligands.

In addition to ethanol, isopropanol and methanol were also examined as target molecules in Capture-SELEX experiments. No binding between RNA and the ligand could be detected for methanol. Six different RNA sequences could be identified for ethanol and isopropanol using cloning and sequencing techniques. These sequences were evaluated for their ability to distinguish between the two alcohols, which led to the 'aptamer I' that preferentially binds isopropanol. Based on the prediction of a secondary structure, various truncations of aptamer I were made subsequently. These were again assayed for their ability to distinguish ethanol and isopropanol as ligands. Certain truncations led to a loss of the binding ability of the RNA to the applied ligands. Others still exhibited binding but did not show any improvement in specificity. Attention has to be paid to the possibility that the monohydric alcohols ethanol and isopropanol are ligands that are capable of forming non-specific interactions with RNA. Therefore, further research is needed to determine whether it is a 'classical' aptamer-ligand binding. The *in vitro* selection against levofloxacin resulted in an enrichment of target-binding aptamers. Subsequently, the entire selection was analysed using Next Generation Sequencing. The resulting data were bioinformatically evaluated in cooperation with the research group 'Self-Organising Systems' of the Department of Electrical Engineering and Information Technology. In addition to assessing the enrichment process of levofloxacin-binding RNA molecules, eight different sequences of potential aptamers were identified. These were tested for their ability to distinguish between two closely related ligands. In addition to the intended target molecule, the structurally very similar ciprofloxacin was used. This resulted in the aptamer LXC, which had the best distinguishing ability and a dissociation constant in the low micromolar range for binding to levofloxacin. Subsequently, based on the predicted secondary structure of LXC, truncations as well as mutations of the sequence were carried out. These were evaluated by isothermal titration calorimetry (ITC). It resulted in the levofloxacin-binding aptamer trLXC. Based on the ITC mutation studies and subsequent in-line probing experiments, the predicted secondary structure could be confirmed. Furthermore, it allowed the identification of regions involved in ligand binding. Thus, a levofloxacin-binding aptamer ready to be used as a receptor in a biosensor was successfully developed and characterised.

Zusammenfassung

Die Verschmutzung der Umwelt durch verschiedenste Substanzen ist ein zentrales Thema der heutigen Zeit. Der Mensch bringt durch industrielle Prozesse, der Nutzung bestimmter Substanzen in der Landwirtschaft sowie der Anwendung von Medikamenten in der Massentierhaltung unterschiedlichste Schadstoffe in die Natur ein. Diese Verunreinigungen können durch ihre Anwesenheit oder spezifische Wirkung negative Effekte auf die Umwelt sowie Lebewesen ausüben und gelangen durch verschiedene Kreisläufe wieder zurück zum Menschen. Die Detektion solcher Stoffe in Umweltproben oder Lebensmitteln ist somit für die Aufdeckung ihrer Eintragungswege sowie Verbreitung essentiell. Dafür nutzt man bereits Analysemethoden wie die Hochleistungsflüssigkeitschromatographie (HPLC) oder Massenspektrometrie (MS). Beide Verfahren bieten eine präzise Untersuchung und können sogar geringste Spuren verschiedener Substanzen ermitteln. Dafür werden jedoch geschultes Personal, umfangreiches Laborequipment sowie sehr teure Messinstrumente benötigt. Zusätzlich beanspruchen die Analysen eine gewisse Zeit und können nicht flexibel oder mobil eingesetzt werden. Untersuchungsmethoden, welche diese Nachteile nicht aufweisen, stützen sich auf die Sensorik mittels biologischer Elemente. Sie stellen schnelle, einfache, vergleichsweise preisgünstige sowie vor Ort einsetzbare Analyseplattformen dar. Diese werden auch als Biosensoren bezeichnet und basieren auf einem aufeinander abgestimmten Zusammenspiel aus verschiedenen Komponenten. Die Grundlage des Erkennens eines Analyten bieten dabei die Biorezeptoren. Diese können aus ganzen Mikroorganismen, isolierten Proteinen wie Enzymen oder Antikörpern oder auch kurzen DNA- oder RNA-Molekülen bestehen. Sie übernehmen das ‚sensing‘ und ermöglichen die Erzeugung eines Signals. Dieses wird anschließend von einem weiteren Sensor, dem Transducer, in ein sicht- oder messbares Signal umgewandelt. Final kann es noch mittels einer dritten Komponente zur Signalverstärkung und -verarbeitung kommen. Biosensoren gewährleisten somit neben einer qualitativen auch eine quantitative Auswertung von verschiedensten Analyten. Auf Grundlage der Probleme durch Verunreinigungen von Umwelt sowie Lebensmitteln war das Ziel der hier vorgelegten Arbeit geeignete Biorezeptoren in Form von kurzen einzelsträngigen RNA-Sequenzen zu entwickeln. Diese werden auch als Aptamere bezeichnet und ihre Nutzung als Erkennungselemente in Biosensoren machen diese zu Aptasensoren. Aptamere sind in der Lage eine Vielzahl von verschiedenen Liganden zu binden. Dazu zählen ganze Zellen, Proteine, aber auch Ionen oder kleine molekulare Verbindungen. Im Rahmen dieser Arbeit wurden letztere als Zielmoleküle für RNA-Aptamere ausgewählt. Dabei wurde sich genauer auf die Substanzklassen der synthetischen Süßungsmittel als Zuckerersatzstoffe, die Bisphenole, welche zur Herstellung von Kunststoffen benötigt werden sowie die in Human- und Veterinärmedizin genutzten Antibiotika festgelegt. Die einzelnen Vertreter dieser Klassen waren Acesulfam K, Cyclamat, Saccharin und Sucralose als Süßstoffe, die Bisphenole A, F, S und 4-Hydroxyaceto-phenon, ein Abbauprodukt von Bisphenol A, sowie die Antibiotika Kanamycin A und Levofloxacin. Einige dieser Stoffe können bereits in der Umwelt detektiert werden und verursachen teilweise Schäden in der Natur sowie Lebewesen oder werden diesbezüglich verdächtigt. Sie stellen somit interessante Analyten für Aptamer-basierte Biosensoren dar. Ausgangspunkt für die Entwicklung entsprechender Aptamere bildeten verschiedene *in vitro* Selektionen von Liganden-bindenden RNA-Molekülen, welche aus einer umfangreichen Sequenz-Bibliothek stammten. Die dafür verwendete Methode leitete sich von der 1990 entwickelten SELEX (systematic evolution of ligands by exponential enrichment) ab. Sie wird als Capture-SELEX bezeichnet und basiert auf einem iterativen Prozess. Dieser umfasst die Immobilisierung von RNA-Molekülen, Elution dieser durch Interaktion mit dem

gewählten Liganden, Amplifizierung der selektierten Sequenzen sowie ihrer Verwendung als neuer RNA-Pool für die nächste Selektionsrunde. Dies führte für die Zielmoleküle Bisphenol A, Kanamycin A sowie Levofloxacin zu einer Anreicherung von potentiellen Aptameren. Im Falle der Selektion gegen Bisphenol A kam es jedoch nicht zur Bindung an den Liganden selbst sondern Ethanol, welches für die Löslichkeit des Bisphenols in wässriger Lösung benötigt wurde. Aufgrund dieser Erkenntnis wurden weitere Schritte der Entwicklung eines RNA-Aptamers auf einwertige Alkohole als Liganden ausgerichtet. Neben Ethanol wurden so auch Isopropanol und Methanol als Zielmoleküle in Capture-SELEX-Experimenten untersucht. Für Letzteres konnte keine Bindung zwischen RNA und dem Liganden festgestellt werden. Somit konnten mittels Klonierung und Sequenzierung für Ethanol sowie Isopropanol sechs verschiedene RNA-Sequenzen identifiziert werden. Sie wurden nach ihrer Fähigkeit zwischen beiden Alkoholen zu unterscheiden bewertet. Dies führte zu dem bevorzugt Isopropanol-bindenden ‚Aptamer I‘. Anhand der Vorhersage einer Sekundärstruktur wurden anschließend verschiedene Verkürzungen des Aptamers I vorgenommen. Diese wurden erneut auf ihre Fähigkeit untersucht, Ethanol und Isopropanol als Liganden zu unterscheiden. Bestimmte Verkürzungen führten dabei zum Verlust der Bindungsfähigkeit der RNA zu den verwendeten Liganden. Andere zeigten zwar noch eine Bindung, aber keine Verbesserung der Spezifität. Die Möglichkeit, dass es sich bei den einwertigen Alkoholen Ethanol und Isopropanol um Liganden handelt, die in der Lage sind, unspezifische Wechselwirkungen mit der RNA zu bilden, sollte in Betracht gezogen werden. Daher sind weitere Untersuchungen erforderlich, um festzustellen, ob es sich um eine "klassische" Aptamer-Liganden-Bindung handelt. Die *in vitro* Selektion gegen Levofloxacin führte zu einer Anreicherung von Zielmolekül-bindenden Aptameren. Anschließend wurde die gesamte Selektion mittels Next Generation Sequencing analysiert. Die daraus resultierenden Daten wurden anschließend in der Kooperation mit der Arbeitsgruppe ‚Selbstorganisierende Systeme‘ des Fachbereichs Elektrotechnik und Informationstechnik bioinformatisch ausgewertet. Zusätzlich zu der Evaluation des Anreicherungsprozesses Levofloxacin-bindender RNA-Moleküle wurden acht verschiedene Sequenzen potentieller Aptamere identifiziert. Diese wurden auf ihre Fähigkeit getestet, zwischen zwei sehr ähnlichen Liganden zu unterscheiden. Dabei wurde neben dem eigentlichen Zielmolekül das strukturell sehr ähnliche Ciprofloxacin verwendet. Daraus ergab sich das Aptamer LXC, welches die beste Unterscheidungsfähigkeit und für die Bindung zu Levofloxacin eine Dissoziationskonstante im niedrigen mikromolaren Bereich aufwies. Anhand der vorhergesagten Sekundärstruktur von LXC wurden anschließend Verkürzungen sowie Mutationen der Sequenz durchgeführt. Diese wurden mittels isothermaler Titrationskalorimetrie (ITC) untersucht. Daraus resultierte final das Levofloxacin-bindende Aptamer trLXC. Anhand der ITC-Mutationsstudien sowie den darauffolgenden In-line Probing-Experimenten konnte die vorhergesagte Sekundärstruktur bestätigt werden. Weiterhin war eine Identifizierung von Regionen, welche an der Bindung des Liganden beteiligt sind, möglich. Somit konnte erfolgreich ein Levofloxacin-bindendes Aptamer, welches für den Einsatz als Rezeptor in einem Biosensor bereit ist, entwickelt und charakterisiert werden.

1 Introduction

1.1 New methods are needed to detect harmful substances in the environment and in food

Mankind and its industry have a significant impact on the environment. Through various pathways, substances are released into the environment and can cause damage. These substances also return to humans as part of a circuit and lead to unwanted impacts. Pathways of entry are, for example, industrial processes, inappropriate waste disposal, factory farming, but also the discharge of wastewater from the aforementioned sources into the environment. Industrial chemicals, agrochemicals, heavy metals or even drugs are suitable representatives of such pollutants that are undesirable in nature. For example food additives, industrially used chemicals and pharmaceuticals can already be found in environmental samples.¹⁻⁶ Some of them are suspected of causing damage to humans and nature, or such impacts have already been proven.⁷⁻¹⁰ Thus, some negative effects of potentially environmentally harmful substances are already known. It can be assumed, however, that the majority is still undiscovered and unknown. The more important is the prevention of the entry of dangerous substances into the environment. The detection of such contaminants in diverse samples like water or food is an essential first step in this process. This enables tracking of their dispersion, but also of the pathway of entry. Both can contribute to better protection of nature, as the sources of pollutants can be identified. Methods like high-performance liquid chromatography (HPLC)¹¹ or mass spectrometry (MS)¹² already exist for such detection. These allow a precise analysis of the samples to be examined and enable an accurate identification as well as quantification of contaminants. However, both methods are dependent on a complex laboratory set-up and are time-consuming as well as cost intensive. Hence, these methods lack mobility and straightforwardness.

Sensors, especially biosensors, are an available alternative. They provide an option for detecting certain substances in environmental samples or food.¹³ Sensors offer the advantage of being quick, easy to use and usually feasible on site. Besides qualitative¹⁴, they also provide quantitative¹⁵ information about the analytes. Thus, sensors are a suitable addition to laboratory-based methods for the analysis of environmental and food samples.

1.1.1 Biosensors

Biosensors are biotechnological measurement devices that combine biological components for sensing with physicochemical transducers for signal transformation.^{16,17} The term 'biosensor' was introduced in 1977 by the German chemist Karl Cammann.¹⁸ A biological element is also called bioreceptor and interacts with the analyte. For example, such receptors can be microorganisms or cellular structures, enzymes, antibodies or antigens, but also nucleic acids such as deoxyribonucleic acid (DNA) or ribonucleic acid (RNA).¹⁹ The transducer is also described as a detector. It converts the signal of the biological component into a physicochemical one.²⁰ Such detectors can for example provide optical²¹, electrochemical²² and gravimetric or piezoelectric²³ signals. If necessary, the subsequent signal handling can be carried out with linked electronic systems. In addition to processing, the signal can also be amplified and displayed. The development of this kind of biological sensor requires therefore several different components. All of them have to be compatible with each other to create a functioning detection system.

1.2 RNA aptamers

The basis of biosensor systems is always a receptor that recognises an analyte. It is the source of the actual sensing process. Therefore, this study is based on the development of RNA aptamers, which are intended to serve as bioreceptors. The following section will provide more detailed information on the characteristics of RNA, the development of aptamers and their use in biosensors.

Ribonucleic acid (RNA) is a macromolecule that plays various important roles in cells. Its structure consists of three essential components: one of four different organic bases, the pentose sugar ribose bound to this base, and a phosphate group linking the individual sugar molecules to one another.^{24, 25} Possible bases for the formation of RNA are the purines adenine, guanine and the pyrimidines cytosine and uracil, which can be abbreviated with their initial letters. In contrast to DNA, RNA does not have uracil, but no thymine as the fourth available base.^{24, 25} Another difference between the nucleic acids involves the structure of ribose. RNA features the basic structure of the monosaccharide and accordingly contains a hydroxyl group on the second carbon atom. In the structure of DNA, this 2'-OH is replaced by a hydrogen atom, resulting in the prefix 'deoxy' of its name. Due to this hydroxyl group on the RNA sugar, hydrolytic cleavage is easily possible, which makes it less stable than DNA.^{24, 25} The primary structure of RNA is a sequence of nucleotides (nt) that form only a single-stranded polynucleotide. This is another difference to DNA, which is usually always double-stranded due to the presence of a complementary strand in cells.^{24, 25} However, RNA can also have such double-stranded regions. They are created by base pairings of A and U or G and C as well as other rather rarely occurring special pairings like the G·U wobble base pair.^{24, 26, 27} These pairings lead to the folding of the RNA and the formation of a secondary structure. This new spatial arrangement can be defined by various structural features. Base pairing results in the formation of stems, which can be capped by a non-paired region, a loop. This is called a stem loop or hairpin.²⁸ Interruptions in base pairing can also be called internal bulges or internal loops.^{29, 30} Pseudoknots consisting of two interacting stem loops are also possible.³¹ Their classification depends on their localisation in the structure. This single-strandedness with its various possibilities for forming secondary structures also enables the formation of complex three-dimensional structures. For example, this allows a special form of RNA to catalyse chemical reactions in the same way as enzymes do. Based on this mode of function, they are called ribozymes.³² Other important duties of RNA include coding and decoding, but also the regulation of gene expression. The mRNA, which enables the translation of genetic information into proteins, is an example of such a functional unit.^{24, 25} In addition, the catalytic component of the ribosomes, the rRNA, as well as the transporters of amino acids, the tRNAs, are essential for protein synthesis.²⁴ Among other regulatory units, antisense RNA (aRNA)³³ and riboswitches³⁴ can regulate the expression of genes. The latter can be found in the untranslated region of mRNA, where they are able to control gene expression by binding metabolites. They are capable of regulating either transcription or translation, usually by changing their conformation.³⁵ These purposes of RNA in cells have inspired scientists to develop synthetic RNA with a wide variety of functionality, both *in vivo* and *in vitro*. These developments include, for example, artificial riboswitches, but also the domain of the RNA aptamers.

The term aptamer is derived from the Latin *aptus* 'fit' and the Greek *meros* 'part'. Aptamers are short single-stranded DNA or RNA oligonucleotides that can specifically bind other molecules through their three-dimensional structure.³⁶ In this work, the focus lies on RNA aptamers. Possible binding targets for these aptamers can be proteins such as blood clotting factors³⁷ or

methylases³⁸, but also ions such as $Pb(2+)$ ³⁹. Other ligands can be small compounds like antibiotics⁴⁰ or xanthines⁴¹ as well as whole cells from tumours⁴² or *Staphylococcus aureus* cells⁴³. The three-dimensional structure of aptamers is precisely adapted to the target. The connection between the ligand and the RNA involves electrostatic interaction, stacking as well as the formation of hydrogen bonds.⁴⁴ This perfectly coordinated interaction enables aptamers to achieve dissociation constants up to the picomolar range.⁴⁵ In addition, they exhibit high specificity and affinity for their ligand.

These properties enable a wide range of applications. In addition to their use as regulatory elements for gene expression⁴⁶, they can also be used as bioreceptors in analytical sensing⁴⁷. In some of these applications, aptamers compete with antibodies. In sensor technology, for example, both can be used as receptors.⁴⁸ Furthermore, aptamers are playing an increasingly important role in medical research. In this field, they can be used for the diagnostics of diseases⁴⁹ as well as for therapeutic treatments^{50, 51}.

Aptamers also provide decisive advantages like an inexpensive and comparatively simple *in vitro* synthesis. Furthermore, it is also possible to modify them to significantly increase their otherwise disadvantageous stability and also expand their functionality as well as their potential applications.⁵² The *de novo* development of aptamers is a challenging task, but can be achieved using the process of *in vitro* selection.

1.2.1 Selection of aptamers

RNA can adopt a wide variety of three-dimensional structures. It is important that this structure is precisely adapted to binding to a target molecule. Therefore, powerful methods to identify RNA aptamers have been developed. Since the sequence of an aptamer is crucial for its structure, large numbers of different RNA molecules are possible. Among these numerous potential aptamers, the one that binds perfectly to the desired target molecule has to be found. This can be achieved with the help of dedicated methods such as the systematic evolution of ligands by exponential enrichment (SELEX), which was developed in 1990.^{36, 53} In this method, RNA molecules are designed according to a specific sequence scheme with constant and randomised regions. The randomised regions lead to the creation of numerous different RNA sequences, which in turn generates a large sequence library. It could also be described as a pool.

RNA aptamers can be developed against a wide variety of target molecules, also known as ligands. However, it is crucial that these ligands can be immobilised on a solid surface. This is necessary to ensure partitioning of binding and non-binding RNA molecules. Therefore, immobilisation enables the selection of specific aptamers. If binding occurs between a sequence and the ligand, the respective RNA is also immobilised via this interaction. Subsequently, all non-binding aptamers can be washed away. Only the ligand-binding RNAs are retained and can be eluted. By amplifying these eluents, a pre-sorted RNA pool is available to start the same procedure again. Repeating this method several times enables the selection of RNA aptamers that can bind to target molecules.

However, this classical SELEX is limited in the variety of ligands. Only target molecules that are immobilisable can be used. Hence, this *in vitro* selection method has been adapted to specific requirements.⁵⁴ This led to the development of the Capture-SELEX.^{55, 56} The input material for this selection is also a pool containing RNA molecules with certain randomised regions within their sequence. Besides those random sequences, there are several constant regions. One of them is a specific sequence that is complementary to a DNA oligonucleotide. The complementarity

enables hybridisation of both nucleic acids and immobilisation of the resulting hybrid on a solid base. This immobilisation of aptamers creates the major difference to the already described classical SELEX, in which the target molecules are bound to a solid surface. Thus, the aptamers are kept free in solution.^{36, 53} In contrast, the ligands remain free in Capture-SELEX, which is a great advantage for small molecules. These are often very difficult or even impossible to immobilise. Furthermore, none of their functional groups are required for surface fixation, which increases the interaction possibilities with the RNA. If binding between aptamer and ligand occurs in the Capture-SELEX under certain conditions, the aptamer can be released from immobilisation by dissolving the hybridisation. These recovered RNA molecules are potential aptamers that can be used for a further round of selection.^{55, 56}

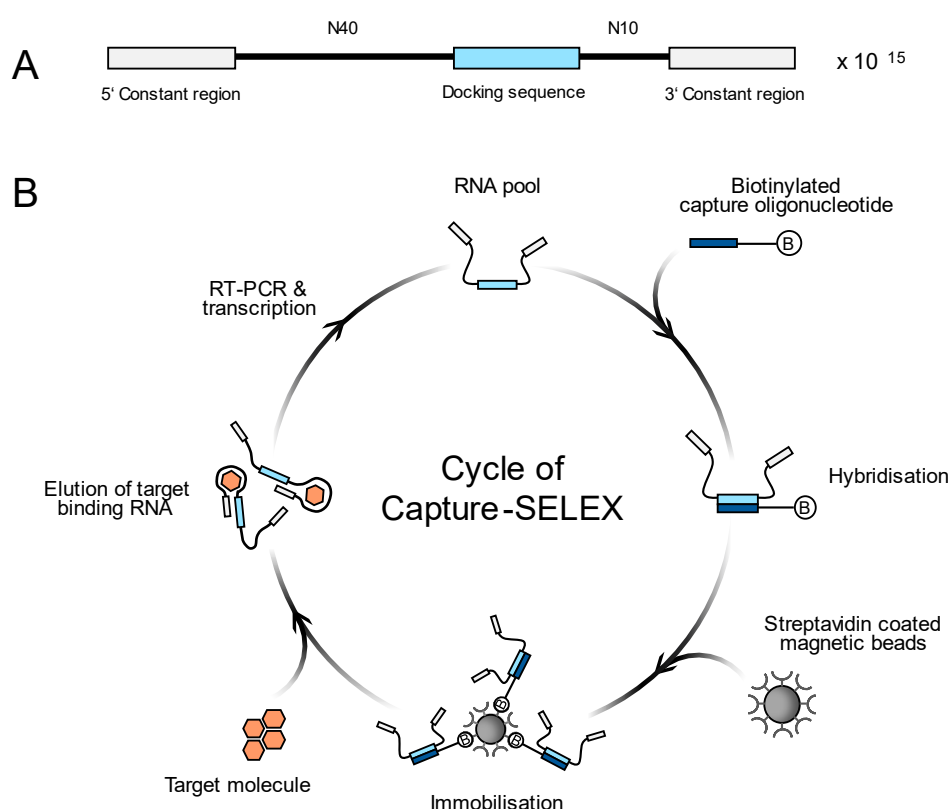


Figure 1 The RNA Capture-SELEX method. **A** The RNA pool used for the selections presented in this work consists of constant regions localised at the 5' and 3' ends. Additionally, a docking sequence (also capture sequence) separates two randomised regions containing 40 (N40) and 10 (N10) nucleotides, respectively. The start of selection is carried out with approximately 10^{15} RNA molecules to cover a wide variety of potential three-dimensional structures. **B** Initially, the RNA pool is hybridised to a biotinylated DNA capture oligonucleotide (CO) via its docking sequence. Subsequently, this RNA-DNA hybrid will be immobilised to streptavidin-coated magnetic beads using the biotin group (B) of the CO. This is followed by the addition of a target molecule solution (hexagons) with a specific concentration. The aptamers, which can detach from the CO by binding to the target molecule, will be eluted. These sequences are amplified by reverse transcription and PCR. Finally, *in vitro* transcription provides a new RNA pool for the next selection round. Adapted from Kramat J and Suess B.⁵⁷ Copyright 2022. The Author(s), under exclusive license to Springer Science+Business Media, LLC, part of Springer Nature. Reproduced with permission from Springer Nature.

The method chosen to develop aptamers for this study utilised the Capture-SELEX approach (Figure 1). The selection is started with an RNA pool consisting of approx. 10^{15} different molecules. The sequence specific layout is composed of a 5' and 3' constant region and a constant docking

sequence (also called capture sequence) located between two randomised regions. These randomised regions comprise 40 and 10 nucleotides respectively, resulting in the docking sequence lying asymmetrically between them. This sequence layout leads to RNA molecules with a total length of 123 nucleotides. (Figure 1A) A selection round is started by hybridising biotinylated DNA oligonucleotides (capture oligonucleotide; CO) to the RNA molecules. This was enabled by the complementarity of the docking sequence to the CO. Subsequently, the resulting RNA-DNA hybrid can be immobilised on streptavidin-coated magnetic beads via the biotin group of the CO. The application of magnetic beads in this selection method allows a rapid and easy separation of the beads from the aqueous supernatant by magnetic force. Various washing steps precede the addition of ligand solution. The presence of the target molecules leads to the elution of RNA. In order to release the nucleic acid macromolecules from the beads, a sufficiently strong interaction between them and the ligand is required. The hybridisation with CO needs to be dissolved.⁵⁸ A prerequisite of the target molecules used in the Capture-SELEX is their solubility in water at pH values close to the neutral point. This can also be achieved by using additives such as ethanol or DMSO. Subsequently, reverse transcription, amplification and *in vitro* transcription are necessary to amplify the eluted RNA and to provide a new pool for a further selection round. The selection continues until an enrichment of potential aptamers can be obtained.

Tracking of the enrichment process can be accomplished, for example, by radioactive labelling of RNA.⁵⁷ An enrichment is considered as soon as the selection step elutes approximately twice as much input as the washing step (see 5.1.2). After obtaining an enrichment, it is feasible to increase the stringency of the selection. For this purpose, it is possible to reduce the concentration of the target molecule in order to elute only RNA that binds very well to the ligand. Furthermore, a counter elution can be introduced before the actual selection to increase the specificity. This requires the use of a counter molecule that is structurally very similar to the target molecule.^{58, 57, 59} The subsequent steps for determining a specific aptamer sequence are described in the results and methods sections (see 2 and 5).

1.2.2 Aptamers in biosensors

The development of a biosensor requires the availability of a specific sensing unit. This unit needs to be adapted to the desired analyte and the function as a bioreceptor. DNA or RNA aptamers can fulfil both requirements. However, an adequate aptamer has to be developed before a biosensor with this type of receptor can be engineered. For example, a suitable DNA/RNA sequence could be found via SELEX using the analyte as the target molecule, as described previously. Biosensors using aptamers as bioreceptors are also called aptasensors.⁶⁰ In this system, the nucleic acid macromolecules provide the first necessary biological signal through their interaction with the analyte. This was achieved in 2013 by Elaheh Farjami and colleagues for the detection of dopamine using an RNA aptamer.⁶¹

The introduction of nucleic acid-based bioreceptors into biosensors often takes place via immobilisation on a supporting material. Such immobilisations may be, for example, the interaction of biotinylation of the nucleic acid and the coating of the material surface with avidin or the hybridisation of the aptamer with complementary, small oligonucleotides that are attached to the support. Other possibilities include the binding of aptamers to gold nanoparticles (AuNP) or a covalent bond via functional groups on the aptamer and the support structure.⁶² For example, the former has been applied in a colourimetric biosensor for the detection of theophylline. In addition to the immobilisation of the aptamer on AuNPs, the ability of these particles to change colour

played an important role. In this system, an RNA aptamer split into two parts prevents the aggregation of AuNPs by coating them. Therefore, this RNA shell increases the tolerance of the particles to raised salt concentrations. The presence of the ligand leads to the detachment of the RNA from the AuNPs, which then aggregate due to the addition of salt. Thus, the biosensor provides a visual signal output through the colour shift from red to blue.⁶³

The same theophylline-binding RNA aptamer was used to develop another biosensor.⁶⁴ Despite the similarity of the RNA aptamers, the two aptasensors differ in their composition and signal output. The second sensor system is based on a fluorescence readout. Therefore, the RNA is hybridised with a small complementary DNA oligonucleotide, which carries a fluorescent label (FL-DNA). The RNA:FL-DNA hybrid shows a weak fluorescence. Addition of the ligand causes this hybrid to dissociate and an RNA:ligand complex is formed. The fluorescence of the released FL-DNA oligonucleotide is now stronger and thus indicates the detection of the analyte.⁶⁴ This demonstrates that different biosensors can be developed with almost exactly the same RNA aptamer. Thus, in addition to the method of immobilisation, such sensors could also be categorised according to their set-up and output signal. Examples of such categorisations are signal-on⁶⁵ and signal-off⁶⁶ sensors according to the signal alterations caused by analyte detection. Furthermore, a separation can be made based on the changes in the sensor system due to ligand-binding. For electrochemical biosensors, this is divided into configuration, conformation or conductivity changes.⁶⁷ However, it is also possible to differentiate whether an aptamer is used modified or in its original form. Biosensors based on native aptamers are described as label-free⁶⁸, while those with modified aptamers are termed as labelled⁶⁹. For example, a sensor based on label-free detection was developed by Fatemeh Shafiei and her colleagues in 2020. This was achieved by fusing a tetracycline-binding aptamer to the fluorogenic RNA aptamer broccoli. The latter induces strong green fluorescence by binding to DFHBI-1T. However, this interaction between broccoli and the fluorogen is affected by the structure-altering fusion with the tetracycline aptamer. Therefore, only with the presence of the analyte and the binding of it to the RNA aptamer, a change in the structure of broccoli occurs and binding to DFHBI-1T is possible. Both aptamers thus form a sensor platform.⁷⁰

Therefore, there are various types of aptasensors that use different approaches for the identification of analytes. They all have major benefits for the straightforward detection of specific substances. An additional advantage is the ability to recognise very small target molecules.^{71, 72} Therefore, contaminants in food or environmental samples can also be used as analytes.

1.3 Target molecules with potentially harmful effects on environment or organisms

Food contaminants and environmental pollutants can be a wide variety of substances. They have the potential to cause serious problems to nature or to the human organism itself. Despite this knowledge, more and more of these undesirable compounds are entering the environment and its organisms. Therefore, it is necessary to come up with new ways to detect such pollutions.

Since contaminants and pollutants include numerous possible ligands for RNA aptamers, three substance classes and individual members of these were chosen as target molecules for Capture-SELEX experiments in this study. Thus, attempts were made to find RNA aptamers that bind targets classified as food additives, industrial chemicals and pharmaceuticals. Representatives of all of these can already be found in the environment. In this work, the focus in these classes was specifically on synthetic sweeteners, compounds used in the production of synthetic materials, and antibiotics. All three substance types provide interesting analytes for RNA aptamer-based biosensors, as their entry into the environment is already ubiquitous and some of them are assessed as potentially harmful to the human organism.

1.3.1 Sweeteners

Artificial sweeteners are widely used food additives that replace the classic sugar saccharose and are supposed to be a healthier alternative. However, they can have undesirable side effects.⁷³ In some cases, they are minimally metabolised in the human body or in other excreted completely unchanged. They enter sewage treatment plants via wastewater, where only a few of them can be degraded almost completely. Some of them are even only broken down to a small extent.⁷⁴ Therefore, it is already possible to detect certain artificial sweeteners in surface waters.⁷⁵ The candidates selected for this group of substances for the Capture-SELEX are acesulfame K, cyclamate, saccharin and sucralose (Figure 2).

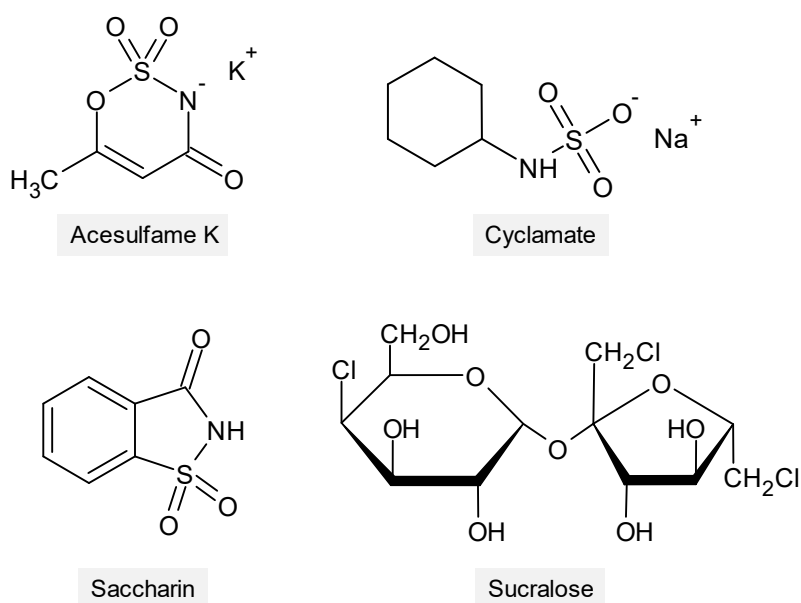


Figure 2 Chemical structural formulae of synthetic sweeteners. Chemical structural formulae of the synthetic sweeteners acesulfame K, cyclamate, saccharin and sucralose. All compounds have been used as target molecules for *in vitro* selections according to the Capture-SELEX method.

The first member of the group of synthetic sweeteners is acesulfame K. It is labelled as E950 in foods and is 130-200 times sweeter than saccharose. It was discovered by chance in 1967 by Karl Clauß at Hoechst AG during the synthesis of oxathiazinone dioxide, which he first published in 1973.⁷⁶ The maximum daily dose is 15 mg/kg and should not be exceeded.⁷⁷ Applications include beverages, fruit yoghurt, toothpaste, protein shakes, but also pharmaceutical products such as chewable or liquid medication. It is not metabolised by the human body and is therefore excreted unchanged.⁷⁸ Even in sewage treatment plants, degradation is only partially successful.⁷⁹ Consequently, it can be detected in the double-digit milligram per litre range in rivers, lakes and drinking water.^{1, 80}

Another ligand from the group of synthetic sweeteners used for *in vitro* selection is cyclamate. It is labelled as E952 in food products. Cyclamate tastes 30-50 ml sweeter than saccharose and is therefore the weakest sweetener of those chosen here. It was discovered in 1937 by the chemist Michael Sveda at the University of Illinois.⁸¹ The maximum daily dose of 1 mg per kilogram of body weight is the lowest of the four synthetic sweeteners selected.⁷⁷ It is used, for example, in calorie-reduced foods, flavoured drinks, spreads, jams and marmalades and canned fruit. Cyclamate is excreted by the human body almost completely unchanged.^{78, 82} It then passes through wastewater into sewage treatment plants, where its biodegradation can be relatively effective. However, it is still detectable in the environment.^{2, 75} For example, it has been found in groundwater in urban environments.^{83, 84}

The first official artificial sweetener saccharin is the third member of this ligand group. Foods containing this substance are labelled with E954. It is 300-500 times sweeter than sucrose and is therefore the second strongest sweetener used here. The chemists Constantin Fahlberg and Ira Remsen discovered saccharin in 1878 at John Hopkins University in the USA.⁸⁵ The maximum daily dose of 5 mg/kg should not be exceeded.⁷⁷ It is commonly used in light products, jams, canned fruits and vegetables, sugar-reduced drinks, but also as a flavour enhancer or in dental care products. As it passes through the human body without being metabolised, it is excreted unchanged.⁸⁶ Although saccharin is effectively degradable in sewage treatment plants⁸⁷, it can still be detected in aquatic environments^{88, 89} and in soil². This is due to its additional use in agriculture. It strongly increases the entry of saccharin into surface waters and soil.²

Sucralose is the last ligand of artificial sweeteners analysed in this study. It is labelled as E955 in foods and has a sweetening power 600 times stronger than saccharose. This makes sucralose the strongest sweetener of those used in this work. It was developed in 1976 in a collaboration between the Tate & Lyle company and Queen Elizabeth College, University of London.⁹⁰ Its recommended daily dose is 5 mg/kg, the same as for saccharin, and should not be exceeded.⁷⁷ Sucralose can be found in beverages, candy, cereal bars, coffee pods and canned fruits. Like the other sweeteners, it is excreted from the human body mainly unchanged.⁹¹ Its entry into wastewater treatment plants and the environment, and very slow degradation rates^{92, 93}, have led to its detection in aquatic samples. For instance, it could already be found in surface waters such as rivers^{3, 94}.

Due to their presence in environmental probes, these artificial sweeteners are a source of interesting analytes for RNA aptamer-based biosensors. As they are partly degraded very slowly in sewage treatment plants and the environment, they have a lasting impact on flora and fauna.

1.3.2 Bisphenols

Bisphenols are chemical compounds consisting of two hydroxyphenyl groups (Figure 3). They include numerous representatives that are used in industry to manufacture a wide variety of products. However, this extensive use also leads to already known problems such as hormone-like effects or the suspected promotion of diseases such as diabetes, infertility or obesity. The possibility of detecting bisphenols can be used to determine the contamination of water, soil, food or other sources. This makes it easier to trace the pathways of contamination or to prevent the consumption of polluted products. As part of this work, the development of such aptamers was attempted for three different bisphenols as well as a degradation product of one of them. Therefore, the chosen target molecules for *in vitro* selection were bisphenol A (BPA), bisphenol F (BPF), bisphenol S (BPS) and the BPA degradation product 4-hydroxyacetophenone (HAP).

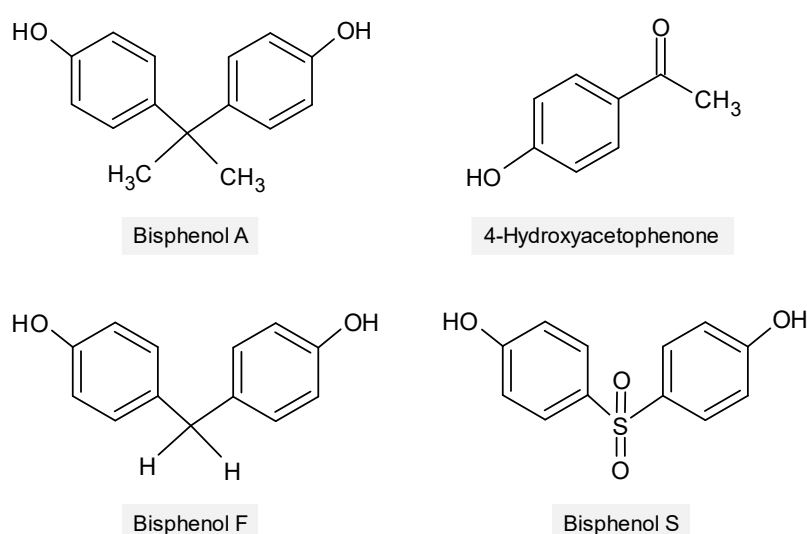


Figure 3 Chemical structural formulae of bisphenols and a degradation product. Chemical structural formulae of the bisphenols bisphenol A, bisphenol F, bisphenol S and the degradation product 4-hydroxyacetophenone of bisphenol A. All compounds have been used as target molecules for *in vitro* selections according to the Capture-SELEX method.

The first ligand used for the Capture-SELEX was bisphenol A. Its initial chemical synthesis was accomplished by the Russian chemist Alexander Dianin.⁹⁵ BPA can be found, for example, in bottles and toys made of plastic, thermal papers, the inner lining of food cans, but also in floor coverings such as epoxy resin. Hence, it is present in plastic objects used in everyday life, where it sometimes comes into direct contact with food. BPA can be released from the material in which it is enclosed by the effects of heat, acids and bases.⁹⁶ In this way, BPA is released into the environment, where it has already been detected in aquatic systems.^{97, 98} But it can also enter the human body through contact with food, which has negative effects on health. BPA has been classified as an endocrine disruptor. It creates an estrogen-like effect through its action as a xenoestrogen.⁷ This has led to suggestions that it may be linked to various diseases. Among these are infertility⁹⁹, diabetes and obesity¹⁰⁰, cardiovascular diseases^{7, 101} and the disease molar incisor hypomineralisation^{7, 101}, which is also called chalky teeth. Therefore, BPA is an interesting target molecule for aptamer-based detection of the compound in environmental or food samples. In this way, contaminations could be rapidly discovered, investigated or combated.

4-hydroxyacetophenone is, along with 4-hydroxybenzoic acid, a main metabolite of BPA biodegradation.¹⁰² (Figure 3) Although HAP is itself rapidly degraded, it can still serve as an indicator of BPA pollution in environmental samples. It has already been detected in surface waters⁴, where it could serve like a tracer of BPA contamination.

Another target molecule used for *in vitro* selection of aptamers has been bisphenol F. It is structurally very similar to BPA and only differs in the lateral groups of the methylene linkage of both hydroxyphenyl groups (Figure 3). It is often used as a substitute for BPA due to emerging concerns about BPA's harmful effects on health. It is therefore used in inner linings for tanks and pipes, in road construction materials, adhesives, paints and lacquers, but also in food packaging and dental materials. Due to this extensive use in industry and household products, BPF enters the environment. It has already been detected in various environmental samples such as water^{103, 104}, sediment and dust^{105, 106}. Furthermore, it has been detected in food^{107, 5} and in human excreta¹⁰⁸. Similar to BPA, BPF has the risk of being harmful to health. It exhibits potential hormone activity and has shown estrogenic, anti-androgenic and thyroidogenic effects in *in vivo* studies. It is therefore also classified as an endocrine disruptor.^{8, 109} Further *in vivo* research indicates that it is also potentially liver toxic.¹¹⁰ *In vitro* data further suggest that BPF can cause effects such as cytotoxicity, cellular dysfunction, DNA damage and chromosomal anomalies.⁸ Considering the possible damage to humans and nature, BPF does not represent a better alternative to BPA.¹¹¹

The last ligand of the bisphenol group chosen was bisphenol S, which is structurally different to BPA and BPF. It contains a sulfonyl bridge between the hydroxyphenyl groups instead of a methylene bond. (Figure 3) BPS is also used as an alternative to BPA in manufacturing a wide range of products. It is a component of epoxy resins, adhesives, anti-corrosion agents, flame retardants and thermal papers. It can also be found in household plastic containers and food packaging. BPS is more stable to light and heat than BPA, making it less susceptible to release from materials.¹¹² However, it is less biodegradable than BPA.¹¹³ BPS is able to enter the body through human skin¹¹⁴, where it can potentially cause harm. Another gateway in the human organism relates to the transfer of the bisphenol from thermo-labels on food packaging into contained food.¹¹⁵ Therefore, in addition to industry, BPS also enters the environment through human excretions.^{116, 117} In common with the other two bisphenols described above, BPS presumably acts as an endocrine disruptor.^{8, 9} Thus, it is also potentially dangerous for humans and nature. For example, *in vivo* studies indicate that the growth of the nervous system in foetuses could be disturbed. The influence of the oestrogenic effect of BPS on thyroid hormone levels and activity is thought to interfere with the development of nerves.¹¹⁸ Furthermore, a correlation is suspected between strong deviations from a normal weight and the exposure to BPS.¹¹⁹ Additional *in vivo* data suggest that the bisphenol also exhibits estrogenic activity to a similar extent as BPA.¹²⁰ Therefore, BPS is an unsuitable alternative to BPA when considering the potential health effects of BPS.⁸

1.3.3 Antibiotics

Antibiotics have their origin in low-molecular metabolic products of bacteria and fungi. These inhibit the growth of other microorganisms or even kill them. Mankind has been able to take advantage of this property and developed a widely used class of drugs. The application is not only limited to humans but is also possible in animals and has become indispensable due to factory farming. Antibiotics are produced at least partially or even completely synthetically or by genetic engineering.¹²¹⁻¹²³ The group of antibiotics can be divided into different classes according to the structural properties of the individual drugs. For example, beta-lactams such as the well-known penicillins or polyketides, which include tetracycline. The use of antibiotics has risen significantly in recent decades. However, this has also led to the development of resistance to antibiotics by the microorganisms to be targeted.^{124, 125} Antibiotic resistance in bacteria is defined as the ability of the microorganisms to withstand the treatment and to grow without being inhibited or killed. Bacteria are even able to resist several antibiotics, which gives them multi-drug tolerance.¹²⁶ The development of resistance is a natural process that follows the principle 'survival of the fittest'. However, excessive and unnecessary use of antibiotics can further promote the development of resistance. For example, antibiotics are prescribed for viral diseases due to incorrect or uncertain diagnosis.¹²⁷ In factory farming, it is also common practice to feed antibiotics to accelerate the growth of the animals. Preventing the outbreak of diseases is only incidental to this. Consequently, resistant bacteria, but also not fully metabolised antibiotics, can be released into the environment.^{128, 129} For example, animal excreta containing antibiotics can be used directly as fertiliser. This leads to an input into nature and as a result, antibiotics can already be detected in soil¹³⁰, groundwater and surface water¹³¹ and even drinking water¹³². Consequently, the antibiotics enter animals again via plant products and water. This also applies to humans, who additionally take up the drugs again unintentionally through consumption of antibiotic-polluted animal products. This creates a kind of circulation that leads to undesired resistance development. Thus, antibiotics represent another interesting group of substances for the *in vitro* selection of aptamers. Their presence in water and plant but also animal products make their detection important to prevent resistance promotion or unnecessary pollution.

For the development of antibiotic-binding aptamers, kanamycin A (KM) and levofloxacin (LX) were selected as target molecules for Capture-SELEX (Figure 4). The former belongs to the class of aminoglycoside antibiotics and is usually used as a drug in a mixture with kanamycin B and C. It was first isolated from *Streptomyces kanamyceticus* in 1957 by Hamao Umezawa and his colleagues.¹³³ KM inhibits bacterial protein biosynthesis. This is realised by the binding of the antibiotic to the 30S subunit of membrane-associated ribosomes. This leads to incorrect annealing to the mRNA, causing it not to be read correctly. As a result, incorrect amino acids are incorporated into the peptide chain that is formed and the resulting protein is non-functional.¹³⁴ KM is active against aerobic Gram-negative bacteria. These include *Pseudomonas*, *Enterobacter* and *Acinetobacter*. It can also treat *Mycobacterium tuberculosis* and Gram-positive bacteria. However, the latter are more likely to be treated with other antibiotics.¹³⁵ In addition to this medical use in humans as well as animals, KM is very important in genetic engineering. There, it is often used as a selective antibiotic.^{136, 137}

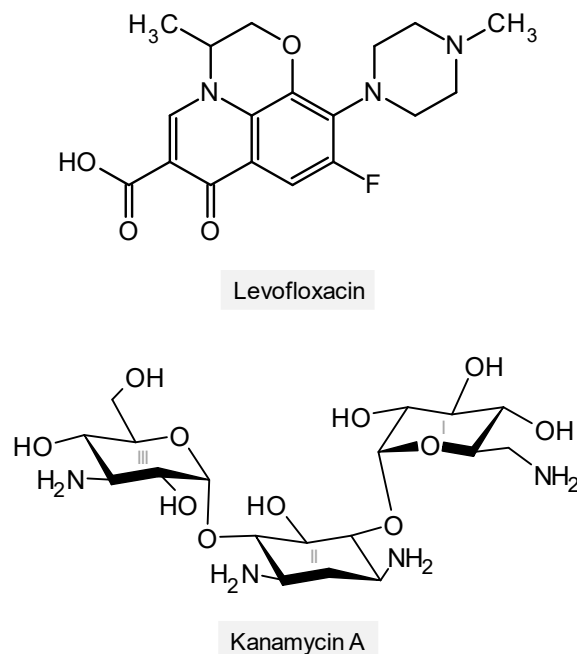


Figure 4 Chemical structural formulae of antibiotics. Chemical structural formulae of levofloxacin and kanamycin A. Both compounds have been used as target molecules for *in vitro* selections according to the Capture-SELEX method. The individual rings of kanamycin A are labelled with the Roman numerals I-III.

The second antibiotic used for the *in vitro* selection of aptamers was levofloxacin (LX). It is a third-generation fluoroquinolone and a member of the quinolone antibiotic class. LX was developed and synthesised by scientists at the Japanese healthcare company Daiichi Sankyo Co., Ltd. in 1985.¹³⁸ This antibiotic has a bactericidal effect by inhibiting various enzymes. These include the gyrase, the topoisomerase IV and two bacterial type IIA topoisomerases.¹³⁹ The inhibition of topoisomerase IV prevents the separation of DNA that was previously replicated for cell division. Subsequently, the gyrase would supercoil the DNA so that it would fit into the newly formed cells. If both mechanisms are inhibited, cell division is not successful and cell death occurs.¹⁴⁰⁻¹⁴² LX is effective against both Gram-positive and Gram-negative bacteria. For example, infections with *Helicobacter pylori*, acute bacterial sinusitis, pneumonia as well as urinary tract infections can be treated.¹⁴³ In addition to these human applications, LX is also used in veterinary medicine. There it is used when antibiotic-resistant bacterial infections can no longer be treated with traditional drugs. Thus, it is intended to serve as a type of reserve antibiotic, but it is also misused for animal fattening. This depends on the regulations of the particular country. The European Union (EU) severely limits the use of antibiotics in veterinary medicine. In some non-EU countries, however, levofloxacin can be used in factory farming without any restrictions.^{144, 145} This has also led to increased research interest in its veterinary use.¹⁴⁶⁻¹⁴⁸ After application of LX, it is excreted unchanged in the urine after a while.¹⁴⁹ This leads to its entry into the environment via sewage treatment plants and later especially into aquatic systems. Thus, the antibiotic was first detected in wastewater and later in rivers.⁶ This can lead to environmental problems because it affects microbial aquatic life. It may even promote the development of LX-resistant microorganisms.¹⁰

1.4 Aim of this thesis

The field of RNA aptamers is an emerging research area in many aspects. In addition to medical applications, scientific applications such as conditional gene regulation using RNA aptamers, e.g. riboswitches, are also a growing field of research. Furthermore, the interest in aptamer-based biosensors used for analytical approaches as well as rapid diagnostics, is increasing strongly. Therefore, new RNA aptamers should be developed in this work using the *in vitro* selection method of Capture-SELEX. The target molecules used were potentially environmentally harmful substances such as food additives, industrially used chemicals and pharmaceuticals. These groups of substances are already present in the environment and some of them are even known to have a negative impact on flora and fauna.

The chosen targets from the groups of sweeteners (acesulfame K, cyclamate, saccharin, sucralose), chemicals for plastics synthesis (bisphenol A, bisphenol F, bisphenol S, 4-hydroxyacetophenone) and antibiotics (kanamycin A, levofloxacin) were used for *in vitro* selections. If an enrichment of target-binding RNA molecules can be achieved, potential aptamers have to be identified. Different methods like cloning, Sanger and high-throughput sequencing, bioinformatic analyses and specificity assays will be used for this identification process. A detailed characterisation of the aptamers will then be conducted using isothermal titration calorimetry, mutation studies and inline probing. Thereby, properties such as binding affinity, ligand specificity, the secondary structure and localisation of the binding site should be elucidated. The final aim of this thesis is the development of aptamers that can be used as a receptor in a biosensor such as the lateral flow assay.

2 Results

2.1 Set-up of the Capture-SELEX method

The development of RNA aptamers started with *in vitro* selection using the Capture-SELEX method. The chosen target molecules originated from the substance classes of synthetic sweeteners, bisphenols and antibiotics. For the experimental set-up, a test SELEX was performed. Since selections with aminoglycoside antibiotics have been shown to be successful^{56, 150-152}, it was decided to use kanamycin A as the target molecule. The chemical structure of the antibiotic is shown in Figure 4. It is important to note that the first selection rounds were carried out without radioactive labelling and are therefore missing in analyses (see 5.1.2). The results of the test SELEX are shown in Figure 5.

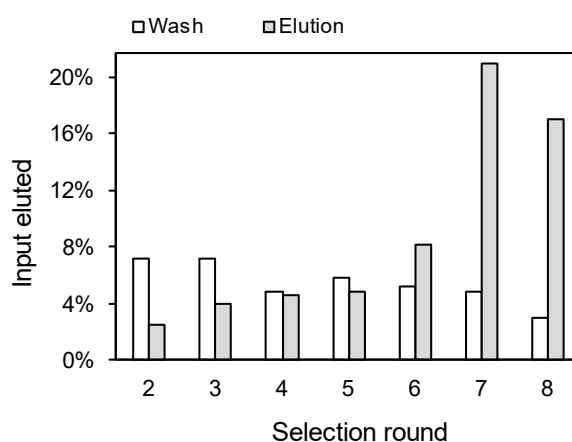


Figure 5 Test Capture-SELEX against kanamycin A. Result of selection against kanamycin A as a graph of the eluted input plotted against the selection rounds. For the specific elution, a concentration of 1 mM target molecule was used. The last washing step (white bars) and the specific elution (grey bars) are shown. The first round was not radioactively labelled.

The selection with the aminoglycoside kanamycin A resulted in an enrichment of ligand-binding RNA molecules (Figure 5). It was observed that the eluted input of the washing step decreased across the rounds. In contrast, elution with the target molecule resulted in increasing values over the selection process. In the 6th round, the eluted input of 8% due to ligand addition exceeded the value of the washing step. The following round showed a significant enrichment. The value of the eluted input by specific elution was almost 21%, whereas the value of the washing step was only about 5%. A similar ratio between elution and wash fraction could be achieved again in the last round. Therefore, the enrichment has been confirmed.

The results obtained were consistent with the expectations of a successful selection process. As the number of rounds progressed, the proportion of eluted RNA molecules due to washing decreased. At the same time, the addition of the ligand led to significantly higher eluted input values in the last two rounds. This showed an accumulation of kanamycin A-binding RNA molecules. An enrichment of target molecule-binding RNA sequences requires at least a factor of 2 higher elution of the input by ligand addition than by the washing step. Ideally, this enrichment should be reproducible in a subsequent round. Based on these results for the ligand kanamycin A, the selections against the synthetic sweeteners were evaluated. Furthermore, this test SELEX served as a guide for the following Capture-SELEX experiments to assess the enrichment of target binding RNA aptamers.

2.2 Targeting synthetic sweeteners

The sweeteners used as target molecules for Capture-SELEX included the synthetic sugar substitutes acesulfame K, saccharin, cyclamate and sucralose. These substances were chosen because of their already proven presence in the environment (see 1.3.1). Their chemical structures are shown in Figure 2. Capture-SELEX was performed for all four sweeteners and the results are summarised in Figure 6.

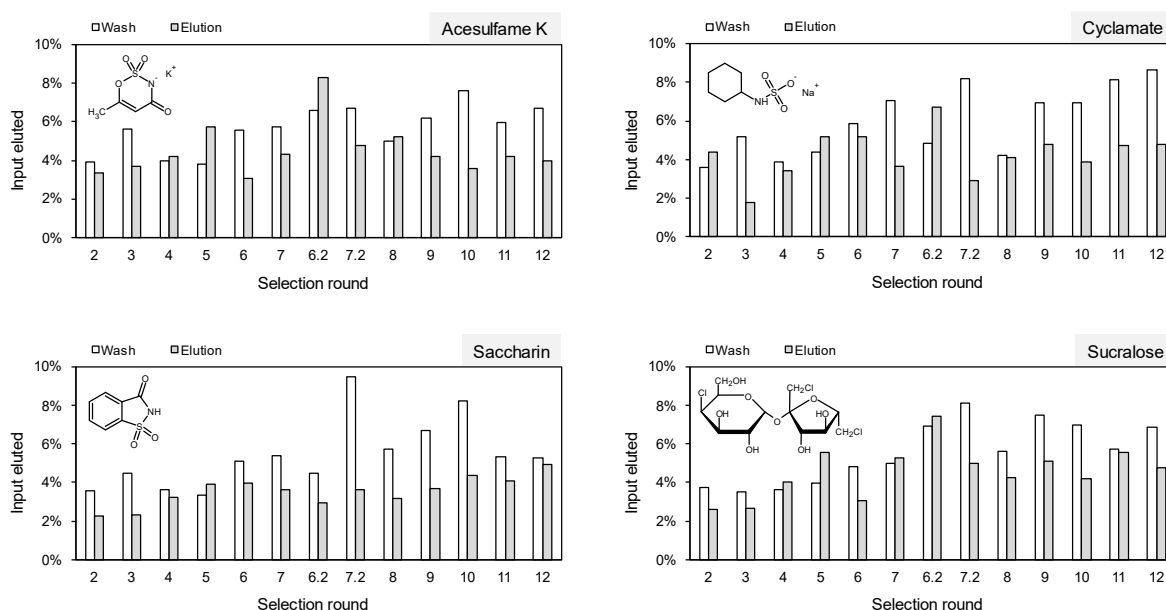


Figure 6 Capture-SELEX against synthetic sweeteners. Results of selection against acesulfame K (top left), saccharin (bottom left), cyclamate (top right) and sucralose (bottom right) as a graph of the eluted input plotted against the selection rounds. For each of the target molecules, 1 mM solution was used for the specific elution. Repeated rounds are marked with the suffix '.2'. The last washing step (white bars) and the specific elution (grey bars) are shown. The first rounds were not radioactively labelled. Chemical structures of the target molecules are shown in Figure 2.

Selection target: Acesulfame K

The addition of target molecule increased the eluted input up to round 5 and resulted in the specific elution giving a higher value than the wash fraction (Figure 6 top left). This incipient enrichment could not be further increased in the following rounds 6 and 7 and there was a drop in the specific elution. Therefore, these rounds were repeated. For this purpose, the RNA pool from the 5th round was used for the round 6.2. This led to an increase in the elution due to ligand addition to over 8%. However, the value of the eluted input of the washing step also increased to nearly 7%, so the ratio of elution to washing did not improve compared to round 5. In round 7.2 the specific elution decreased drastically again and the subsequent rounds showed no significant enrichment for this selection. Therefore, it was decided to stop the Capture-SELEX experiment after 12 rounds.

Selection target: Cyclamate

The selection with the target molecule cyclamate yielded similar results to that of acesulfame K (Figure 6 top right). Up to round 5, the eluted input by ligand addition increased to approx. 5%. Although round 6 showed a comparable specific elution, the eluted input of the wash fraction exceeded it. This trend of increasing wash fraction subsequently continued in round 7. The elution with the ligand even dropped to below 4% in this round. Thus, rounds 6 and 7 were also repeated for this Capture-SELEX by using the pool from round 5 again. In contrast to the selection with acesulfame K, round 6.2 now achieved a better ratio of elution to washing compared to round 5. However, this was reversed in the repeated 7th round, as the specific elution dropped again significantly and the washing step showed an increased value for the eluted input. In the following rounds, the values of both elution fractions fluctuated. However, the elution with cyclamate did not exceed the wash step any more. Thus, this selection was also stopped after 12 rounds.

Selection target: Saccharin

At the beginning of the selection with saccharin as a target molecule, a similar process was obtained compared to the two ligands already described (Figure 6 bottom left). Until round 5, the specific elution increased continuously. In the two subsequent rounds, the value of the ligand dependent elution remained at a similar level of 4%. However, the washing step now exceeded this value. The repetition of rounds 6 and 7, which was also carried out in this experiment, did not lead to any improvements. The wash fraction remained with its eluted input above the values of the specific elution. It even reached its maximum in round 7.2 with over 9%. In the following rounds, no higher elution values could be achieved by ligand addition compared to the wash fraction. Finally, the selection was terminated after 12 rounds.

Selection target: Sucralose

Sucralose, the fourth ligand applied in a Capture-SELEX experiment, also yielded very similar selection results in comparison to the previously tested sweeteners (Figure 6 bottom right). The specific elution showed slowly increasing values in the first rounds, resulting in eluted input values above those of the washing step in rounds 4 and 5. However, round 6 revealed a significant decline in the specific elution. Although it recovered in the following round, it was now only minimally higher than the wash fraction. Therefore, rounds 6 and 7 were also repeated for the selection against sucralose. In round 6.2, the elution due to ligand addition reached its maximum value with over 7%. However, the wash fraction was only slightly lower, resulting in a worse ratio than in round 5. The next round revealed another drop in specific elution. In this round, however, the washing step reached its highest value of eluted input with over 8%. Thus, the specific elution was again below the wash fraction, which continued for the subsequent rounds. Therefore, the Capture-SELEX experiment was also stopped after 12 rounds.

The *in vitro* selections were repeated for acesulfame K, cyclamate and saccharin (data not shown). Experimental problems could be excluded as the test SELEX with kanamycin A was carried out simultaneously (see Figure 5). Since only four selections can be performed in parallel, sucralose could not be used again as a target molecule. However, these repetitions did not lead to an enrichment, so the selection was stopped after 8 rounds. Due to the inability to predict the success of a Capture-SELEX and the failure of many selections to achieve enrichment, no further repetition of the selection against synthetic sweeteners was carried out.

2.3 Targeting bisphenols

Further target molecules for the Capture-SELEX were chosen from the group of bisphenols. Therefore, bisphenol A (BPA), bisphenol F (BPF), bisphenol S (BPS) and the degradation product of bisphenol A, 4-hydroxyacetophenone (HAP), were analysed. Their chemical structures are shown in Figure 3. All of them can be detected in environmental samples and the bisphenols A, F and S are suspected of being damaging to health (see 1.3.2).

All ligands except BPA could be dissolved in aqueous solution in the concentration of 1 mM required for the Capture-SELEX. BPA was only soluble at a concentration of 0.75 mM with the addition of 10 % (v/v) ethanol. The results obtained are shown in Figure 7.

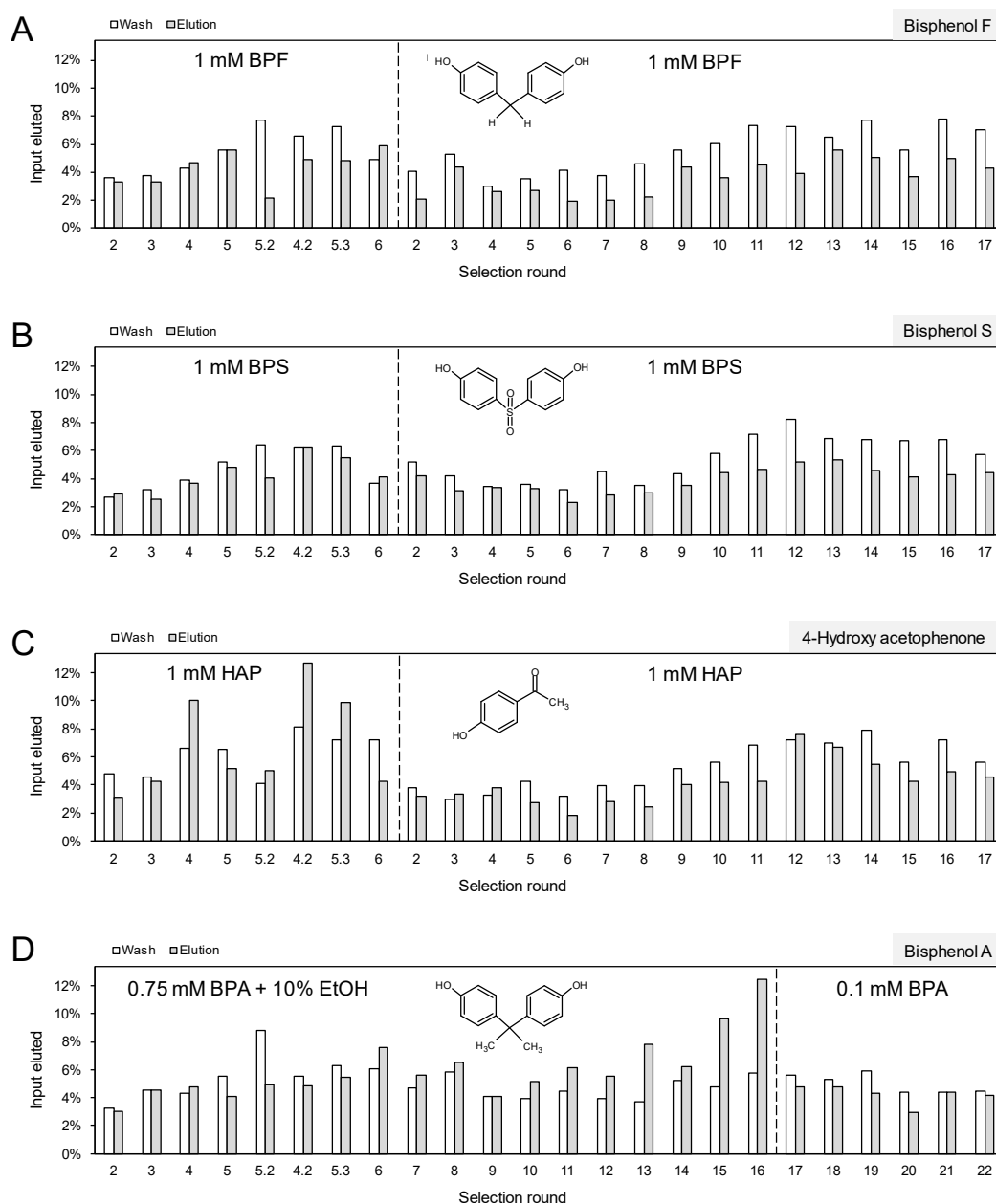


Figure 7 Capture-SELEX against bisphenols A, F, S and the possible bisphenol A degradation product 4-hydroxyacetophenone. Results of selection against bisphenol A (BPA, A), bisphenol F (BPF, B), bisphenol S (BPS, C) and 4-hydroxyacetophenone (HAP, D) as a graph of eluted input plotted against the selection rounds. The last washing step (white bars) and the elution fraction (grey bars) are shown. The selection of BPA started with 0.75 mM solution containing 10% (v/v) ethanol for the specific elution, which was reduced

to 0.1 mM from the 17th round onwards. For the selections against BPF, BPS and HAP, a 1 mM solution was used for the specific elution. Repeated rounds are indicated with the suffix '.2' or '.3' and were given in chronological order. Increases in stringency (BPA) or restarts of selection (BPF, BPS, HAP) are indicated with dashed lines. The first rounds were not radioactively labelled. Chemical structures of these target molecules are shown in Figure 3.

Selection target: Bisphenol F

The results of the selections against BPF are shown in Figure 7A. In the selection against BPF, the addition of ligand increased the elution until the 5th round to a value of over 5%. However, the input eluted by the washing step also increased continuously, leading to the repetition of the 5th selection round. However, this resulted in a major deterioration, as the specific elution dropped to approx. 2% and the wash fraction increased significantly to nearly 8%. Thus, the pool from the 3rd round was used for a new repetition starting one round earlier. The resulting rounds 4.2 and 5.3 again showed that the washing step yielded higher elutions than the elution with ligand. Only in round 6 the specific elution of approx. 6% exceeded the wash fraction again. However, it did not increase significantly compared to round 5, where it was similarly high.

Based on the previous strong fluctuations, it was decided to restart the selection completely, despite the positive trend in round 6. However, for all rounds conducted, the eluted input of the washing step was always higher than that of the specific elution. Therefore, no enrichment could be obtained. However, it was noticeable that both elution fractions of the selection appeared to increase or decrease almost synchronously. The Capture-SELEX experiment was terminated for the ligand BPF after 17 rounds.

Selection target: Bisphenol S

The *in vitro* selection against BPS showed very similar results to the selection with BPF and is displayed in Figure 7B. Besides the specific elution, the washing step also increased continuously up to the 5th round. However, the elution by ligand addition did not exceed the wash fraction in this round. In order to achieve an improvement of the specific elution, first only round 5 and then round 4 together with 5 were repeated. However, the former (round 5.2) resulted in a slight decrease in the specific elution and an increase in the washing step. On the other hand, round 4.2 showed that both values of the eluted input were equal at about 6% and thus the ligand induced elution as well as the wash fraction increased compared to round 4. However, in the following round, the specific elution decreased again to approx. 5% and was again below the wash fraction. Only in round 6 it exceeded the value of the washing step.

Similar to the selection against BPF, the Capture-SELEX experiment was restarted due to the strong fluctuations of the previous results. Interestingly, the results of this repetition were very similar to those of the ligand BPF. The specific elution did not exceed the value of the eluted input of the washing step in any of the rounds conducted. Likewise, almost synchronous increases and decreases in the elutions due to washing or ligand addition could be observed. These follow a rough trend similar to the results of the BPF selection. The Capture-SELEX experiment with the ligand BPS was stopped after 17 rounds.

Selection target: 4-Hydroxyacetophenone

The results for the bisphenol A degradation product HAP are shown in Figure 7C. They deviated for the first attempted selection in comparison to the BPF or BPS selection. After 4 rounds, a first increased specific elution of 10% could be observed, which was significantly higher than the washing step. However, this apparently emerging enrichment could not be further enhanced in

the following round. The elution by ligand addition decreased to about half, whereas the eluted input by washing remained nearly the same. A repetition of the 5th round did not improve the specific elution, which remained at 5%. The use of the pool from round 3 for the repetition of round 4 allowed a new maximum value for the specific elution of nearly 13%. In the following two rounds, the elution with the ligand dropped significantly, so that in round 6 it was again below the elution of the wash fraction. Only a third of the specific elution from round 4.2 could be achieved.

These strong fluctuations for the target molecule HAP were already observed to a lesser extent with BPF and BPS. Thus, a new Capture-SELEX experiment was also started for this ligand. In contrast to the target molecules already described, a higher value was obtained in various rounds for the specific elution than for the washing step (cf. rounds 3, 4, 12). However, none of this led to an enrichment of HAP-binding RNA molecules. The collectively fluctuating values of the specific elution and washing could also be observed in this selection. As in the BPF and BPS selections, the general trend of increases and decreases was also clearly recognisable. The *in vitro* selection against the ligand HAP was therefore stopped after 17 rounds.

Selection target: Bisphenol A

As shown in Figure 7D, an enrichment could be achieved with BPA. Promising increases in the elution with BPA were repeatedly observed (cf. rounds 4.2-6 and 9-13). At the beginning of the selection, the 4th and 5th rounds were repeated in the same way as for the other ligands. Here, increasing elutions with the ligand also occurred (rounds 2-4), which, however, collapsed again (round 5). Round 6 yielded with approx. 8% the highest specific elution at this point. Although the results were similar to those of the selection against BPF, it was decided to continue this selection because of the more pronounced increase in specific elution compared with previous rounds. This similarity in the progression of the selections against BPA or BPF enabled an investigation of whether different results can be obtained when one SELEX was restarted and the other was maintained. The selection with BPA appeared to be more promising for the continuation.

The following rounds until round 9 showed decreasing elution values for the selection. However, they were always above or equal to the wash fraction. Starting in round 10, an increase in the specific elution could be observed. Although this was slightly reduced in rounds 12 and 14, the first enrichment was achieved in round 15. In this round, the elution with BPA was about 10% and the wash fraction about 5% of the eluted input. This was followed by a confirmation of the enrichment. The values for round 16 were over 12% for the specific elution and under 6% for the washing step.

After this enrichment, the concentration of BPA was reduced from 0.75 mM to 0.1 mM to increase the stringency of the specific elution. The addition of 10% (v/v) ethanol was no longer required to maintain BPA's solubility. A decrease of the value of specific elution after concentration reduction had been expected and was observed in round 17. For the first time since round 5.3, the selection was clearly below the elution of the washing step. Also in the following rounds, the specific elution did not exceed the wash fraction. Only in round 21 the specific elution did approach the value of the washing step again and both were at approx. 4%. However, in round 22, the elution with BPA again dropped slightly. The reduction from 0.75 mM to 0.1 mM BPA may have been a too severe increase in stringency. Therefore, different approaches were used to optimise the selection process.

2.3.1 Optimisation of the selection against bisphenol A

In order to increase the selection pressure on the enriched RNA sequences, different attempts were made to reduce the ligand concentration and to introduce a counter elution. The obtained results are presented in Figure 8.

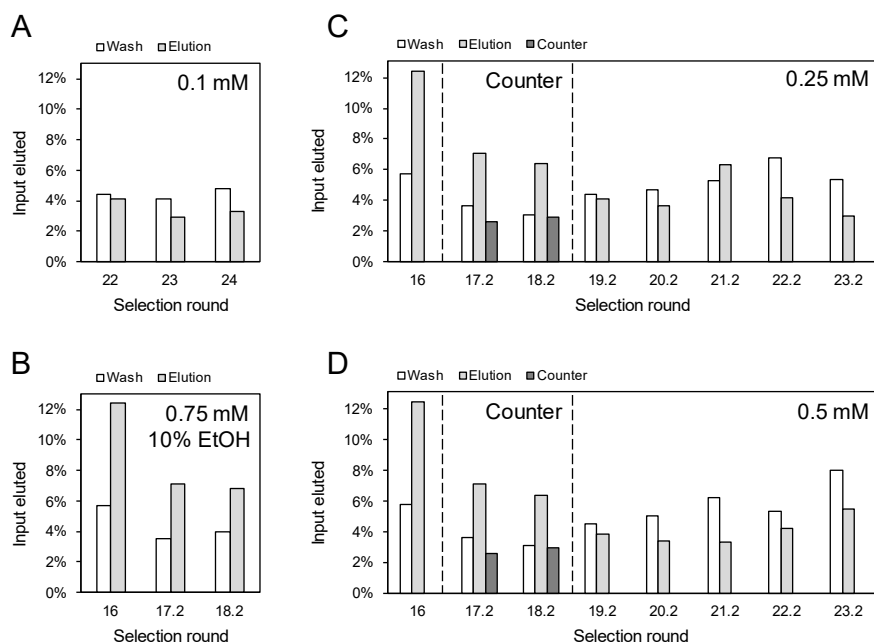


Figure 8 Capture-SELEX variations for optimising the selection against bisphenol A. Results of the different continuations of the bisphenol A (BPA) selection as graphs of the eluted input plotted against the selection rounds. Repeated rounds are indicated with the suffix '.2'. Changes in selection stringency are marked with dashed lines. The last washing step (white bars) and the specific elution (grey bars) are shown. In addition, partial counter selections (dark grey bars) were performed with 0.75 mM solution of bisphenol F (BPF) and bisphenol S (BPS). **A** Continued selection as in Figure 7 with 0.1 mM BPA applied in the specific elution for another 2 rounds. **B** Repeated rounds 17 and 18 with 0.75 mM BPA containing 10% (v/v) ethanol in the specific elution. **C** Repeated rounds 17 and 18 with 0.75 mM BPA containing 10% (v/v) ethanol in the specific elution as well as additional counter elution with BPF/BPS solution. Starting with round 19.2, 0.25 mM BPA solution was used for the specific elution and no counter elution was performed. **D** Repeated rounds 17 and 18 with 0.75 mM BPA containing 10% (v/v) ethanol added for specific elution and additional counter elution with BPF/BPS solution. Beginning with round 19.2, 0.5 mM BPA solution was used in the specific elution and no counter elution was performed.

Initially, the increase in stringency was continued as before by reducing the concentration of the ligand from 0.75 mM to 0.1 mM for two more rounds (see Figure 8A). However, this did not lead to any further enrichment of BPA-binding RNA molecules. This approach was therefore terminated after the 24th round.

A second optimisation approach for BPA selection aimed to increase the first enrichment and is shown in Figure 8B. For this purpose, two further rounds with 0.75 mM BPA and 10% (v/v) ethanol were carried out using the RNA pool of round 16. This should lead to an increase in enrichment. Unexpectedly, the values of the elution due to the addition of ligand dropped significantly to less than 8%. In round 17.2, enrichment was still obtained despite the falling values. The specific elution still exceeded the wash fraction by a factor of about two. In round 18.2, this relationship could no longer be observed and thus no distinct enrichment of ligand-binding aptamers could be

obtained. Due to these results, which were contrary to expectations, this optimisation strategy was stopped after two rounds.

The last two attempts to increase the stringency of the selection against BPA were both based on the introduction of a counter elution step with a 0.75 mM BPF and BPS solution. Subsequently, the BPA concentration was reduced once again. However, this was only done with a decrease to 0.25 mM and 0.5 mM, respectively. The corresponding results are shown in C and D of Figure 8. The application of the RNA pool from round 16 allowed the introduction of a counter elution prior to elution with 0.75 mM BPA and 10% (v/v) ethanol. The resulting rounds 17.2 and 18.2 both showed higher values for the specific elutions than for the wash fractions or the counter elutions. The latter, which reached less than 3%, were even lower than the elutions of the washing steps. In contrast, the specific elutions achieved about twice the eluted input than the wash fractions in both rounds. Due to this still existing enrichment and the lack of influence of the elution with BPF and BPS on the previously enriched RNA molecules, the counter elution was suspended in the following rounds.

Starting in the subsequent round 19.2, this selection process was split into two different approaches. The stringency was therefore increased by reducing the BPA concentration from 0.75 mM to 0.25 mM (see Figure 8C) as well as 0.5 mM (see Figure 8D). Both concentration reductions, like the first decrease to 0.1 mM BPA (see Figure 7D and Figure 8A), did not lead to further enrichment of ligand-binding aptamers. Although a higher specific elution than the wash step was obtained using 0.25 mM BPA in round 21.2, the subsequent rounds did not show any new enrichment. The selection with 0.5 mM BPA never achieved a specific elution that was similar to or higher than the wash fraction. Thus, both final attempts to improve the selection against BPA were terminated after the respective 23.2 round.

The results of these optimisation strategies showed that the conducted attempts were not able to introduce an increase in stringency in the selection against BPA. Especially the lack of influence of the counter elution with the structurally very similar counter targets BPF and BPS (cf. Figure 8C/D) suggested that the obtained enrichment might not represent BPA-binding RNA molecules. The necessity of adding 10% (v/v) ethanol for the solubility of 0.75 mM BPA in an aqueous solution led to the assumption that it could be ethanol-binding RNA. To verify this hypothesis, further tests were performed on the enrichment obtained in rounds 15 and 16 from the initial *in vitro* selection against BPA.

2.3.2 Investigating the enrichment of the bisphenol A selection

In order to test whether the enrichment obtained was an elution caused by the solvent ethanol, a counter elution with 10% (v/v) ethanol was carried out. In addition, an examination was performed to assess any unspecific elution caused by the alcohol. For this purpose, the elution behaviour of an enriched pool from a selection against kanamycin A was tested using 10% (v/v) ethanol. The results are shown in Figure 9.

The hypothesis that the enrichment obtained in the selection against BPA is an enrichment of ethanol-binding RNA molecules was tested by two different approaches (Figure 9). First, the RNA pool from round 15 of the BPA Capture-SELEX experiment was used again to perform a counter elution with 10% (v/v) ethanol. The specific elution was carried out as previously with 0.75 mM BPA containing 10% (v/v) ethanol. The value of the eluted input was significantly higher with the addition of ethanol than with the addition of BPA (Figure 9 'Counter_EtOH').

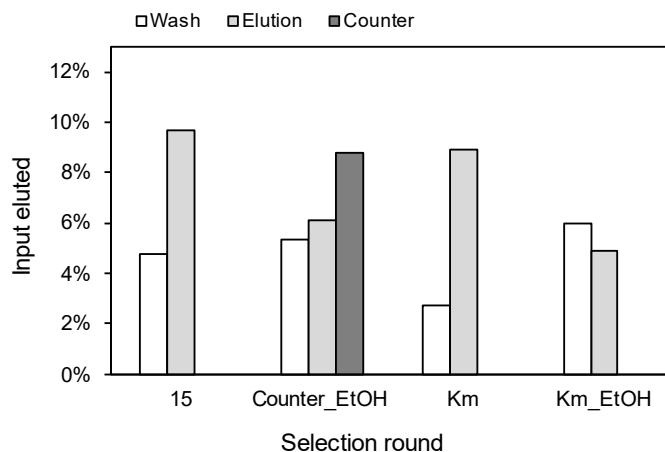


Figure 9 Analysis of the ethanol-based enrichment of the bisphenol A Capture-SELEX with non-specific elution control using an enriched kanamycin A Capture-SELEX pool. Results of the verification of ethanol-based enrichment of bisphenol A (BPA) selection and specificity control as a graph of the eluted input plotted against the selection rounds. The last washing step (white bars) and the specific elution (grey bars) are shown. **15:** The RNA pool of the bisphenol A selection (Figure 7) resulting from round 15 was used for an ethanol-based elution test. **Counter_EtOH:** A counter elution with 10% (v/v) ethanol (dark grey bar) and a specific elution with 0.75 mM BPA with 10% (v/v) ethanol were performed. **Km:** The determination of whether this ethanol induced elution was non-specific or specific was done using an RNA pool from the enriched round 9 of the kanamycin A (Km) Capture-SELEX (Figure 15). **Km_EtOH:** Therefore, 10% (v/v) ethanol was used for the specific elution.

Thus, the counter elution with ethanol yielded nearly 9%, whereas the elution with BPA resulted in only approx. 6%. The second approach addressed the possibility of non-specific elution of RNA molecules in the Capture-SELEX experiment due to the presence of ethanol. For this purpose, the enriched pool of round 9 from the selection against the aminoglycoside antibiotic kanamycin A was used (see Figure 15 and Figure 9 'Km'). The subsequent elution with 10% (v/v) ethanol showed a value of roughly 5%, which was below the input eluted by the wash fraction. Therefore, non-specific elution of RNA molecules by adding ethanol in a Capture-SELEX experiment was not achieved.

Based on these results, it was assumed that this could indeed be an ethanol-induced specific elution of RNA molecules. Therefore, the Capture-SELEX experiments with bisphenols were not repeated, but the enrichment obtained from the BPA selection was used as a basis for new selections. It was decided to use the three simplest monohydric alcohols, methanol, ethanol and isopropanol, as target molecules.

2.3.3 Development of RNA aptamers binding monohydric alcohols

Since the sample volume of the enriched RNA pool of round 16 had already been reduced by using it for optimisation attempts of the selection against BPA, the pool resulting from round 15 was used for the subsequent Capture-SELEX experiments. Furthermore, this pool could exhibit a higher sequence diversity than the pool from round 16. This could be advantageous for the selections against the three monohydric alcohols.

2.3.3.1 Selection against monohydric alcohols

The Capture-SELEX experiments using the monohydric alcohols methanol (MeOH), ethanol (EtOH) and isopropanol (i-PrOH) were started with an already enriched RNA library derived from the bisphenol A selection. Subsequently, different attempts were made to introduce an increase in stringency. The results obtained are summarised in Figure 10.

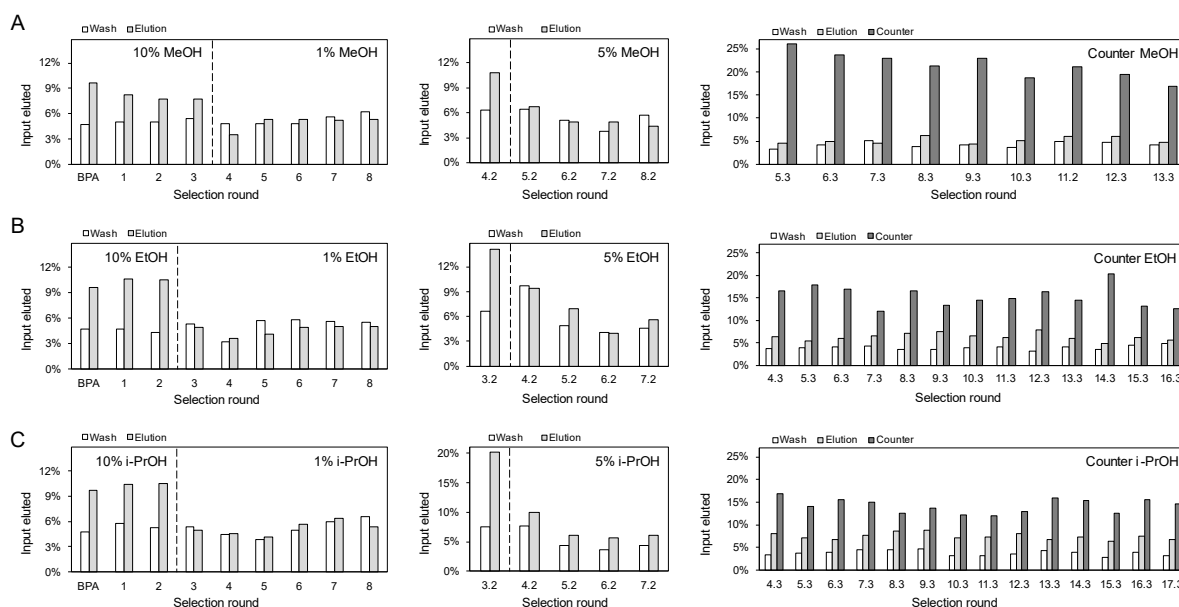


Figure 10 Continuation of the former bisphenol A Capture-SELEX against the monohydric alcohols methanol, ethanol and isopropanol. Results of the selections against methanol (MeOH), ethanol (EtOH) and isopropanol (i-PrOH) as graphs of the eluted input plotted against the selection rounds. Repeated rounds are indicated with the suffix '.2' or '.3' and were given in chronological order. Changes in selection stringency are marked with dashed lines. The last washing step (white bars) and the specific elution (grey bars) are shown. **A Left** Three rounds with 10% (v/v) MeOH in specific elution were carried out using the enriched RNA pool from round 15 of the BPA selection 'BPA' (Figure 7). Subsequently, the concentration was reduced to 1% (v/v) MeOH. **A Centre** The repetition of the 4th round was conducted using the RNA pool from round 3 (A left). Again 10% (v/v) MeOH was used for the selection. Afterwards the concentration was reduced to 5% (v/v) MeOH. **A Right** The introduction of a counter elution with 10% (v/v) EtOH and i-PrOH was started with the pool from round 4.2 (A centre) and stopped after 9 additional selection rounds. **B Left** Two rounds with 10% (v/v) EtOH in specific elution were carried out using the enriched RNA pool from round 15 of the BPA selection 'BPA' (Figure 7). Subsequently, the concentration was reduced to (v/v) 1% EtOH. **B Centre** The repetition of the 3rd round was conducted using the RNA pool from round 2 (B left). Again 10% (v/v) EtOH was used for the selection. Afterwards the concentration was reduced to 5% (v/v) EtOH. **B Right** The introduction of a counter elution with 10% (v/v) MeOH and i-PrOH was started with the pool from round 3.2 (B centre) and stopped after 13 additional selection rounds. **C Left** Two rounds with 10% (v/v) i-PrOH in specific elution were carried out using the enriched RNA pool from round 15 of the BPA selection 'BPA' (Figure 7). Subsequently, the concentration was reduced to 1% (v/v) i-PrOH. **C Centre** The repetition of the 3rd round was conducted using the RNA pool from round 2 (C left). Again 10% (v/v) i-PrOH was used for the selection. Afterwards the concentration was reduced to 5% (v/v) i-PrOH. **C Right** The introduction of a counter elution with 10% (v/v) MeOH and EtOH was started with the pool from round 3.2 (C centre) and stopped after 14 additional selection rounds.

Methanol

For the first rounds, the selection against MeOH showed decreasing values for the specific elution with 10% (v/v) of the ligand. However, the input eluted by the washing step increased slightly up to round 3, so that it was no longer considered an enrichment (Figure 10A left). Nevertheless, an attempt was made to increase the stringency by reducing the concentration of MeOH to 1% (v/v). This led to a significant decline in specific elution to under 4% and below the value of the wash fraction (Figure 10A left). In the following rounds, the elution due to ligand addition rose again to over 5%, but no significant enrichment of MeOH-binding RNA molecules could be obtained. After 5 rounds under this increase in stringency, elution was stopped after round 8.

A further attempt to increase the selection pressure by reducing the concentration of the ligand was started by repeating round 4 with 10% (v/v) MeOH. Subsequently, the stringency was increased again by using only half of the MeOH concentration (Figure 10A centre). This resulted in a drop in specific elution from nearly 11% (round 4.2) to about 7% (round 5.2). In the following rounds, no new enrichment could be obtained either.

After terminating this approach of increasing the stringency after round 8.2, a final attempt was made by introducing a counter selection (Figure 10A right). The counter molecules applied were EtOH and i-PrOH in a 10% (v/v) solution. The RNA pool resulting from round 4.2 was used to start the introduction of the counter elution. It was evident that over one quarter of the input could be eluted by the counter solution (cf. round 5.3). This increase in stringency was carried out for a total of 9 rounds. It was observed that the elution with the counter alcohols was always significantly higher than with 10% (v/v) MeOH or the wash fraction. There were slight fluctuations in all elution fractions examined, but the counter elution always dominated and the specific elution with MeOH was at a similar level as the washing step.

Ethanol

The *in vitro* selection against EtOH partly exhibited similar results to the Capture-SELEX experiment with MeOH as target molecule (Figure 10B). However, at the beginning, the use of 10% (v/v) EtOH for the specific elution still showed an enrichment (Figure 10B left). Thus, in both rounds 1 and 2, the eluted input value was at least twice as high with the elution using the alcohol than the value due to the washing. Hence, from round 3 onwards, the concentration of the ligand was reduced to one tenth (Figure 10B left). However, this led to a significant decline in the specific elution from over 10% in round 2 to under 5% in round 3. In the following 5 rounds, there was no new accumulation of EtOH-binding RNA molecules, leading to the termination of this approach after round 8.

Similar to the selection against MeOH, a further reduction of concentration was attempted (Figure 10B centre). The start was also based on the repetition of a round with 10% (v/v) EtOH in specific elution (here round 3). This repeated round showed a distinct enrichment and achieved more than 14% of eluted input for specific elution. From round 4.2 onwards, the reduction of the EtOH concentration by half again led to a drop in the elution due to ligand addition. In rounds 5.2 and 7.2, the elution rose above the value of the wash fraction, but no new enrichment could be obtained. Thus, the attempt to increase the selection pressure by reducing the concentration of the ligand was also terminated for the selection against EtOH.

Another possibility to increase the stringency was the introduction of MeOH and i-PrOH as counter molecules. This was carried out for a total of 13 rounds, starting with the RNA pool of round 3.2 (Figure 10B right). It was evident that counter selection here also led to high eluted input values. However, the maximum input eluted by counter ligand was approx. 20%. Furthermore, it was

observed that the specific elution with EtOH was always higher than the wash fraction and in some cases exceeded it by a factor of two (cf. rounds 9.3 and 12.3). Selection using counter elution was stopped after round 16.3.

Isopropanol

The third monohydric alcohol used as a ligand, i-PrOH, showed results similar to those of the preceding target molecule EtOH (see Figure 10C). Here, as well, a slight enrichment was seen at the beginning of the selection (Figure 10C left). In round 2, an enrichment occurred with values of the eluted input of approx. 5% due to the washing step and over 10% due to the specific elution. A concentration reduction to 1% (v/v) i-PrOH in order to increase the stringency led to a decline in the elution due to ligand addition (Figure 10C left). The values of the specific elution only partially and very slightly exceeded those of the wash fraction (cf. rounds 5-7). They reached a maximum of only approx. 6%. After 6 rounds of this increase in stringency, it was decided to adjust the ligand concentration to a lesser extent for the selection against i-PrOH (Figure 10C centre).

For this purpose, round 3 was first repeated using the RNA pool resulting from round 2. In this round 3.2, one fifth of the input was eluted by adding 10% (v/v) i-PrOH. Subsequently, the reduction of the elution concentration by 5% (v/v) led to a halving of this high value of the specific elution. Although the eluted input by ligand addition always remained at a higher level than by the washing step, no new accumulation of i-PrOH-binding RNA molecules could be obtained. This second attempt to increase stringency by concentration reduction was terminated after round 7.2. The subsequent introduction of a counter selection with MeOH and EtOH led to similar results as in the selection against EtOH (Figure 10C right). It was started using the RNA pool resulting from round 3.2. Here, too, the counter elution dominated the proportion of eluted input among all the elution fractions examined. The highest value of approx. 17% eluted input was obtained (cf. round 4.3). However, the specific elution with the target molecule always showed higher values than the washing step. For example, in the rounds 4.3 and 12.3, the elution with i-PrOH exceeded the elution of the washing by a factor of two. After a total of 14 rounds, the last attempt to increase the stringency by introduction of a counter elution for the selection against i-PrOH was terminated.

2.3.3.2 Cloning and sequencing of single selection rounds

The analysis of individual enriched pools was carried out for the respective rounds 12.3 of the *in vitro* selections against EtOH as well as i-PrOH (see Figure 10B and C). The respective PCR products of the chosen pools were cloned into the pJET1.2/blunt Cloning Vector. Subsequently, 48 clones each were picked and sequenced using Sanger sequencing service from Microsynth SeqLab GmbH. This resulted in 47 (EtOH pool) and 48 (i-PrOH) pool) sequences. The sequences identified are represented in Table 1.

The analysis of the enriched selection rounds against EtOH and i-PrOH yielded a total of six different sequences of potential RNA aptamers (Table 1). The abundance also included point mutations, as these were sequences that had evolved together and not completely differently. All six sequences were found at least 3 times in the RNA pool of the 12.3. round of i-PrOH selection. The examined RNA pool of the EtOH selection contained only multiple copies of sequences I to IV. The potential RNA aptamers V and VI could only be detected once each. Sequence I significantly dominated the pool of the selection against EtOH with 32 copies.

Table 1 RNA sequences of potential aptamers against the monohydric alcohols EtOH and i-PrOH

Name ¹	Sequence ²	Abundance ³	
		EtOH	i-PrOH
I	5'- GGGCAACUCCAAGCUAGAUCUACCGGUGUAUUUAGUA AGCACACGGUAAUGCGACUGGGCAAGUCUUCUACUGGCU <u>UCUACAGCGCCCUUAAAAUGGCUAGCAAAGGAGAAGAACU</u> UUUCACU-3'	32	18
II	5'- GGGCAACUCCAAGCUAGAUCUACCGGUACCAAUGCAU CGUGGUGCCGGUACCUUUCAGGGAGUCUUCUACUGGCUU <u>CUACUGGACUGGAAAAUGGCUAGCAAAGGAGAAGAACUU</u> UUCACU-3'	5	12
III	5'- GGGCAACUCCAAGCUAGAUCUACCGGUAGAAAUCAAUA ACUCCCGGUACCAACCGACAAGUCUCUUACUACUGGCUU <u>CUAGGCAAUGGUUAAAAUGGCUAGCAAAGGAGAAGAACUU</u> UUCACU-3'	4	4
IV	5'- GGGCAACUCCAAGCUAGAUCUACCGGUUGUACAAUUGC UUGCACAACCCCGCUGCCAGAGCAGUCUUCUACUGGCUU <u>CUACUGGGGCGGCAAAAUGGCUAGCAAAGGAGAAGAACU</u> UUUCACU-3'	2	4
V	5'- GGGCAACUCCAAGCUAGAUCUACCGGUAACGGUCCUUC GUAGGAUACCUACGUGCAUGUGACGUCUUCUACUGGCUU <u>CUAUGACACGAGCAAAAUGGCUAGCAAAGGAGAAGAACUU</u> UUCACU-3'	1	4
VI	5'- GGGCAACUCCAAGCUAGAUCUACCGGUACGUGAACGAU AGUACAGUGUAGAUAAACGUCGAGGUCUUCUACUGGCUU <u>CUACCAUUGUGACAAAAUGGCUAGCAAAGGAGAAGAACUU</u> UUCACU-3'	1	3

¹ The sequences were named with the Roman numerals I to VI.

² Identified sequences: The 5' and 3' constant regions are marked in bold letters. The capture sequence is highlighted with an underline.

³ Information about the abundance of the sequences (one point mutation allowed)

In the i-PrOH selection, this sequence could only be identified 18 times. Together with sequence II, which had a frequency of 12, it dominated the pool of the i-PrOH selection. The other sequences II to VI occurred with similar abundance in the i-PrOH pool, but significantly less than I and II. In the EtOH pool, a small difference in abundance was observed between sequences II to VI. The potential aptamers II and III were found five and four times, respectively. Thus, they occurred with similar frequency. The other sequences IV to VI could only be identified two times or only once. Therefore, they could be considered as not enriched. Sequences V and VI, which occurred only once each, were included in further work despite their low frequency. The aim was to investigate whether the lack of enrichment in the EtOH pool also showed a difference in their specificity. The missing sequences to reach the total number of sequences detected were not included in this subsequent work, as they only occurred once in the analysis of the respective pool.

2.3.3.3 Testing the specificity of potential aptamers

Based on the sequencing data, the six sequences already described (see 2.3.3.2) were used for a determination of their specificity. The required RNA was prepared by *in vitro* transcription of each candidate and tested for binding to EtOH and i-PrOH. This assay was identical to the Capture-SELEX procedure starting in the second selection round. However, no pool consisting of different sequences was used, but the single-species pools, which contained only those sequences of each potential aptamer. The respective RNA molecules were immobilised on streptavidin-coated beads using biotinylated capture oligonucleotides. The same three washing steps as in the Capture-SELEX procedure were performed, followed by elution with 10% (v/v) EtOH or i-PrOH. The experiment was then stopped and only the measured values of the individual fractions were evaluated. This allowed the determination of the eluted input due to the addition of EtOH or i-PrOH. The results obtained are shown in Figure 11.

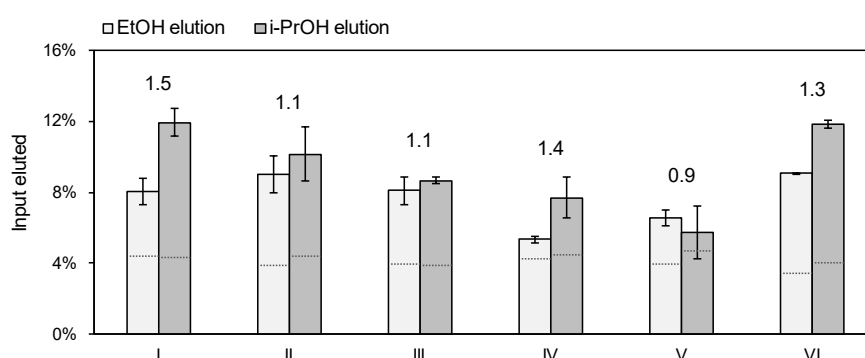


Figure 11 Capture-SELEX-based elution assay with potential monohydric alcohol-binding aptamers. Six different potential aptamers were tested against ethanol (EtOH) and isopropanol (i-PrOH) named I-VI. The light grey bars show the amount of RNA eluted after addition of 10% (v/v) EtOH. The dark grey bars show the amount of RNA eluted with 10% (v/v) i-PrOH. The numbers above the bars represent the ratio of the RNA eluted with i-PrOH to the RNA eluted with EtOH. The dotted lines mark the elution by the last washing step. The procedure was repeated at least two times.

The analysis of the elution behaviour allowed an assessment of the specificity of the tested potential aptamers. The eluted input values obtained by EtOH or i-PrOH addition were plotted for each candidate. Additionally, the ratio of the two values was determined (Figure 11). The individual candidates showed varying elutions and thus also a differing ability to distinguish between the monohydric alcohols EtOH and i-PrOH. The RNA sequences II, III and V showed no or only very limited ability to discriminate between the two ligands. Both of their values of the input eluted by the monohydric alcohols were almost equal, indicating ratios close to 1. The remaining candidates I, IV and VI exhibited more distinct differences in elution with the ligands. The tested RNA sequence VI yielded approx. 9% eluted input with the addition of EtOH and nearly 12% due to elution induced by i-PrOH. Thus, it was possible to elute almost a third more input with i-PrOH. An even better result of the elutions measured was achieved by IV with a ratio of 1.4. The elutions by the two ligands, however, were lower than those of VI, at approx. 5% for EtOH and less than 8% for i-PrOH. Furthermore, the elution by i-PrOH showed a relatively high standard deviation. Candidate I probably had the best ability to distinguish between the used monohydric alcohols. The ratio between the elutions with the alcohols showed that a 1.5-fold higher elution of RNA molecules was possible with i-PrOH. Furthermore, the candidate achieved the highest value of eluted input with 12% when i-PrOH was used.

Based on these results, it was decided to continue to work with the probably most specific binding candidate I. Since previous studies have shown that truncation of the sequence can lead to improved binding to the ligand¹⁵³⁻¹⁵⁵, the potential aptamer I should be shortened in various ways. Therefore, the secondary structure was initially predicted using the web tool RNAfold web server¹⁵⁶. The prediction is shown in Figure 12. According to this secondary structure, three different truncations were made, depending on the structural features of the sequence. Ten further shortenings resulted from the systematic reduction of the 5' or 3' end by 5 to 25 nt in steps of five. All truncations are indicated in Figure 12.

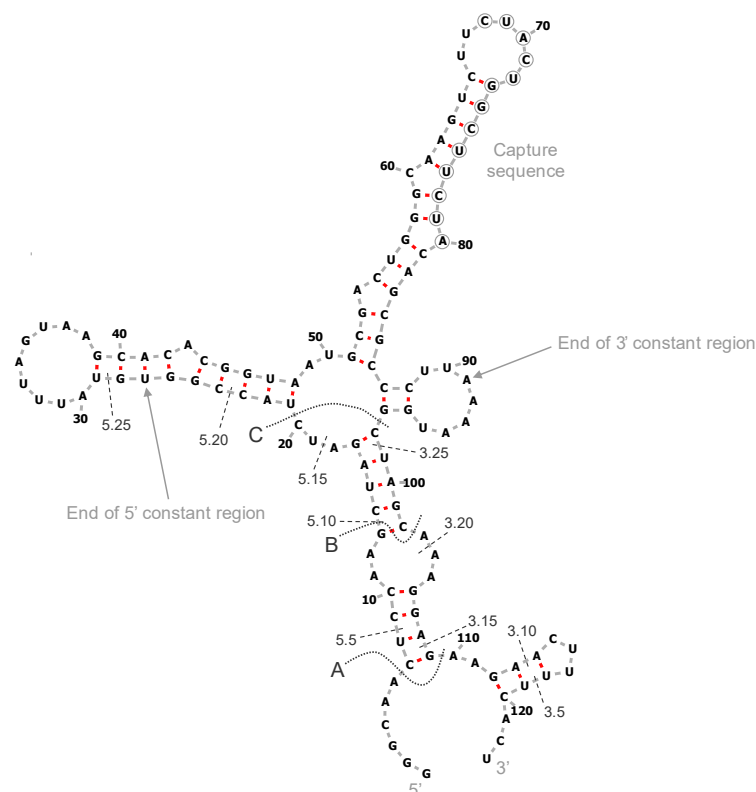


Figure 12 Predicted secondary structure of the potential isopropanol aptamer I. The ends of the 5' and 3' constant regions are indicated with arrows. The capture sequence is marked with outlined nucleotides. The major truncations A-C are indicated by dotted lines. The 5.5-5.25 and 3.5-3.25 truncations of the 5' and 3' ends of the aptamer by 5-25 nucleotides are indicated by dashed lines. Prediction of secondary structure was performed with the web tool RNAfold web server¹⁵⁶ and representation of the structure was created with the Forna tool¹⁵⁷.

The prediction revealed a complex secondary structure (Figure 12). In addition to several stem loops and an asymmetric internal loop, a four-way junction could be possible. Furthermore, four single nucleotide bulges were predicted at A43, A54, C60 and A80. The 5' constant region is involved in the secondary structures of the internal loop, the junction and the stem of the first stem loop. The capture sequence is located in the second large stem loop. It is present both in the loop and in the stem area. Like its 5' counterpart, the 3' constant region participates in the junction and the internal loop. In addition, it is involved in the formation of two smaller stem loops, one at the four-way junction, the other at the end of the sequence.

The first approach of truncating the structure followed this prediction. The shortenings A, B and C cut off different parts of the secondary structure (see dotted lines in Figure 12). In A, a part of both constant regions and the small stem loop contained therein were removed. The truncation B resulted in the asymmetric internal loop additionally being cut away. The largest reduction of the

structure was made by C. The four-way junction had been trimmed leaving only the two large stem loops and the smaller one at the 3' end. The second approach of truncation involved cutting off a maximum of 25 nt from the 5' or 3' end in steps of 5 nt (cf. dashed lines in Figure 12).

It is important to consider that such structural reductions can lead to refolding and thus to a new secondary structure. In order to examine whether such refolding events would be possible due to the performed truncations, secondary structures were also predicted for all shortenings using the web tool RNAfold web server¹⁵⁶. The secondary structures obtained are shown in Figure 13.

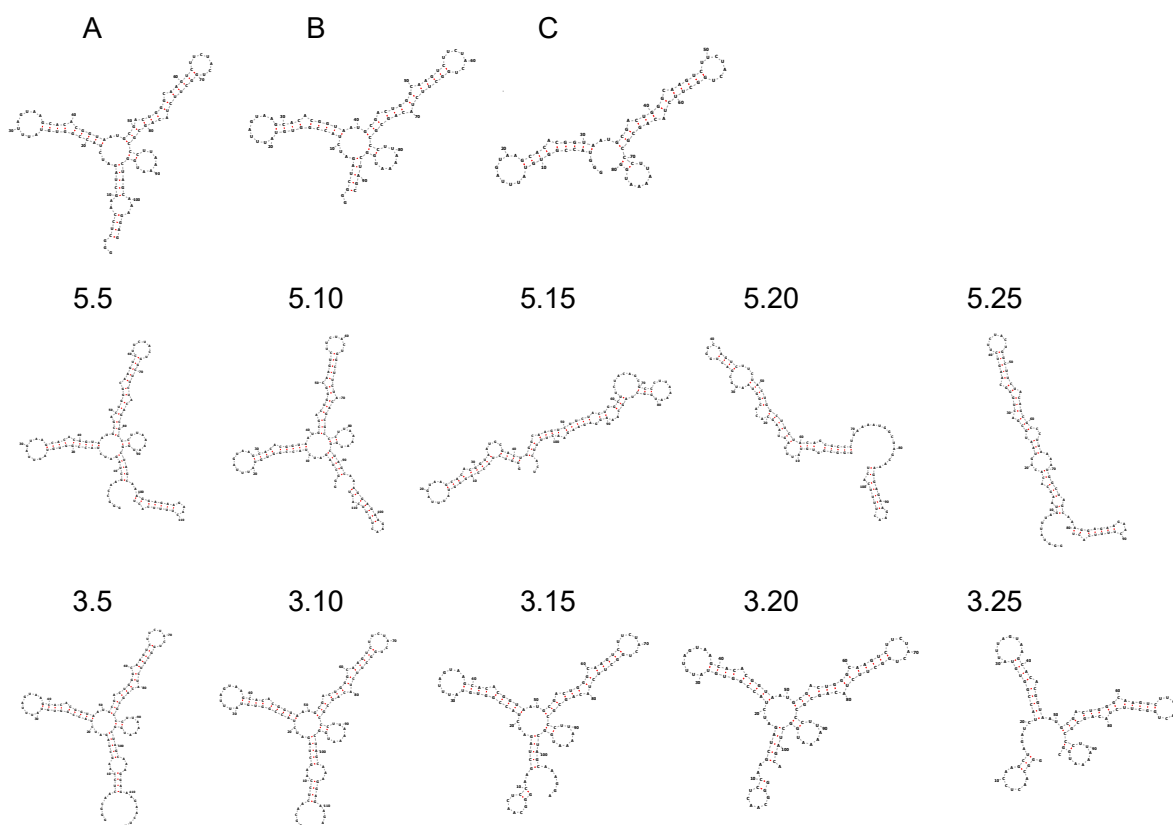


Figure 13 Predicted secondary structure of all truncations of the potential isopropanol aptamer I. The major truncations A-C as well as the 5.5-5.25 and 3.5-3.25 truncations of the 5' and 3' ends by 5-25 nucleotides are shown as secondary structure predictions. The names of the individual truncations are given above the respective structure. Prediction of secondary structure was performed with the web tool RNAfold web server¹⁵⁶ and representation of the structure was created with the Forna tool¹⁵⁷.

Based on the secondary structure prediction of all shortenings of aptamer I, it can be assumed that some truncations led to a significant change in the secondary structure (Figure 13). With the shortenings A and B, 5.5 and 5.10 as well as 3.5 to 3.20, a certain basic structure similar to the parent aptamer I could be maintained. They differed from each other mainly in the length and structure of their closing stem. Such a stem could no longer be predicted for the secondary structure of truncation C. However, it still exhibited the three stem loops of the parent aptamer. A similar structure was predicted for shortening 3.25. This truncation also lacked a closing stem and thus consisted mainly of stem loops connected at their base by a few nucleotides. Complete refolding may have occurred in truncations 5.15 to 5.25. All three showed a completely different secondary structure prediction compared to aptamer I. Thus, the presumed refoldings of these truncations tended to consist of two arms of different lengths formed by complex stem loops with bulges and internal loops.

Due to these differences in the predicted secondary structures, a new elution assay was subsequently carried out with all truncations. This served as an assessment of the influence of the applied shortenings on the specificity of potential aptamer I. The assay was performed identically to the previously conducted one (see above). The obtained results are presented in Figure 14.

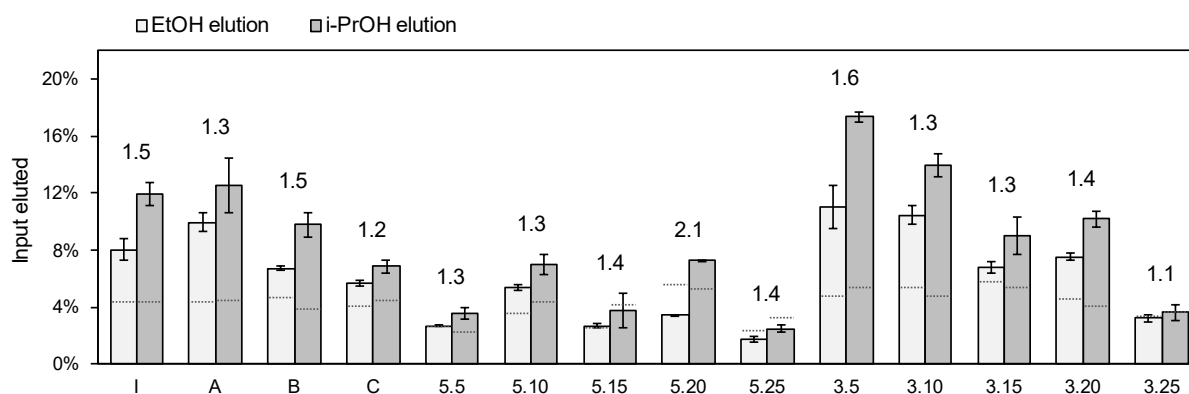


Figure 14 Capture-SELEX-based elution assay with truncations of potential isopropanol-binding aptamer I. 13 different truncations of aptamer I were tested against ethanol (EtOH) and isopropanol (i-PrOH). The light grey bars show the amount of eluted RNA after addition of 10 % (v/v) EtOH. The dark grey bars show the amount of RNA eluted with 10 % (v/v) i-PrOH. The numbers above the bars represent the ratio of the RNA eluted with i-PrOH to the RNA eluted with EtOH. The results of the parent aptamer I were plotted for comparison. The dotted lines mark the elution by the last washing step. The procedure was repeated at least twice.

The analysis of the elution behaviour allowed an evaluation of the specificity of the tested truncations of aptamer I. Furthermore, the influences of these truncations on the elution itself could be investigated. The eluted input values, which were obtained by adding EtOH or i-PrOH, were plotted for each shortening and the parent aptamer. In addition, the ratio of the two values was determined (Figure 14). The individual truncations yielded varying results. It becomes evident that certain shortenings had a distinct negative effect on the elution behaviour. In particular, the truncations C, those of the 5' end and the 15 to 25 nt shortened 3' ends exhibited significantly weaker elutions than aptamer I. Thus, it could be assumed that in the case of these changes in the sequence, a disturbance of the binding ability of RNA to the ligands could have occurred. This might be partly related to the predicted secondary structures (see Figure 13). Especially for the truncations C, 5.15 to 5.25 and 3.25, these structures were significantly different from the predicted structure of the parental aptamer. However, such a correlation between strong secondary structure deviation and elution behaviour could not be detected for the truncations 5.5 and 5.10 as well as 3.15 and 3.20.

In contrast, the remaining truncations A, B, 3.5 and 3.10 achieved comparable or even better values of the eluted input. Shortening A yielded comparable elutions by EtOH and i-PrOH to the original aptamer, while shortening B showed rather weaker elutions. Interestingly, opposite values were obtained for the ratio calculations. B had the same ratio of 1.5 as aptamer I and A could only achieve a ratio of 1.3. An improvement of the values of the eluted input by adding EtOH or i-PrOH could be achieved with the shortening 3.10. However, an increase in the values of the eluted inputs by approx. 2% could not lead to a better ratio between i-PrOH and EtOH-based elution. The ratio achieved was merely 1.3. The only improvements of this ratio could be achieved by the shortenings 5.20 and 3.5. However, 5.20 showed significantly weaker elutions for both monohydric alcohols than the original aptamer. Finally, 3.5 exhibited a slightly improved ratio of

1.6 as well as significantly stronger elutions due to addition of EtOH or i-PrOH. With a value of eluted input of over 17% by i-PrOH and of 11% by EtOH, it clearly exceeded the values of the parent aptamer. In general, it achieved the highest values of the entire elution assay.

Therefore, a monovalent alcohol-binding RNA could be successfully found with the truncation 3.5 of aptamer I. It showed a very good response especially to i-PrOH in the specificity assay. The further characterisation of this monohydric alcohol-binding aptamer was not continued in this work due to time constraints. It was suspected that the use of alcohols as ligands could cause methodological problems in the investigation of the aptamer. In addition, the development of the levofloxacin-binding aptamer was already at an advanced stage, so the focus was shifted to this project.

2.4 Targeting antibiotics

Antibiotics were another class of substances used as target molecules for Capture-SELEX experiments. The *in vitro* selections were performed against the aminoglycoside kanamycin A and the fluoroquinolone levofloxacin. Both antibiotics are widely used in human medicine and factory farming and can partly already be detected in the environment (see 1.3.3). A treatment with antibiotics always involves the risk of microorganisms developing resistance to them. This environmental occurrence and the risk of resistance development make them interesting ligands for RNA aptamers.

2.4.1 *In vitro* selection against kanamycin A

The *in vitro* selection against kanamycin A (KM) was performed using the Capture-SELEX method. In addition to the successful test SELEX with the antibiotic as the target molecule (see 2.1 Figure 5), a further selection against KM was carried out. However, this selection was more extensive due to the introduction of stringency increases. The results are shown in Figure 15.

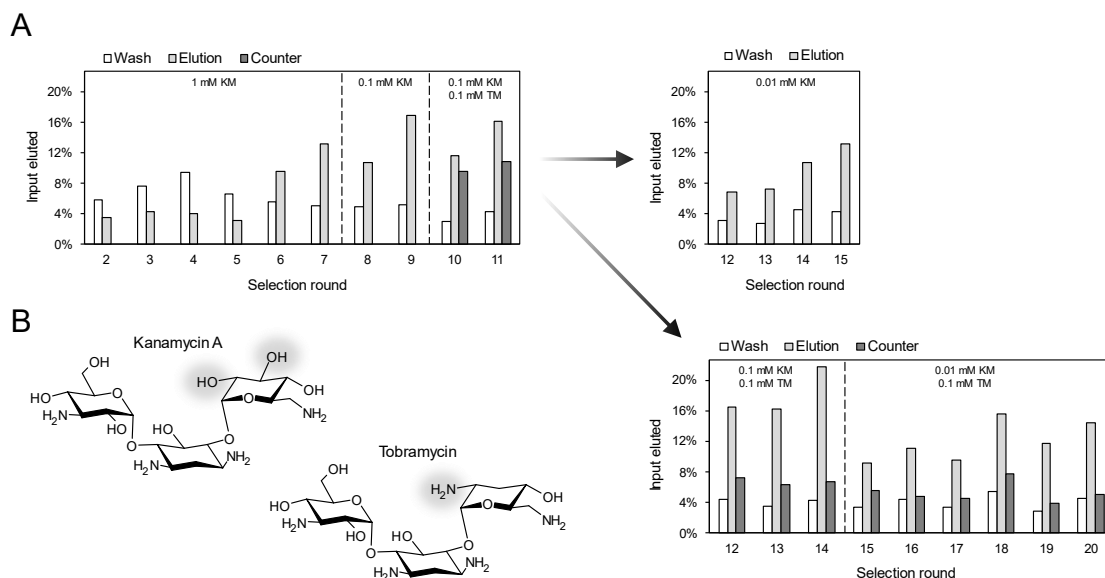


Figure 15 Capture-SELEX with the target molecule kanamycin A. A Results of selection as a graph of eluted input plotted against selection rounds. The white bars show the amount of eluted RNA in the last washing step. The medium grey bars represent the amount of eluted RNA after addition of 1 mM (rounds 2-7) and 0.1 mM (rounds 8-9) kanamycin (KM). In order to specifically select KM-binding RNA, a counter selection with 0.1 mM tobramycin (TM) was introduced starting in round 10. The amounts of RNA eluted in this process are shown with dark grey bars. Dashed lines mark increases in stringency due to reduction of KM concentration (starting from round 8) or introduction of a counter target (beginning from round 10). The first round was not radioactively labelled. To test further increases in stringency, the selection was split from round 12 onwards. First, the counter selection was cancelled but the concentration of KM was reduced again to 0.01 mM (top right). In addition, the selection was continued for another 3 rounds as it was done in round 11. After round 14, the KM concentration was reduced to 0.01 mM (bottom right). **B** Chemical structures of the used ligands KM and TM. Different residues are highlighted by grey shading.

In vitro selection against the aminoglycoside antibiotic KM resulted in enrichments under various conditions (Figure 15A right). The Capture-SELEX experiment started with the application of 1 mM ligand solution. The specific elution increased only slightly in the first rounds. In rounds 4 and 5, it even slightly declined again. In round 6, the elution with KM showed a significant increase. It rose from about 3% in round 5 to almost 10%. However, reliable enrichment could first be obtained in round 7. The value of the specific elution increased further to over 13%, whereas the value of the input eluted by the washing decreased to approx. 5%. Thus, the elution by ligand addition exceeded the washing step more than twice.

As a result of this enrichment, stringency was increased by reducing the concentration of KM to 0.1 mM. This already resulted in a new enrichment in the first round carried out under this condition. Round 9 then even showed a further increase in the eluted input by ligand addition to almost 17%, resulting in the elution by wash fraction being only a third of this amount.

Due to this continued significant accumulation of KM-binding RNA molecules, a counter elution with tobramycin (TM) could be introduced as early as round 10. This counter molecule differs from KM only in two functional groups (see Figure 15B). Therefore, it was a suitable ligand for counter selection. Despite the great structural similarity, elution with TM yielded only lower values for the eluted input than elution with KM. Even though the TM elution increased slightly to almost 11%, it remained below the elution with the target molecule of the selection. Furthermore, it was observed for rounds 10 and 11 that the wash step continued to decrease and thus the elution by KM addition exceeded this by almost three (round 10) or four (round 11) times.

From round 12 onwards, the selection against KM was split (Figure 15A left). This allowed two different approaches to be tested for a further increase in stringency. First, elution with the counter target TM was stopped and the concentration of KM was again reduced by one tenth (see Figure 15A top right). This resulted in a significant drop in the specific elution. It decreased to a value of under 7%. However, this elution could be increased again in the next three rounds. In the 15th round, it reached a value of over 13%. Thus, the eluted input due to addition of KM was again almost three times greater than that due to the washing step. This test of further concentration reduction was terminated after this round.

A final change of conditions to increase the stringency of the selection was initially carried out using the previous settings from round 11 (see Figure 15A bottom right). counter elution with 0.1 mM TM was carried out for another 3 rounds. This led to a further enrichment of KM-binding RNA molecules. Hence, the specific elution in round 14 resulted in the elution of more than one fifth of the applied RNA molecules. Compared to the value of the input eluted by the washing step of approx. 4%, the specific elution now exceeded this by a factor of more than five. On the other hand, the counter elution with TM decreased further. In order to increase the selection pressure on the KM-binding RNA molecules again, the concentration of the ligand was reduced to 0.01 mM. There was a major decline with only approx. 9% eluted input by specific elution. However, this recovered again by round 18, leading to almost 16% of the RNA molecules being eluted by the addition of KM. In rounds 19 and 20, the values for specific elution decreased again slightly, but remained significantly greater than for counter elution or the washing step. The *in vitro* selection against KM was terminated completely after round 20 of this stringency increase test.

The development of a kanamycin A-binding aptamer was not pursued further in this work due to time constraints. The presented study focused on the development of a levofloxacin-binding aptamer since none had been published at this time. However, the successful selection against the aminoglycoside antibiotic was further utilised in another project within the research group.

2.4.2 Development of the levofloxacin-binding aptamer trLXC

In vitro selection against fluoroquinolone antibiotic levofloxacin (LX) was conducted using the Capture-SELEX method. The results of the selection process are presented in Figure 16.

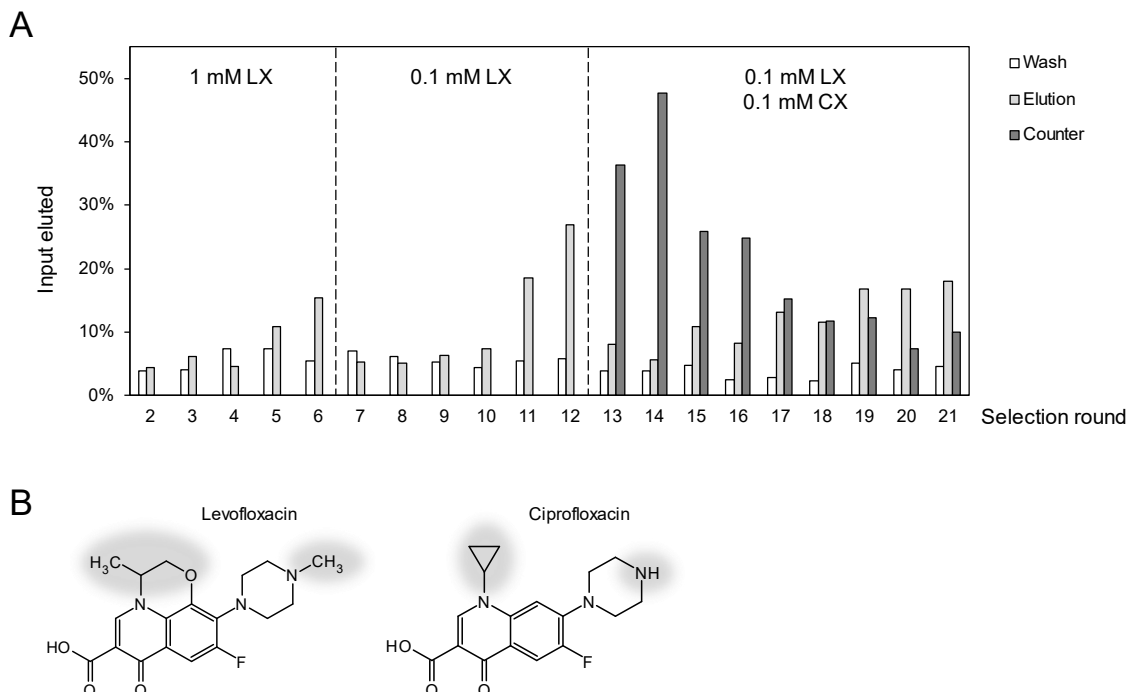


Figure 16 Capture-SELEX with the target molecule levofloxacin. **A** Results of selection shown as a graph of eluted input plotted against selection rounds. The white bars show the amount of eluted RNA in the last washing step. The medium grey bars show the amount of eluted RNA after the addition of 1 mM (rounds 2-6) and 0.1 mM (rounds 7-12) levofloxacin (LX). In order to be able to specifically select LX-binding RNA, a counter selection with 0.1 mM ciprofloxacin (CX) was introduced starting in round 13. The amounts of RNA eluted in this process are shown with dark grey bars. Dashed lines mark increases in stringency due to reduction of LX concentration (from round 7) or introduction of a counter target (from round 13). The first round was not radioactively labelled. **B** Chemical structures of the used ligands LX and CX. Different residues are highlighted by grey shading.

The *in vitro* selection against the antibiotic LX resulted in an enrichment of ligand-binding aptamers (Figure 16A). In the first rounds, the elution with 1 mM LX led to a gradual increase in the specific elution. In round 6, the first valid enrichment was observed. With more than 15%, the value of the input eluted by LX exceeded the value of the wash fraction almost threefold.

Due to this accumulation of LX-binding RNA molecules, the concentration of ligand was reduced to 0.1 mM starting in round 7. This initially led to a significant decrease in the specific elution. However, it slowly recovered until a new enrichment was observed in round 11. It was also evident that this accumulation was further enhanced in round 12. In this round, the elution of RNA by the addition of LX reached its maximum of almost 27% eluted input for the entire selection process. The value of the washing step with less than 6% was therefore lower than the specific elution by nearly factor 5.

The enrichment in round 11 and the confirmation of it in the following round enabled the introduction of a counter selection from round 13 onwards. The structurally very similar ciprofloxacin (CX) was used as a counter ligand. It differs from LX in only two areas (see Figure 16B). The counter elution with CX was carried out with a 0.1 mM ligand solution. This resulted in

significant elution by CX addition in the first rounds. Almost 50% of the RNA molecules used in round 14 could be eluted by counter ligand addition. However, this very dominant elution by CX weakened continuously. In round 18, the elution with LX and CX were almost equal. Finally, the specific elution with the target molecule of the selection exceeded the counter elution in round 19 with a value of almost 17%. A further decrease in elution due to the addition of CX was observed in the last rounds of selection. Thus, the elution with LX, which did not increase by itself, significantly exceeded the elution with CX in round 20 and 21. The *in vitro* selection with the target molecule LX was ended after this 21st round.

2.4.2.1 Next Generation Sequencing of the *in vitro* selection

The Capture-SELEX experiment with the target molecule LX were to be investigated using Next Generation Sequencing (NGS). Therefore, the PCR products of all conducted selection rounds as well as the DNA template pool were prepared and sent to the service provider GENEWIZ (Leipzig) for sequencing. The sequencing carried out corresponded to the Amplicon-EZ service. Using Illumina sequencing technology, a read count of at least 50,000 reads per sample was guaranteed. The total number of sequences obtained was about 1.3 million for the 22 examined samples. Thus, an average of approximately 68,000 sequences could be identified for each round. Besides all 21 rounds of selection, the RNA library, which was used to start every Capture-SELEX experiment was also analysed as round '0'. In addition to tracking the enrichment processes throughout the selection, sequences of potential RNA aptamers were identified. In cooperation with the research group Self-Organising Systems of the Department of Electrical Engineering and Information Technology, various analyses of the NGS data received were carried out. The results are summarised in Figure 17.

Most abundant 25 sequences of each selection round

Monitoring of the 25 most enriched sequences (Top25) of each selection round showed a distinct enrichment process (Figure 17A). Up to round 5, the abundance of the Top25 initially remained at a low level. However, with the first significant accumulation of LX-binding RNA molecules in round 6 (cf. Figure 16), the number of reads per million (RPM) also rose. In the following rounds, this incipient accumulation took a steep course and increased to a value of almost 10,000 RPM by round 10. Between rounds 5 and 10, the *in vitro* selection only showed one recognisable enrichment in round 6 according to the evaluation method applied. This was significantly reduced by lowering the ligand concentration, starting in round 7 (cf. Figure 16). The abundance of the Top25 of each round did not increase distinctly from the 10th round onwards. Although there were slight fluctuations, the RPM remained at the high level of just under 10,000.

Percentage and absolute number of orphans

Another interesting analysis is the observation of the sequences that occur only once in the RNA pool of each round (Figure 17C and D). These sequences are also called orphans and have a frequency k less than or equal to 1. The analysis of the absolute number of orphans (Figure 17D), but also the percentage of these in the total sequence number (Figure 17C) were evaluated. The percentage of these uniquely occurring sequences was over 60% both in the RNA start pool and until round 6 of the selection. Thereafter, the share of orphans decreased significantly. This was in line with the first increase in stringency by reducing the LX concentration in *in vitro* selection (cf. Figure 16).

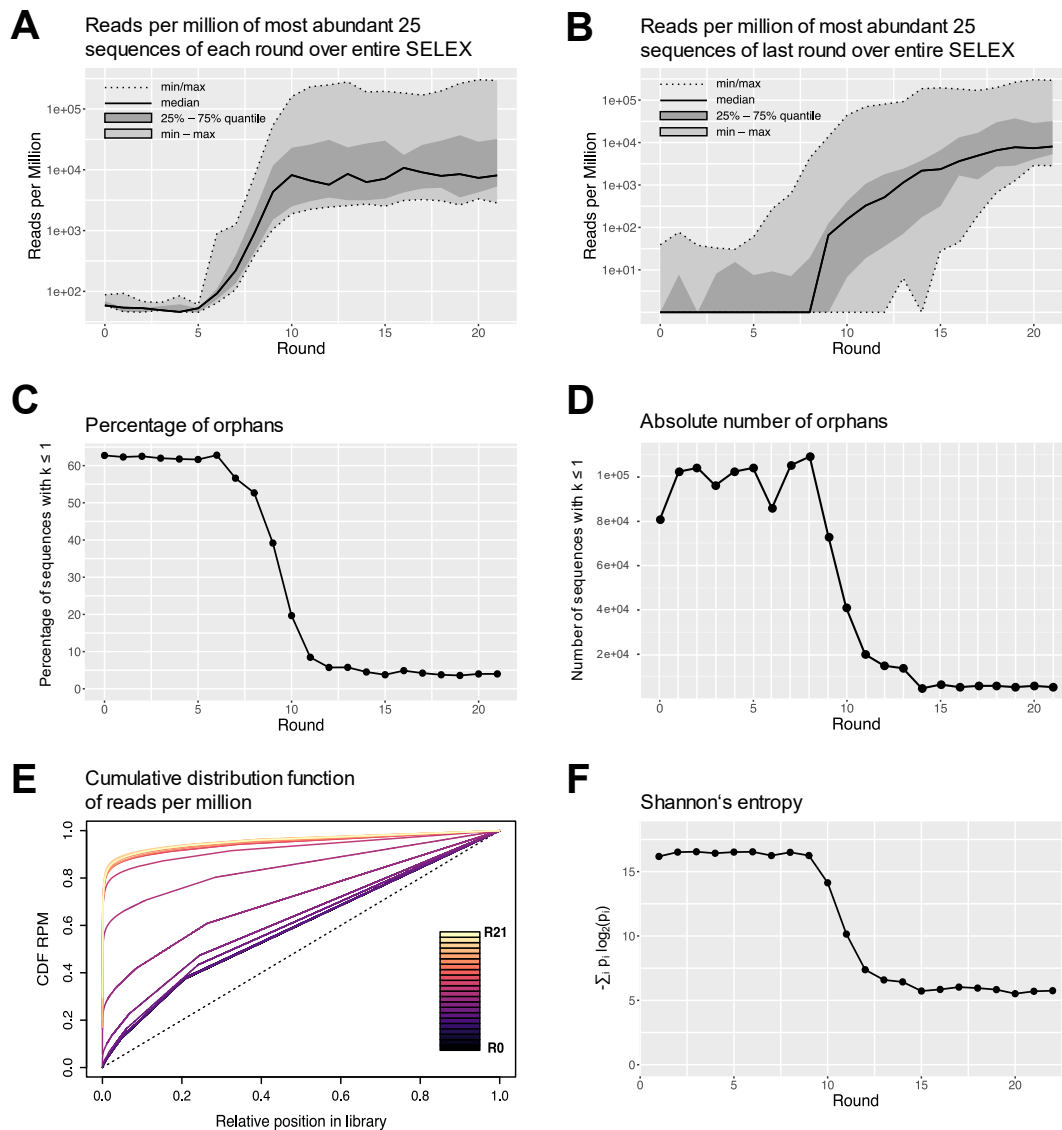


Figure 17 Multiple analyses of the data obtained from Next Generation Sequencing (NGS). **A** Graph of the 25 most frequent sequences (Top25) of each round in logarithmic scaled reads per million (RPM), plotted against the selection rounds. The median frequency of the Top25 for each selection round is shown by a solid line (median). The interquartile range (IQR) from 25% to 75% is highlighted in dark grey. The range between maximal and minimal frequency of the Top25 is represented in light grey with a dashed border line. **B** Graph of the 25 most frequent sequences (Top25) of the last selection round in logarithmic scaled reads per million (RPM), plotted against the selection rounds. The median frequency in each round of the Top25 of the last round is shown by a solid line (median). The interquartile range (IQR) from 25% to 75% is highlighted in dark grey. The range between maximal and minimal frequency of the Top25 is represented in light grey with a dashed border line. **C** Graph of the percentage of orphans with frequency $k \leq 1$ within the total number of sequences plotted against the selection rounds. **D** Graph of the absolute number of orphans with frequency $k \leq 1$ plotted against the selection rounds. **E** Lorenz curve of the cumulative distribution function (CDF) of reads per million (RPM) against all sequences according to their position in library (least to most abundant). This can be used to evaluate the sequence diversity and overall enrichment. Perfect diversity of the RNA pool, i.e. no enrichment, is represented by a dashed line. This can be used as a guide to estimate the enrichment of the RNA pool of a round. Inlay: Each round can be matched with a coloured line. As the round number increases, the colour becomes brighter. **F** Graph of Shannon's entropy value $-\sum_i p_i \log_2(p_i)$ plotted against the selection rounds. It represents a measure of the expected value of the information contained in a random variable (e.g. an RNA pool). The information content decreases for enriched sequences in the entire sequence space. This results in reduced entropy as the distribution shifts

to a few dominant sequences. Graphical evaluations were provided by Philipp Fröhlich (Department of Electrical Engineering and Information Technology, TU Darmstadt, Self-Organizing Systems, 64283 Darmstadt, Germany). They have been modified for the presentation.

By round 12, the orphan's percentage had decreased to less than 10%. This can also be applied to the results obtained from the selection, as a second enrichment was obtained by round 12 (cf. Figure 16). The orphans remained at this low level during a further increase in stringency by introducing a counter elution (see Figure 16) until the end of the selection in round 21.

A similar course can be observed in the absolute numbers of orphans. The selection start pool '0' had slightly more than 80,000 unique sequences. This number even increased in the first 5 rounds, so that up to more than 100,000 orphans could be detected. In round 6, there was a first decline, causing the number of orphans to fall below 90,000. In this round, a first enrichment of LX-binding RNA was obtained in the Capture-SELEX experiment (cf. Figure 16). After an increase in the number of orphans in rounds 7 and 8, the number decreased significantly to approx. 20,000 in round 11. In this round, the second enrichment was obtained in the *in vitro* selection (see Figure 16). In the following 3 rounds, the number of unique sequences declined again. It was now less than 5,000. The absolute quantity of orphans remained at this low level until the end of the selection. During these rounds, counter elution with CX was introduced and LX-binding RNA molecules were again enriched (cf. Figure 16).

Cumulative distribution function

The function of the cumulative distribution allowed to assess developments in sequence diversity and thus in the enrichment of the RNA pool across the *in vitro* selection (Figure 17E). A pool with a perfect composition, i.e. a complete diversity of the sequences, would result in a linear curve like the dashed line shown in Figure 17E. The lower the diversity of the pool examined, the more the resulting curve would bend. The RNA pool '0' used here for the start of selection against LX exhibited a slight curvature (dark blue curve in Figure 17E). The first selection rounds 1 to 4 also had a similar shape. The curve only steepened from round 5 onwards. Diversity continued to decrease even more with rounds 6-8. In the *in vitro* selection, a first enrichment was obtained in these rounds and a stringency increase was carried out by reducing the ligand concentration (see Figure 16). From round 9 onwards, all subsequent rounds revealed a very similar curve. Thus, until the end of the selection, there was no major change in the general sequence diversity.

Shannon's entropy

The determination of the Shannon's entropy of each round allowed a further evaluation of the overall enrichment process of the selection against LX (Figure 17F). The entropy provides a measure of the diversity of sequences in the RNA pool. The higher the number of different sequences, the greater the value of entropy. Thus, the entropy decreases with the accumulation of identical sequences through an enrichment. This could be observed for the *in vitro* selection against LX. In the first 8 rounds of the Capture-SELEX experiment, the entropy was at the same high level. Hence, the first enrichment in round 6 did not significantly reduce it (cf. Figure 16). In the subsequent rounds 9 to 11, the diversity in the RNA pools of the respective rounds decreased rapidly. By round 14, it had declined even more. This can be compared with the second enrichment obtained by reducing the ligand concentration and the introduction of counter selection with CX (see Figure 16). Despite slight fluctuations in entropy, it remained at the low level reached in round 14 until the last round of selection. During these rounds, there was a further accumulation of LX-binding RNA molecules (cf. Figure 16).

Eight different RNA aptamers were chosen from the sequencing data of the last selection round. Initially, six of the ten sequences that occur with the highest frequency were picked. These included the three most abundant sequences and those in the 5th, 7th and 9th rank of abundance. The last three were chosen because their frequency decreased more significantly than the frequency of the sequences in the 4th to 6th ranks of abundance. Two of these sequences differed only in one point mutation (LXB1 and LXB2). Such a minor deviation in the sequence can be interesting for subsequent investigations, as it can lead to major effects on the function of the aptamer. Therefore, another pair of sequences was chosen, which also differ only in one point mutation (LXA1 and LXA2). The individual sequences are listed in Table 2.

Table 2 RNA sequences of potential aptamers against LX

Name ¹	Sequence ²	Abundance ³
LXA1/A2	5'- GGGCAACUCCAAGCUAGAUCUACCGGUCUUUUUC (A/U)G GCGGCUUAAAAACCAGGAAAGGUGGAGACUUC <u>CUACUGGCU</u> <u>UCUAUCCAGCCGGUAAAAUGGCUAGCAAAGGAGAAGA</u> ACU UUUCACU -3'	239 (LXA1) 962 (LXA2)
LXB1/B2	5'- GGGCAACUCCAAGCUAGAUCUACCGGUGUGUAACGGAA GCACAAAGGUGCCUCCUACAGCAGGUCUUC <u>CUACUGGCUU</u> <u>CUACUGAUAC</u> (A/G)CUAAAAUGGCUAGCAAAGGAGAAGA AC UUUUCACU -3'	5,093 (LXB1) 2,693 (LXB2)
LXC	5'- GGGCAACUCCAAGCUAGAUCUACCGGUUUGGGUAGUG CGAUUCGCACUGAAUGCCGCGUAGGCUUC <u>CGCUACUGGCU</u> <u>UCUACUACGUACCCAAAAUGGCUAGCAAAGGAGAAGA</u> ACU UUUCACU -3'	4,947
LXD	5'- GGGCAACUCCAAGCUAGAUCUACCGGUCUAGUGCCUCA ACUAGCCGAACCGUGGUCGUCUUC <u>AUGCCUACUGGCUUC</u> <u>UACGAGAUAAAUAAAAUGGCUAGCAAAGGAGAAGA</u> ACUUU UCACU -3'	1,221
LXE	5'- GGGCAACUCCAAGCUAGAUCUACCGGUCGUAGUGGAC CUGUUUAGGUUUGCAUACGUUAGAUGUCUUC <u>CUACUGGCU</u> <u>UCUAAAUCGAACCGAAAAUGGCUAGCAAAGGAGAAGA</u> ACU UUUCACU -3'	24,807
LXF	5'- GGGCAACUCCAAGCUAGAUCUACCGGUGCAGGUCUGG GAACUCGUUCCCGGCUCAGCUGGAUUCUUC <u>CUACUGGCU</u> <u>UCUAGCCCGACCGAAAAUGGCUAGCAAAGGAGAAGA</u> ACU UUUCACU -3'	6,782

¹ The sequences were named with the prefix LX and the letter A to H. The suffix '1' or '2' was used for sequence pairs with a point mutation.

² Identified sequences: The 5' and 3' constant regions are marked in bold letters. The capture sequence is highlighted with an underline. Point mutations are written in brackets.

³ Information about the abundance of the sequence in the last selection round

The presented sequences in Table 2 were chosen from the 21st round of the Capture-SELEX experiment. The three most frequently detected sequences for the last round of selection were LXE with more than 24,800 reads, LXF with almost 6,800 reads and LXB1 with over 5,000 reads. The two sequence pairs with the single point mutation also differed significantly in their abundance. Not only did they differ between each other, but also as general sequence pairs. The sequences

LXA1 and LXA2 were much less frequent than LXB1 and LXB2. LXB1 was the third most abundant sequence. Its sequence partner LXB2 was only the seventh most frequent sequence. Another interesting finding occurred in the sequence of the potential RNA aptamer LXD. Unlike the other sequences, it did not have 40 nucleotides in the N40 randomised region, but only 39.

2.4.2.2 Testing the specificity of potential aptamers

In the following, a specificity test similar to the Capture-SELEX procedure was performed with all eight potential aptamers LXA1 to LXF. After *in vitro* transcription of their RNA sequences, the potential aptamers were tested for their ability to distinguish between LX and the counter molecule CX. The elution assay was performed according to the Capture-SELEX procedure starting in the second selection round. However, single-species pools containing only one sequence were used. After immobilisation of the RNA molecules, the same three washing steps were carried out as in the SELEX routine. Subsequently, elution was carried out with a 1 mM solution of LX or CX. Finally, only the obtained fractions were measured and used to determine the percentage of the elution fraction in the total amount of RNA. Therefore, the evaluation was based on the values of the eluted input caused by the two different ligands. The results are shown in Figure 18.

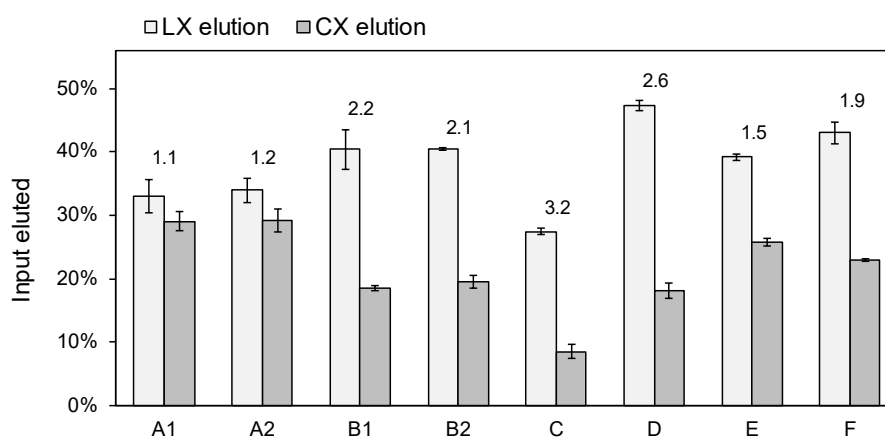


Figure 18 Capture-SELEX-based elution assay with potential levofloxacin-binding aptamers. Eight different potential aptamers were tested. The names LXA1 - LXF were shortened to the last letter for better orientation. The light grey bars show the eluted RNA amount due to the addition of 1 mM levofloxacin (LX). The dark grey bars show the amount of RNA eluted with 1 mM ciprofloxacin (CX). The numbers above the bars represent the ratio of LX eluted RNA to CX eluted RNA. The procedure was repeated at least two times.

The elution assay revealed differences in the recognition between the two ligands tested (Figure 18). LXA1 and LXA2 could only slightly distinguish between LX and CX as ligands in the specific elution. The aptamer LXE, which was the most abundant in the Next Generation Sequencing data of the final selection round, was able to distinguish slightly better between the two antibiotics. At almost 40%, the elution with LX was 1.5-fold higher than with CX. Even better ratios between LX and CX elution appeared for the candidate LXF. With a specific elution by the ligand CX of approx. 23% and by the ligand LX of 43%, the latter elution was almost twice as high. The sequences LXB2 and LXB1 showed an elution better by more than a factor of 2 with the target molecule LX than with the counter molecule CX. The potential aptamer LXD showed the highest specific elution with the addition of LX, at over 47%. The comparatively very low elution with CX of only slightly more than 18% thus produced a 2.6-fold difference. Only the candidate LXC was able to top this very good result. With a ratio of LX elution to CX elution of 3.2, it exceeded that of LXD by 0.6.

Although this aptamer showed a much lower elution with LX of only approx. 27%, a very low elution was also observed with the addition of CX. The value of this specific elution was the lowest of all the candidates investigated, with under 9%. Thus, this led to the best ratio of distinguishability between LX and CX by the potential aptamer LXC.

The later use of an LX-binding aptamer in a biosensor requires high specificity in order to prevent false positive results from structurally similar analytes. Based on the results of the elution assay, it was assumed that LXC was the most specific binding candidate. Therefore, this sequence was used for subsequent work on the development of an LX-binding aptamer.

2.4.2.3 Determination of the dissociation constant of the aptamer LXC by isothermal titration calorimetry

The first investigation of the binding conditions between the aptamer LXC and its ligand was carried out by thermodynamic measurement of the binding event using isothermal titration calorimetry (ITC). Therefore, the RNA was transcribed *in vitro*, gel-purified and used at a concentration of 50 μM . For the ligand LX, a 10-fold higher concentration of 500 μM was applied. In addition, the secondary structure of the aptamer was predicted using the web tool RNAfold web server¹⁵⁶. The results of the binding measurement with ITC and the secondary structure prediction are shown in Figure 19.

Measurement of the ligand binding using ITC

The analysis of the binding affinity was carried out using isothermal titration calorimetry and resulted in the determination of a dissociation constant K_D (Figure 19A). The upper graph shows the measurement of the energy required to maintain the temperature of the RNA solution for each injection of ligand solution (see Figure 19A top). It could be observed that the size of the measured peaks decreased continuously with increasing number of injections. At the beginning of the measurement (1st to 3rd injection) small deviations occurred, these were eliminated with baseline correction. After the 16th injection, no further significant changes in the peaks occurred. The plot of the reaction enthalpy ΔH as a function of the molar ratio yielded a binding curve using the single binding site model of the applied evaluation software (see Figure 19A bottom). A K_D of approx. 3 μM could be determined for the binding between aptamer and ligand. This indicated a 1:1 binding ratio between RNA and ligand. The binding reaction between LXC and the target molecule LX was spontaneous. This could be deduced from the negative free enthalpy ΔG . It could be calculated via the Gibbs-Helmholtz equation using the value of the enthalpy of reaction ΔH (-110 kJ/mol) and the product of the absolute temperature T and the entropy ΔS (-79 kJ/mol). A constant systematic measurement deviation (Offset) of -4.43 kJ/mol occurred, which was included within calculations.

Prediction of the secondary structure

The prediction of the secondary structure of the aptamer LXC resulted in an elongated stem loop (Figure 19B). In addition to the three stem loops, three internal loops of different sizes could be identified. One of the latter could also be regarded as a bulge formed from 5 nucleotides (A18-A22). Furthermore, a three-way junction (J1-3) and two single nucleotide bulges (U52, C57) in the stem P3 were predicted. The capture sequence was found to be part of the stem of the largest stem loop (P3L3) and the three-way junction J1-3. The 5' and 3' constant regions formed all internal loops. In addition, the smallest of the predicted stem loops was located in the 3' constant region.

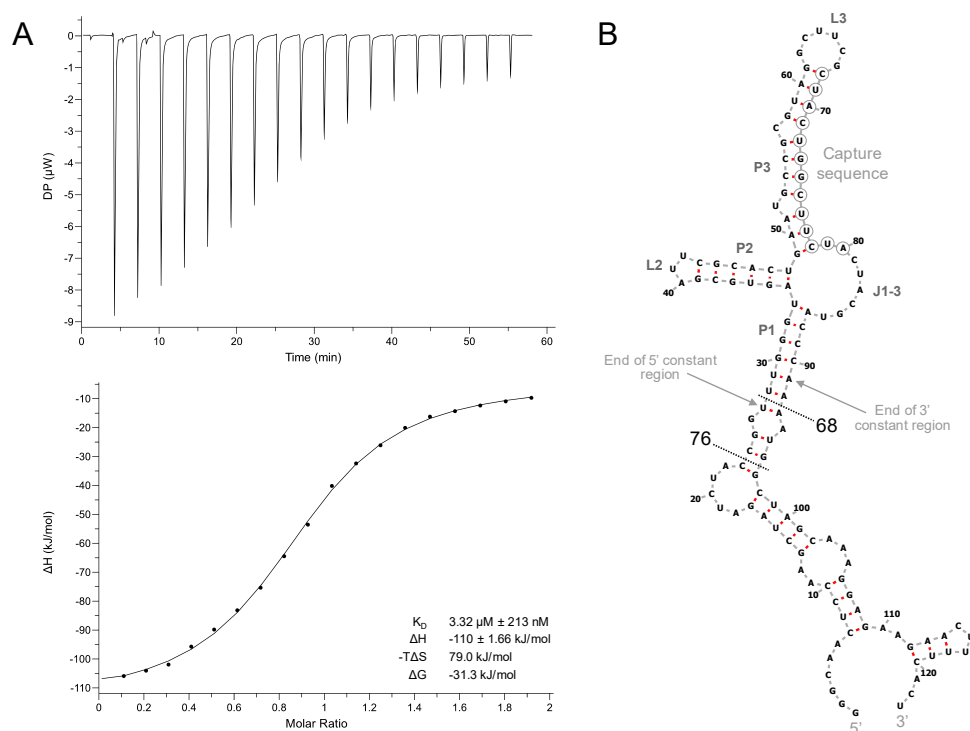


Figure 19 ITC measurement and predicted secondary structure of the aptamer LXC. **A** Measurement of the dissociation constant (K_D) of LXC-binding aptamer LXC. Top: Required power to sustain the temperature of the RNA solution plotted against the time to reach saturation (baseline corrected). Bottom: Plot of the enthalpy of reaction along the molar ratio of LX to RNA fitted to a single binding site model (MicroCal PEAQ-ITC Analysis Software 1.41). The determined values of the K_D , the reaction enthalpy ΔH , the negative multiplication product of temperature and entropy $-\Delta S$ as well as the free enthalpy ΔG are given in the lower right corner. **B** The ends of the 5' and 3' constant regions are indicated with arrows. The capture sequence is marked with outlined nucleotides. The labels of the most important structural features (P1, P2, P3, L2, L3, J1-3) were included and defined for following secondary structures. The later truncations to 68 and 76 nt are represented by dotted lines. Prediction of secondary structure was performed with the web tool RNAfold web server¹⁵⁶ and representation of the structure was created with the Forna tool¹⁵⁷.

Previous developments of aptamers have demonstrated that sequence shortening can improve binding between the aptamer and the ligand.¹⁵³⁻¹⁵⁵ In order to reduce the size of this 123-nucleotide long RNA aptamer, two different truncations were created. Both ended at the marked points of the secondary structure (see Figure 19B) and were named after the length of the resulting aptamers. The truncation 68 left out the entire 5' constant region and, except for two adenines, also the 3' constant region. Thus, all internal loops and the small stem loop at the 3' end were no longer contained in this shortened version. In contrast, truncation 76 retained the smallest of the internal loops and thus also minor parts of the 5' and 3' constant region.

2.4.2.4 Truncation and mutation study using ITC

The first attempt to optimise the aptamer LXC by shortening its structure was carried out using a newly established ITC-based method. The focus was not on the determination of the exact thermodynamic parameters, but on the investigation of whether the aptamer was still able to bind the ligand despite the respective mutation. The original aptamer LXC was used as a reference.

In addition to the truncations 68 and 76, a mutation of 76 was also tested. The stem P1 was closed by changing the bases, resulting in the mutant trLXC. All the required RNA sequences were transcribed *in vitro* and purified using a molecular weight cut-off column. This method enabled a faster purification process but did not yield as clean RNA samples as gel purification. Therefore, the results obtained were evaluated primarily qualitatively and not quantitatively. An obtained K_D value could only be considered as an estimation based on the results. The RNA was used in a concentration of 30 μM and the ligand LX in a concentration of 500 μM . In addition, the secondary structures of the truncations 68 and 76 as well as the mutant trLXC were predicted using the web tool RNAfold Webserver¹⁵⁶. The results of the determination of the binding ability using ITC measurements and the secondary structure prediction are shown in Figure 20.

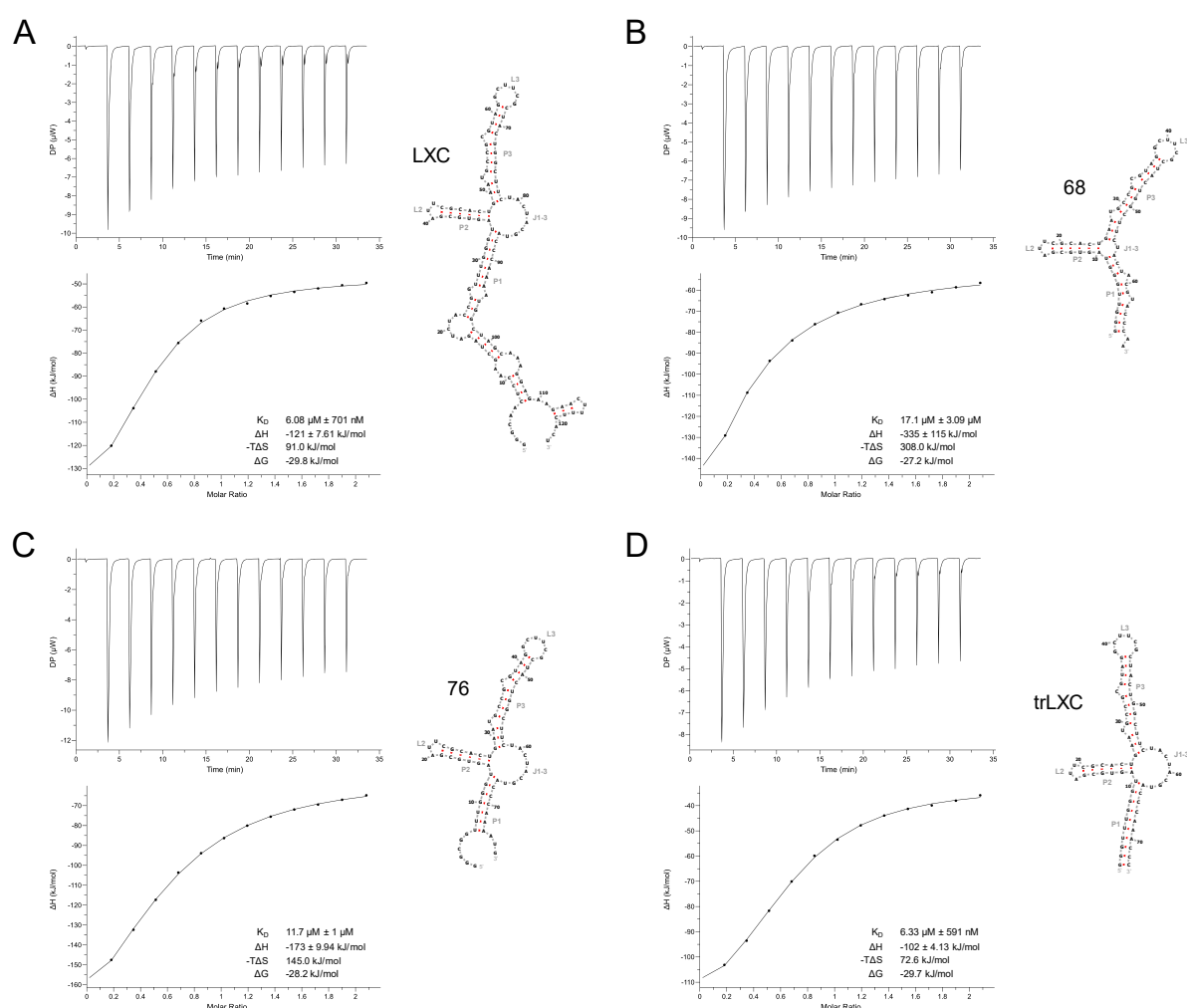


Figure 20 ITC-based analysis of truncations and mutation of the aptamer LXC with predicted secondary structures of LXC, shortenings 68 and 76 as well as the mutant trLXC. Determination of the binding ability of LXC (A), shortenings 68 (B) and 76 (C) as well as trLXC (D). Top graphs: Required power to sustain the temperature of the RNA solution plotted against the time to reach saturation (baseline corrected). Bottom graphs: Plot of the enthalpy of reaction along the molar ratio of LX to RNA fitted to a single binding site model (MicroCal PEAQ-ITC Analysis Software 1.41). The determined values of the K_D , the reaction enthalpy ΔH , the negative multiplication product of temperature and entropy $-T\Delta S$ as well as the free enthalpy ΔG are given in the lower right corners. Next to the respective graphs the predicted secondary structures of LXC (A), truncations 68 (B) and 76 (C) as well as trLXC (D) are shown. The prediction was performed with the web tool RNAfold web server¹⁵⁶ and graphically represented using the Forna tool¹⁵⁷.

The results of the first attempt to truncate the aptamer LXC showed that the shortening to 68 or 76 nt and the mutant trLXC had no significant impact on binding to the ligand (see Figure 20). Only minor changes in the dissociation constants could be detected. The original aptamer and trLXC exhibited K_D values of about 6 μM (see Figure 20A and D). The shortenings 68 and 76 yielded values of approx. 17 μM and nearly 12 μM , respectively (see Figure 20B and C). However, these changes in the K_D were not pronounced enough to be considered as significant deteriorations. Thus, the binding affinity remained in the low micromolar range for all variants.

Examination of the predicted secondary structures revealed that a refolding may have occurred in shortening 68 (see Figure 20B right). The large three-way junction J1-3 reduced massively and an alternative closing stem with two bulges was formed in P1. In the case of shortening 76, these two structural features probably remained almost unchanged (see Figure 20C right). Merely the small internal loop in the closing stem P1 was not able to be formed.

The mutation of the closing stem P1 of 76 led to the mutant trLXC. It presumably also exhibited all the structural features of the parental aptamer LXC (see Figure 20D right). Only stem P1 was completely closed and thus stabilised. Consequently, the parent aptamer LXC could be shortened and its closing stem stabilised by mutation. However, this neither improved nor deteriorated the binding to the ligand LX.

Since a stabilised closing stem is usually advantageous for aptamers, more mutations were carried out using trLXC to improve ligand binding or further reduce its length. Additionally, it was intended to investigate whether it was possible to identify regions that are necessary for the binding to LX. For this purpose, various mutations were introduced in nearly all structural segments of the aptamer trLXC. All mutants produced are shown in Figure 21. The predicted secondary structure is shown with partially deformed bonds for easier orientation.

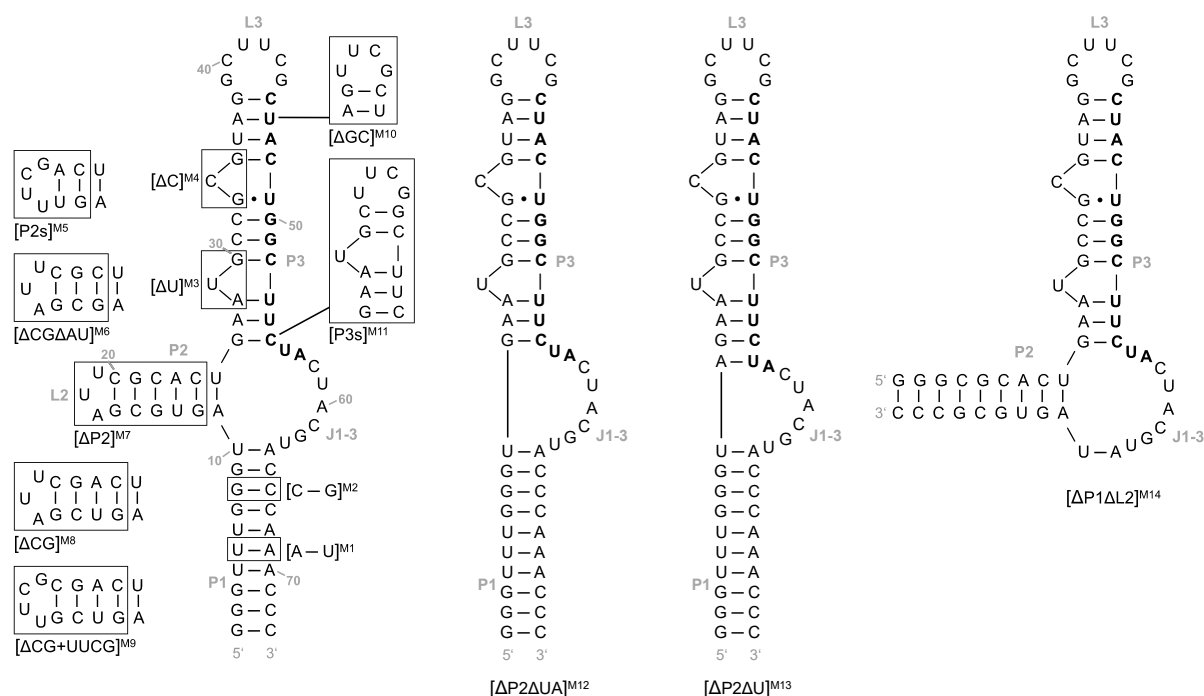


Figure 21 Summary of all mutations applied to the LX-binding aptamer trLXC. The mutations are displayed in frames and named M1 - M14. The changes at P1, P2L2 and P3L3 resulted in the mutations M1-M11. The difference between M12 and M13 was the deletion/retention of A11. The formation of an alternative closing stem P2 in mutation M14 was achieved by deleting P1 and L2. The capture sequence is highlighted in bold.

The impact of each mutation on the binding ability of the aptamer trLXC to its ligand was also determined using the newly established ITC-based method. Therefore, the RNA sequences of all mutations were transcribed *in vitro* and purified with a molecular weight cut-off column. This method enabled a purification process that was faster but did not provide as clean RNA samples as gel purification. Therefore, the results obtained were primarily evaluated qualitatively rather than quantitatively. The K_D values obtained could only be considered an estimate based on the binding curves. The RNA was used in a concentration of 30 μM and the ligand LX in a concentration of 500 μM . The data from the ITC experiments of all mutations are summarised in Figure 22.

The conducted mutation study yielded different results regarding the binding ability of the respective mutations (Figure 22). The loss of the ability of the aptamer trLXC to bind its ligand caused by a certain mutation was assumed as soon as no valid binding curve could be determined. If the interaction between aptamer and LX was not affected, a binding curve could be obtained and a K_D value was estimated.

Single nucleotide mutations in P1 and P3 (M1-M4)

Mutations M1 and M2 were used to test the importance of the sequence in the closing stem of the aptamer. For this purpose, one nucleotide pair each was switched sides. Under the influence of both mutations, the RNA was still able to successfully bind the target molecule LX.

The deletions of the bulged nucleotides U29 (M3) and C34 (M4) were intended to reveal the importance of these structural elements. Both mutations abolished binding and led to complete loss of the aptamer's binding ability.

Mutations in L2P2 (M5-M9, M12-M14)

Several mutations were also made in the L2P2 stem loop. Some of them caused changes in the stem (M6, M8), and others additionally in the loop (M5, M9). Further mutations included deletions of varying extent in the L2P2 stem loop (M7, M12, M13). The last mutation M14 even created an alternative closing stem in P2. Therefore, P1 was almost completely deleted.

The stem altering mutations M6 and M8 varied in the deletion of different base pairs. For M6, both a CG (G14, C22) and an AU (U13, A23) pair were deleted. In contrast, M8 only included the deletion of the same CG pair. The results showed a loss of binding between aptamer and ligand for M6. However, for M8, no change in binding ability was detected.

The mutations M5 and M9 introduced, in addition to stem changes, a replacement of the AUU triple-loop by a UUCG tetra-loop. For M5, the sequence was deleted from G14 to C22. The resulting short stem was formed into a new stem loop using the UUCG tetra-loop. However, this led to a loss of binding between the RNA aptamer and LX. The M9 mutation was derived from the M8 mutation. However, for this mutation, the loop of L2P2 was additionally replaced by UUCG. This change resulted in a binding curve and thus had no effect on the binding ability of the aptamer.

RESULTS

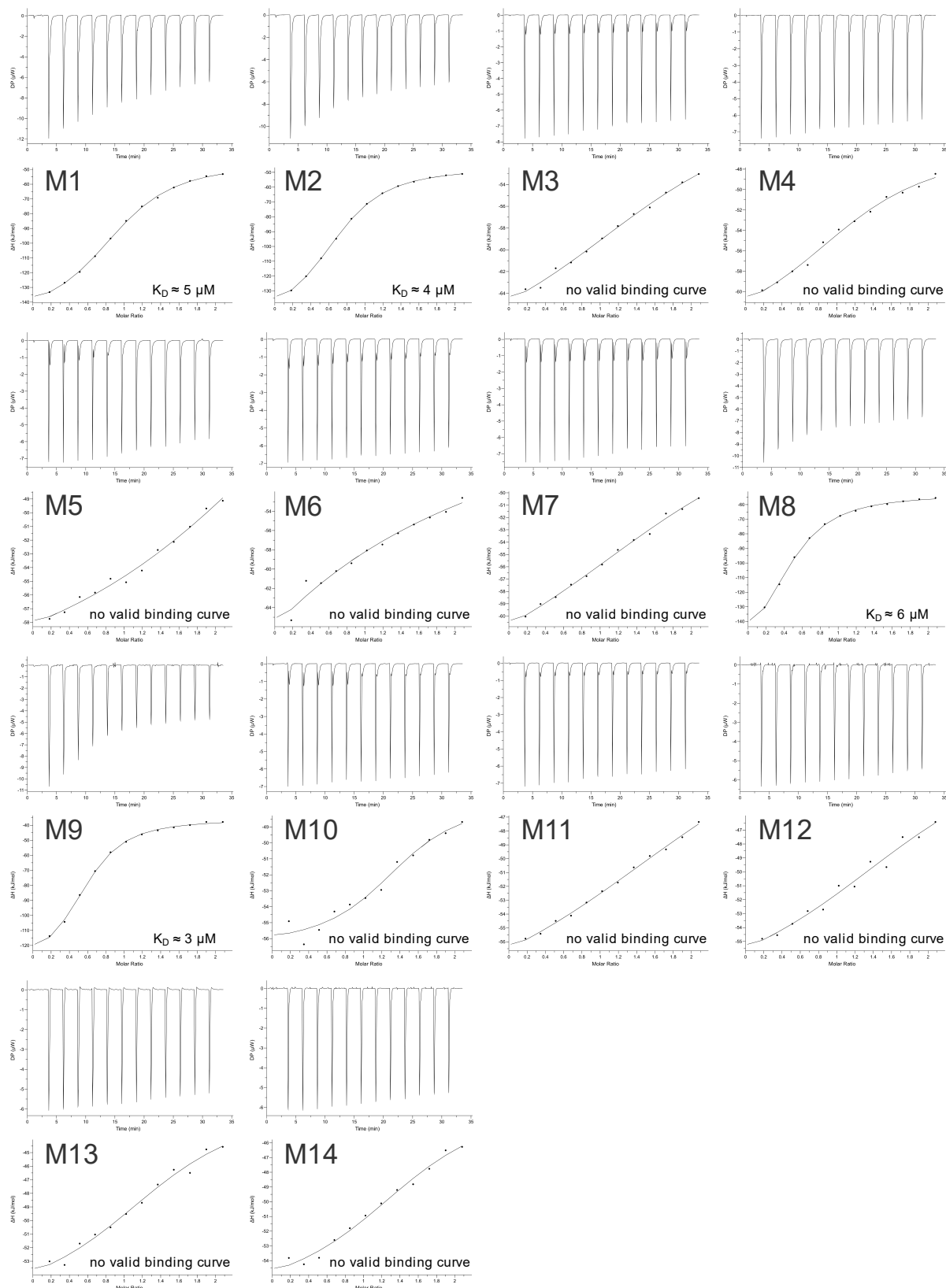


Figure 22 Summary of the ITC-based analysis of mutations of the aptamer trLXC. ITC measurements of the mutations M1 - M14, which were performed on trLXC. Upper graphs: Plot of the required power to maintain the temperature of the RNA solution over time (baselines corrected). Lower graphs: Enthalpy of reaction plotted against the molar ratio of LX to RNA fitted to a single binding site model (MicroCal PEAK-ITC Analysis Software 1.41). If a valid binding curve could be determined, the estimated dissociation constant (K_D) is given in the bottom right corner.

The mutations M7, M12 and M13 differed in their extent of deletion of the entire stem loop L2P2. While the AU pair (A11 and U25) was retained in M7, it was completely removed in M12. M13 formed a compromise between these two mutations, since only the U25 was deleted. By keeping A11, it could be paired with the U56 of the three-way junction. Thus, another base pair was added in the stem P3 (base pairing shown in the structure of M13). However, no valid binding curve could be obtained for any of these mutations in the ITC experiment. All of these changes made to L2P2 thus led to a loss of binding between the respective aptamer variants and the ligand.

The mutation M14 conducted on L2P2 involved the formation of a completely new alternative closing stem of the aptamer. For this purpose, P1 was deleted except for the base pair of U10 and A64. Furthermore, the AUU triple-loop L2 was removed and replaced by a short stem of three CG pairs. However, this very complex mutation of the aptamer did not lead to a valid binding curve. This indicated a loss of the binding ability of the aptamer with an alternative closing stem.

Mutations in L3P3 (M10 and M11)

Two changes were also made to stem loop L3P3. One only changed the loop, the other additionally modified the length of the stem. The first mutation, M10, led to the transformation of the hexa-loop. Thereby, G39 and C40 were deleted, which created a UUCG tetra-loop. However, this mutation did not yield a valid binding curve within the ITC experiment and consequently led to the loss of binding between the aptamer and the ligand.

The second mutation, M11, was primarily directed at shortening the long P3 stem. For this purpose, the sequence between C31 and G51 was deleted. The resulting shorter stem was additionally attached to a UUCG loop. Like the previous mutation, this one also led to the loss of the binding ability of the RNA to the target molecule LX, since no binding curve could be obtained in the evaluation of the ITC experiment.

The conducted truncation and mutation studies revealed that only a few changes could be tolerated by the aptamer trLXC. Besides the shortening of the aptamer, a consistent complementarity could be established in the P1 stem. This led to the stabilisation of the closing stem. Additionally, only a minor truncation in stem P2 and an exchange of loop L2 with a UUCG tetra-loop in combination with this truncation were possible. All other mutants exhibited no binding to the ligand LX. Therefore, it could be assumed that major parts of the aptamer are involved in ligand binding or the formation of the binding pocket.

2.4.2.5 In-line probing

The previous mutation study with the trLXC aptamer provided initial insights into the importance of certain structural features of the aptamer. In order to gain further information on the correlation between structure and binding to LX, in-line probing was performed with trLXC. Although certain mutations did not lead to a loss of binding ability, no significant improvements in binding to the ligand were achieved. Consequently, the unchanged aptamer trLXC was used. In-line probing also provided an opportunity to experimentally verify the predicted secondary structure. The RNA was transcribed *in vitro*, gel-purified and labelled with radioactive nucleotides at the 5' end. The aptamer was subsequently incubated with different concentrations of LX for several days. The natural instability of RNA caused the structure to cleave at flexible regions, which is known as in-line cleavage.¹⁵⁸ This was finally visualised by polyacrylamide gel electrophoresis. The results are shown in Figure 23.

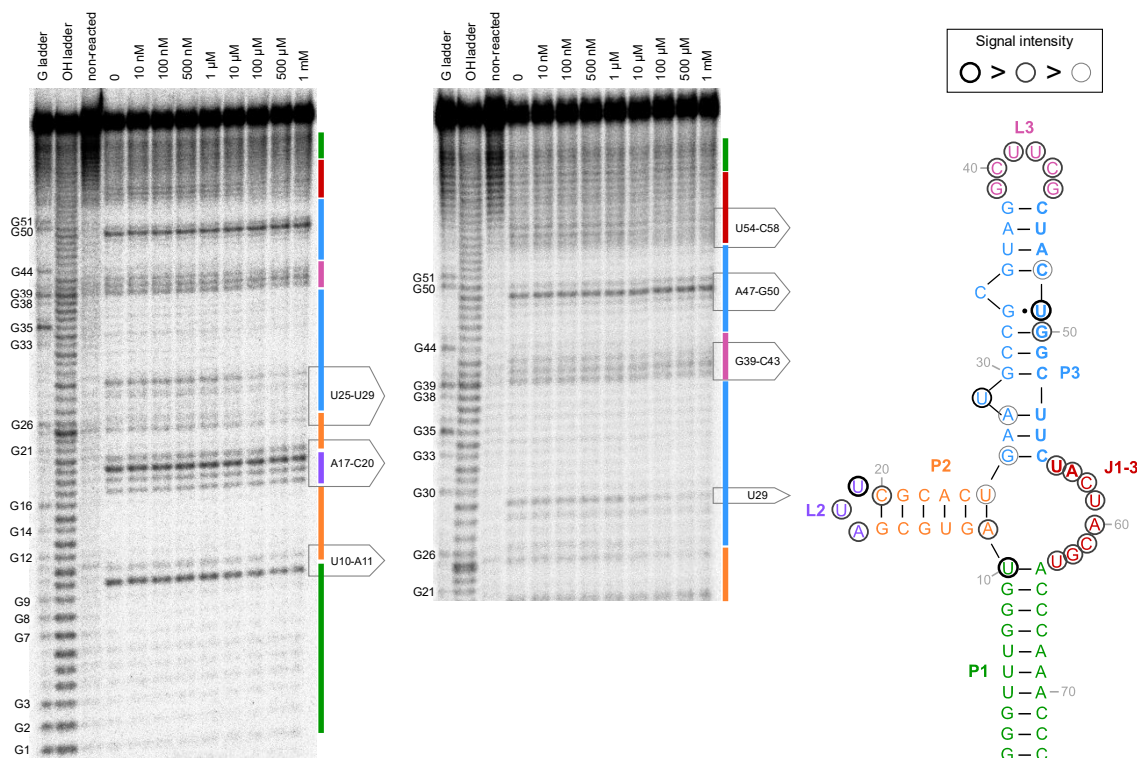


Figure 23 In-line probing experiment for trLXC. In addition to the cleavage pattern of the entire aptamer (10% PAA gel), the region starting at the 21st nucleotide was also examined in more detail (8% PAA gel). The in-line reactions were carried out without and with up to 1 mM LX under alkaline conditions. In order to provide a reference for the guanine bases and individual nucleotide positions two ladders were included (G and OH ladder). The positions of the guanine bases (G) within the sequence were labelled. Using the G localisations and the OH ladder, which shows each individual nucleotide position, the remaining nucleotides could be aligned with the signals. Additionally, a non-reacted RNA sample of the aptamer was incorporated as a control (non-reacted). The areas with visible signals were identified by their nucleotide positions. The predicted secondary structure (right) was marked with the corresponding areas. Therefore, the respective nucleotides were highlighted with circles of different thicknesses depending on the signal intensity (inlay top right). The coloured lines next to the gels match the identified stem, loop and junction regions indicated by the same colour in the predicted secondary structure. The capture sequence is shown in bold (C45-A57). The pentagonal arrows mark the nucleotide positions used for the graphical evaluation of signal intensities (see Figure 24). In regions G21-G26 and G39-G44, it is not possible to clearly identify the individual nucleotides. This is due to gel compression. The in-line probing was performed at least 2 times for each polyacrylamide concentration of the gels.

Different signal intensities were observed in the two gels shown for the conducted in-line probing experiments (Figure 23). The gel which displayed the entire RNA sequence exhibited such varying signals for different nucleotide positions (Figure 23, left). In particular, the signals of U10, U19 and U49 appeared to be the most intense throughout the entire gel. Other areas or nucleotide positions showing signals were A11, A17-C20, U25-U29, G39-C43, A47-G50 and U54-C58. The latter three regions could be better analysed in the in-line probing gel with higher resolution of the 3' end of the RNA (Figure 23, centre). All other nucleotide positions showed no or weak signals. Based on these signals of varying intensity, which could be assigned to specific nucleotide positions, the predicted secondary structure could be aligned to the gels. The individual regions of the aptamer trLXC were marked with different colours (Figure 23 left). The corresponding-coloured labels were then mapped to the signals. Areas with strong signals were considered flexible and those with weak or no signals were regarded as rigid parts of the aptamer. According

to this principle, the results could be correlated with the predicted secondary structure. Thus, in-line probing conducted with the aptamer trLXC confirmed its secondary structure prediction. Almost all regions that were assumed to be flexible could be determined as such. Only the bulged C34 could not be identified as flexible. However, the opposing region between C48 and G50 exhibited increased flexibility. Especially U49 showed one of the strongest signals in the in-line probing gels. Thus, it could be suggested that C34 lies more within the nucleotide string of the P3 stem, causing inflexibility, and that U49 protrudes from the stem.

In addition, the confirmation of the predicted secondary structure, the localisation of the presumed ligand binding site was determined based on the results of the in-line probing experiments. For this purpose, the signal intensities were measured using the ImageJ graphic software. The analysed sections included the regions with distinct signals already labelled in Figure 23 as well as the two regions of the nucleotide positions U4 and G35. These did not exhibit any significant signals and thus served as controls. The measured data was plotted graphically as relative signal intensities against the logarithmically scaled concentration of LX. The obtained results are shown in Figure 24.

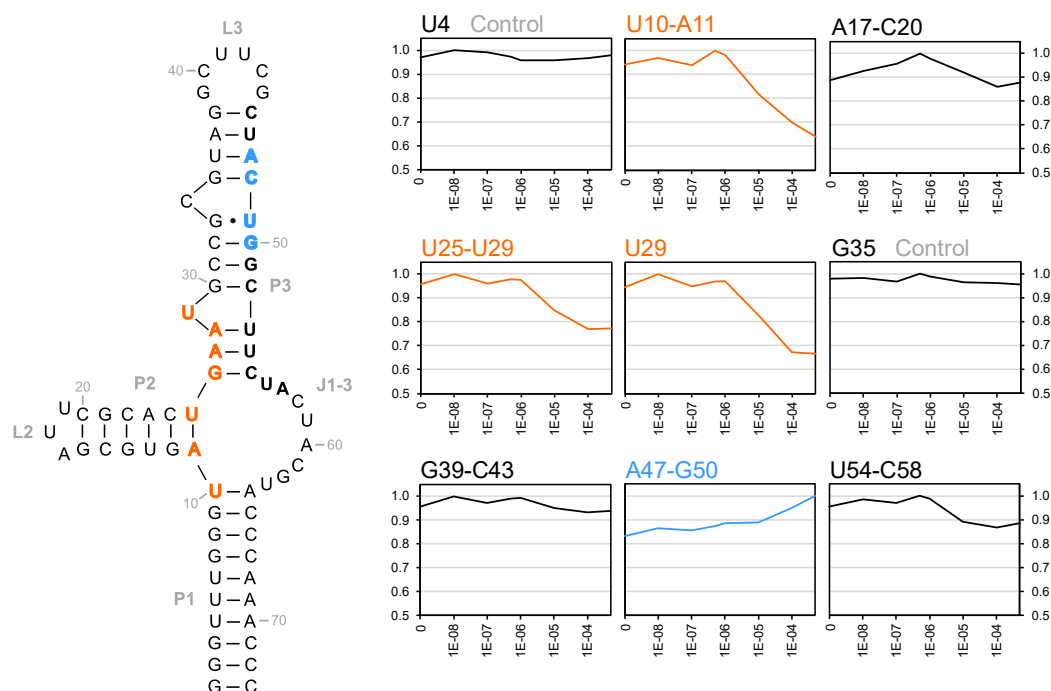


Figure 24 Assessment of the localisation of the ligand binding site by signal intensity quantification as a function of LX concentration. The change in flexibility or rigidity of specific regions of the aptamer was investigated by graphical measurements of signal intensity (ImageJ 1.54b). The monitored areas were named and labelled with the corresponding nucleotides (pentagonal arrows in Figure 23). The graphs display the relative intensity of the measured signals (y axes) plotted against the concentration of LX 8 (x axes). Areas that changed significantly due to ligand binding were highlighted in orange, the one that changed moderately in blue. The areas corresponding to the nucleotide positions U4 and G35 did not exhibit distinct signals and thus served as control measurements. They were not labelled in Figure 23.

Another aspect of in-line probing was the identification of regions involved in the ligand binding. In order to perform such analyses, it was necessary to use a concentration gradient of LX. This allowed the evaluation of changes caused by the interaction with the ligand in certain areas of the structure as well as a graphical estimation of the binding affinity of the RNA aptamer (Figure 24). Both could be performed with the measurement of signal intensity. Subsequently, the relative

signal intensity was plotted against the logarithmically scaled LX concentration (see Figure 24 right). The detailed values are listed in Table 27 in the appendix. The areas analysed with this method included the regions marked with pentagonal arrows on the in-line probing gels (cf. Figure 23). In addition, two areas without distinct signals were included as controls. It is important to note the width of the signals at the edges of the gels (see Figure 23). The lane of the 1 mM ligand concentration produced a much narrower signal than the other lanes. Since no valid graphical evaluation was possible, this concentration was not incorporated into the analyses.

The results obtained showed different curves of the measured signal intensity with increasing LX concentration (see Figure 24 right). For the areas U10-A11, U25-U29 and the individually measured signals of U29, the intensity decreased significantly with higher ligand concentrations (see Figure 24 highlighted in orange). The areas A17-C20, G39-C43 and U54-C58 showed fluctuating values or only a slight decrease in signal intensity (see Figure 24 black curves). Only the region A47-G50 revealed an increase in the intensity of the measured signals (see Figure 24 highlighted in blue).

Based on these measurements of signal intensities, conclusions could be drawn about the analysed regions of the aptamer structure. Regions that did not show a significant increase or decrease in intensity with increasing LX concentration are merely considered flexible. They do not undergo any significant changes caused by the binding of the RNA to LX. Hence, the regions of loops L2 (A17-C20) and L3 (G39-C43), as well as the 3' basis of the P3 stem and part of the J1-3 junction (U64-C58), are only slightly or not at all involved in ligand binding. In contrast, regions U10-A11 and U25-U29 exhibited a distinct decrease in signal intensity. This means that these regions have changed due to the binding between the aptamer and the ligand. Thus, it can be assumed that they are significantly associated with binding to LX. Another region with a change in signal intensity was A47-G50. It appeared that the region became more flexible due to the interaction between the RNA aptamer and LX.

Further evaluation of the in-line probing experiments allowed an estimation of the binding affinity of the aptamer. In the graphical analyses of U10-A11, U25-U29 and the single nucleotide position U29, a significant change in intensity could be observed at a similar ligand concentration. The signals always decreased around the concentration of 1 μ M LX. This could be related to the already determined K_D in the low micromolar range (see 2.4.2.3 and 2.4.2.4).

2.5 Summary of the results

Target molecules: Synthetic sweetener

Using the synthetic sweeteners acesulfame K, cyclamate, saccharin and sucralose, no enrichments of target molecule-binding RNA sequences could be obtained by the Capture-SELEX method. The repeated *in vitro* selections did not yield any success either.

Target molecules: Bisphenols and monohydric alcohols

The *in vitro* selections against bisphenols A, F and S as well as 4-hydroxyacetophenone, a degradation product of bisphenol A, did not result in an enrichment of aptamers that could bind these target molecules. After several attempts to optimise the bisphenol A selection, the enrichment obtained could be attributed to the ethanol, which had to be added for the solubility of the ligand. The assumption that the elution of RNA by ethanol occurred due to non-specific interaction was proven wrong by using an enriched pool of a selection against kanamycin A. This pool showed no elution of RNA molecules in the presence of ethanol. Based on the hypothesis that binding between the aptamers and ethanol may actually have occurred, this development of the bisphenol selections was taken as an opportunity to change the direction of the project. Thus, new Capture-SELEX experiments were not conducted with the bisphenols, but with monohydric alcohols. SELEX was continued with the enriched pool of bisphenol A selection using methanol, ethanol and isopropanol as target molecules. However, this was only successful for ethanol and isopropanol. The analysis of enriched pools from these selections yielded the six potential aptamers I to VI. They were examined regarding their ability to distinguish between the two alcohols. The most specific candidate, aptamer I, was subsequently truncated based on its predicted secondary structure. Each of these shortenings was again tested for specificity, resulting in a slight improvement with the truncation B. The necessary following investigation of the aptamer was not performed due to time limitations and the progress of levofloxacin aptamer development.

Target molecule: Kanamycin A

In vitro selection against the aminoglycoside antibiotic kanamycin A resulted in significant enrichment of ligand-binding RNA molecules. These could be obtained after the introduction of different stringent increases such as ligand concentration reduction as well as counter elution. The selection was split up to introduce different conditional changes from a certain point onwards. Therefore, various increases in selection pressure on the enriched RNA sequences could be tested in parallel. Further work with enriched pools obtained will continue, but not within this study.

Target molecule: Levofloxacin

The successful *in vitro* selection against the antibiotic levofloxacin yielded an enrichment of ligand-binding aptamers. This could be investigated in detail using Next Generation Sequencing and bioinformatic analysis of the obtained data. Furthermore, the high-throughput sequencing method enabled the identification of eight different sequences, which were tested for their specificity as potential aptamers. This indicated that the aptamer LXC showed the best ability to distinguish between the target molecule and the structurally similar ciprofloxacin. The determination of its dissociation constants by isothermal titration calorimetry (ITC) revealed a binding affinity in the low

micromolar range. Based on a secondary structure prediction, the aptamer was first shortened and then investigated in more detail via a mutation study. Both were carried out with a newly established method using ITC. The results of the mutation study provided initial indications of important regions of the aptamer involved in binding to levofloxacin. Finally, in-line probing experiments were performed. These confirmed the secondary structure and allowed the precise determination of the putative binding sites. Therefore, a levofloxacin-binding aptamer was successfully developed, ready to be tested as a receptor in a biosensor.

3 Discussion

3.1 Design of the RNA library for *in vitro* selection

Since a significant part of this work involved *in vitro* selections for the development of RNA aptamers, the used sequence library and design of the Capture-SELEX method will be discussed in more detail first.

The layout of the RNA library used here comprised two randomised regions with 40 and 10 nucleotides, a fixed region between them (docking/capture sequence) and flanking constant regions at the 5' and 3' ends.⁵⁸ By splitting the randomised region, the applied library differs from the classical design. This typically features a 20-60 nt long randomised region bordered by two fixed regions.¹⁵⁹ However, the introduction of the capture sequence made it possible to use the Capture-SELEX method, as it enabled the immobilisation of RNA molecules (see 1.2.1). Furthermore, the process of separating aptamers during the selection process is specifically based on the length and position of this constant sequence. Due to its location between two randomised regions, it can increase the possibilities of RNA refolding by ligand binding. Since both randomised segments can be included in the binding process, detachment of the immobilised RNA from the capture oligonucleotide can take place more easily. Besides this breakdown of the RNA-DNA hybrid, it is also possible to induce a structural change.⁵⁸

Another important aspect to be considered upon library design is the length of the randomised regions. In order to ensure that binding to the target also leads to elution of the RNA in the Capture-SELEX, it is important that the binding event takes place in proximity to the capture sequence. This increases the probability that an interaction between aptamer and ligand will also lead to the release from immobilisation.⁵⁸ Consequently, the randomised regions should not be too large. However, the number of randomised positions also defines the diversity of the resulting sequence library. Theoretically, it can be assumed that the longer the randomised region, the greater the diversity and the probability of the presence of ligand-binding RNA molecules.¹⁵⁹ Nevertheless, in practice it is usually supposed that libraries with 10^{15} different sequences are sufficient for successful selection. Thereby the chemical synthesis of a library also has to be considered. Higher diversity makes the synthesis more complicated and often more expensive.¹⁶⁰⁻¹⁶² Since the amount of 10^{15} different sequences in a library corresponds to a number of 25 randomised positions, it can be assumed that an application of longer non-constant regions would be pointless. The resulting diversity could not be fully covered. However, not only this sequence coverage is important, but also other aspects such as a greater diversity of possible binding pockets and three-dimensional structures due to longer randomised regions.^{162, 163} In addition, several RNA aptamers showing dissociation constants in the nanomolar range have been found with libraries of 40 or more randomised sequence positions.¹⁶⁴⁻¹⁶⁶ Especially for small ligands, such as the ones used in this work, longer randomised regions offer better chances for successful selection. Evidence for this can be found by comparison with naturally occurring riboswitches. They show that larger aptamer domains provide a better fit for smaller ligands. Thus, despite the loss of diversity due to incomplete sequence coverage, it can be assumed that longer randomised regions in the library are beneficial, especially for small compounds.¹⁶⁷

A further disadvantage of too long randomised regions is the resulting increase in the total length of the sequence library. This could negatively affect experimental procedures such as the amplification of eluted RNA via reverse transcription (RT), PCR and *in vitro* transcription, since better results can be obtained with shorter heterogeneous DNA sequences. Thus, RT-PCR leads

to fewer by-products as well as higher dsDNA yields, and *in vitro* transcription shows better efficiency and fewer errors if the sequence library is not too long.¹⁵⁹ Consequently, the applied library was designed to achieve a balance between the increased occurrence of ligand-binding motifs with longer randomised regions and the maintenance of good synthesis as well as feasibility of the selection process with a shorter library design.⁵⁸

3.2 Testing and assessing the selection conditions

The selection against kanamycin A served as a control for the Capture-SELEX experiments performed in this work. The decision to use the aminoglycoside as a target molecule was based, to some extent, on its promising chemical structure and its specific activity as an antibiotic. Kanamycin A binds the rRNA of the 30S subunit of bacterial ribosomes¹³⁴ and thus provided very good prerequisites for the successful selection of RNA molecules. With seven hydroxyl and four amino groups, its molecular structure features numerous functional groups (see Figure 4). These are able to mediate an interaction with the backbone or residues of RNA via electrostatic interaction or by forming hydrogen bonds.¹⁶⁸ In particular, the functional groups of the neamine core, which is present in all aminoglycoside antibiotics and comprises ring I and II¹⁶⁹ (cf. Figure 4), play a decisive role in binding to nucleic acids. Additionally, the electrostatic interaction between the negatively charged RNA and the positively charged ligand also enables binding.¹⁶⁸

Besides this chemical suitability as a target molecule for DNA or RNA aptamers, numerous selections against this and other aminoglycosides have already been successfully performed. In 2012, Stoltenburg *et al.* found a DNA aptamer against kanamycin A using the Capture-SELEX method.⁵⁶ Two years later, Nadia Nikolaus and Beate Strehnitz selected their own DNA aptamers against kanamycin A. Some of these aptamers were able to specifically bind the ligand and others were able to bind a variety of aminoglycoside antibiotics. Thus, they demonstrated that different binding patterns between aptamers and this type of ligands were possible.¹⁷⁰ In addition to DNA aptamers that can bind kanamycin A, it was also possible to select aminoglycoside-binding RNA. For example, Susan M. Lato and her colleagues were able to select RNA aptamers against kanamycin A and lividomycin. They also called them RNA 'lectins' and wanted to determine whether different RNA structures that bind the same ligand must have a related evolutionary development.¹⁵⁰

Successful selections of RNA aptamers against other aminoglycoside antibiotics could also be accomplished. In 1995, Wallis *et al.* found RNA aptamers that were able to bind neomycin via a specific structural motif.¹⁶⁶ In 2008, Weigand *et al.* identified a neomycin-binding aptamer from the same selection that could function as a riboswitch with translational control.¹⁷¹ Another neomycin B-binding RNA aptamer was investigated in 1999 by Licong Jiang and colleagues for its binding to the ligand.¹⁷² A further example of an aminoglycoside antibiotic-binding RNA aptamer was reported by Adrien Boussebayle and colleagues in 2019. They were able to identify a highly specific paromomycin-binding aptamer via the Capture-SELEX method and *in vivo* screening, which could also be used as a riboswitch.¹⁵¹ Since the 1990s, there have also been several RNA aptamers that can also bind tobramycin. In 1995, Wang *et al.* successfully selected RNA molecules against the aminoglycoside.¹⁵² Two years later, Dinshaw J. Patel and colleagues elucidated the structure of a tobramycin-RNA complex.¹⁷³ This was also accomplished by Jiang *et al.* in 1998.¹⁷⁴

The more precise mechanisms of the binding of aminoglycosides to RNA structures have also been investigated by various researchers. It became apparent that electrostatic attraction

between the positively charged antibiotics and the negatively charged RNA plays a predominant role. Even metal ions complexed in the structure of the RNA can be displaced by aminoglycosides, which leads to inhibition of the hammerhead ribozyme, for example.¹⁷⁵⁻¹⁷⁸ Thus, it has been evident for decades that aminoglycoside antibiotics are suitable target molecules for *in vitro* selections. The test SELEX was therefore performed using kanamycin A expecting an enrichment of ligand-binding RNA molecules. Since this expectation could be met, this Capture-SELEX experiment served as a validation of the experimental set-up and a reference for other selections.

3.2.1 The number of selection rounds depends on the target molecule and increases in stringency

The literature usually describes *in vitro* selections using the SELEX method with 5 to 15 rounds until an enrichment of target molecule-binding aptamers is achieved.¹⁵⁹ These empirical data are also consistent with the selections successfully performed in this study. The selection against bisphenol A showed a first enrichment starting in round 13, which could be extended until the 16th round (see Figure 7). The test as well as the extended selection against kanamycin A showed an enrichment in the 7th round respectively (see Figure 5 and Figure 15). But the fastest enrichment of ligand-binding RNA molecules occurred in the levofloxacin selection (see Figure 16). It could already be obtained in round 6.

However, the selections were not stopped thereafter. Various increases in stringency were made, such as reducing the concentration of the ligand or introducing a counter elution. Thus, the respective selection rounds increased to more than 20 in some cases (cf. selection against levofloxacin in Figure 16). These extensions aimed to increase the affinity and specificity of the selected aptamers.

Strategies to improve the affinity of selected aptamers

An improvement of the binding affinity can be promoted by reducing the concentration of the target molecule, but theory and practice diverge here. Theoretical considerations suggest that higher ligand concentrations result in the selection of low-affinity binders. Consequently, low ligand concentrations should increase the chance of selecting high-affinity binders.¹⁵⁹ However, using mathematical modelling, it has been postulated several times that if low-affinity binders dominate over high-affinity binders in the sequence pool, a concentration reduction of the target molecule leads to the selection of low-affinity binders being favoured.¹⁷⁹⁻¹⁸¹ Thus, the aptamers with higher affinity, which are already less abundant due to this, are selected more poorly with a ligand concentration that is too low. They can even be lost via the processing steps of the eluted nucleic acids such as amplification and *in vitro* transcription.¹⁸¹ Thus, a slow reduction of the target molecule concentration over the selection process is recommended to avoid this effect.¹⁸⁰ In the Capture-SELEX experiments conducted in this work, the concentrations of the respective ligands were only reduced after an initial enrichment. However, it became apparent, especially with the ligand levofloxacin, that it took several rounds before a new enrichment could be obtained (see Figure 16). A possible alternative, which might have resulted in a faster enrichment, would therefore be a gradual reduction of the ligand concentration from round to round. Furthermore, the aptamer LXC obtained at the end of the last selection round only showed a K_D value in the low micromolar range. It was possible, however, to select an aptamer against another antibiotic exhibiting an affinity in the low nanomolar range using this method.¹⁵¹

Strategies to improve the specificity of selected aptamers

In addition to this strategy of increasing the affinity of the selected aptamers, counter selection can also be carried out to improve the specificity. It increases the chance of selecting aptamers that can distinguish between the actual ligand and a structurally very similar molecule.^{159, 182} This was successfully achieved for some of the aptamers tested against monohydric alcohols and levofloxacin (see 2.3.3.3 and 2.4.2.2). However, aptamers which did not exhibit a good specificity could still be found. Consequently, the inclusion of a counter elution does not ensure the selection of only highly specific aptamers.

In addition to counter selection, there is also the option of negative selection. This involves selecting against the components of the ligand solution required for the specific elution. This would have been a possibility to prevent an accumulation of ethanol-binding aptamers in the selection against bisphenol A (see 2.3.2). Using a negative selection step with 10% (v/v) ethanol prior to the specific elution with bisphenol A would have reduced the risk of obtaining alcohol binders.

Successful implementation of stringency increases does not provide information about the affinity or specificity of selected aptamers

The selection against kanamycin A showed that it is possible to apply numerous increases in stringency by reducing the concentration of the ligand and introducing counter selection. It is assumed that this is primarily due to the excellent suitability of the aminoglycoside as a ligand in SELEX (cf. 3.2). Thus, the selection served as a test to what extent different stringency increases can be applied. It was evident that there was a very robust enrichment of aptamers that could withstand varying selection pressures. However, it needs to be noted that these reoccurring enrichments alone do not provide any information about the specificity or affinity of the selected aptamers. Without subsequent verification of the K_D and the specificity, it can only be assumed that the stringency increases have improved the chances of finding better and more specific binding aptamers.

Based on the results obtained in this work, the experiences described in literature can be supported. The reduction of the ligand concentration does not necessarily lead to an improvement in the affinity of the selected RNA aptamers. Furthermore, counter selection with a ligand-like molecule does not necessarily ensure that aptamers examined later can distinguish this molecule from the actual ligand. These strategies of increasing the stringency only enhance the chances of improving affinity and specificity, but they do not guarantee it. Furthermore, an enrichment after reduction of the ligand concentration or implementation of a counter selection does not indicate the affinity and specificity of the selected aptamers.

3.2.2 Why is enrichment not achieved in every SELEX?

Repetition of certain rounds does not ensure an improvement of the results

In vitro selections involve very complex methods with numerous parameters that can be adjusted. These include, for example, temperatures, incubation times, number and conditions of washing steps, ligand concentration or the pH value and the composition of buffers. Even the smallest changes in the procedure can lead to altered conditions. However, these changes can be so insignificant that the experimenter does not recognise them, but they have a decisive influence on the selection. Such minor changes can lead to collapses in incipient enrichments. Thus, the repetition of individual rounds is a possible approach to eliminate such experimental deviations.

As soon as an unexpected development occurred during the selections reported in this study, rounds were repeated. If it was noticed in advance that there were inconsistencies in, for example, incubation times, temperatures or other parameters, appropriate adjustments were made to ensure a correct repetition of a round. However, if no exact cause could be identified, rounds were also performed again with the utmost care. This increased the chances that if a round yielded unexpected results, it would show improvement when repeated. However, this required knowledge of potential experimental errors. In the selections against synthetic sweeteners and bisphenols, such repetitions of selection rounds only led to limited success. This in turn showed that this approach does not necessarily result in an improvement of the selection and consequently in an enrichment of ligand-binding aptamers.

The ligand and its applied concentration influence the success of a selection

The concentration of the target molecule influences the success of a selection. Mathematical models are frequently developed and used to study the SELEX process. Many postulate that there is always an optimal ligand concentration that can lead to enrichment. In addition to the concentration of the nucleic acid library and its bulk K_D , it depends on the partitioning efficiency of the selection procedure^{179-181, 183-185} and the number of PCR cycles for pool amplification¹⁸¹. The selections performed in this work were always started with a ligand concentration of 1 mM according to the standard protocol. Adjusting this concentration in new attempts to repeat failed selections would provide the opportunity to obtain enrichments. It would be particularly interesting to determine the bulk K_D of the RNA library for the ligand to be used. This could be carried out relatively easily by isothermal titration calorimetry and provides a first indication of a suitable target molecule concentration. Since this is not yet part of the used Capture-SELEX protocol, it has not been taken into account as a possibility. However, it should be considered to always determine the bulk K_D .

RT-PCR and *in vitro* transcription can introduce bias into selections

Other parameters that can determine the success of aptamer selection are preparative processes such as RT-PCR and *in vitro* transcription.¹⁵⁹ The number of PCR cycles and the method itself play a decisive role. It should always be considered that there is never a perfect amplification of all occurring sequences and thus a bias is introduced by PCR.¹⁵⁹

Therefore, possible sources for the failure of a selection could lie primarily in the RT-PCR amplification of the eluted RNA molecules. A too pronounced influence of the PCR on the diversity of the pool can lead to a reduction in the chance of enrichment, especially in the first selection rounds. Furthermore, DNA overamplification should always be avoided and suitable PCR protocols and conditions should be chosen.¹⁵⁹

During the selections conducted in this study, care was taken to obtain a sufficient, but not overamplified, amount of DNA from the RT-PCR. In order to ensure this, gel electrophoretic separations were prepared as controls for each selection round. However, sequence-specific PCR bias could not be assessed. Thus, verifying whether sequences with low occurrence successfully passed the PCR amplification and were sufficiently amplified was not possible.

In order to reduce the general influence of PCR on selection with RNA molecules, Tsuji *et al.* used an amplification of the RNA via *in vitro* transcription using T7 as an alternative to PCR-based amplification. They did not carry out the usual amplification with RT-PCR, but only used it to transcribe the eluted RNA into cDNA for transcription. The researchers assumed that selection against a macrophage migration inhibitor factor was successful with this exclusion of PCR bias,

as other selection attempts with classical PCR amplification failed.¹⁸⁶ However, this approach would not be practical for the Capture-SELEX method used here in combination with radioactively labelled RNA molecules. During *in vitro* transcription, radioactive nucleotides are incorporated into the RNA sequences. For adequate amplification, not only the reaction volume for transcription, but also the individual components required, would have to be scaled up. In particular, the radioactively labelled nucleic acids are too expensive to use in large quantities. In addition, the bias that occurs during transcription should also be considered. Shorter cDNA is transcribed into RNA more efficiently and with fewer errors than longer cDNA^{187, 188}, which limits the length of the used RNA library. Furthermore, an imbalance in the incorporation of nucleotides can occur. Sequences that are rich in certain nucleotides may be preferentially or poorly transcribed. If ligand-binding RNA molecules contain those nucleotides that are not favoured, this leads to reduced amplification in the transcription process. This in turn can have a negative influence on the enrichment.^{159, 189}

Therefore, a bias can arise in the selection process as a result of various factors, which delays or even prevents enrichment. However, the SELEX method is not predictable in every detail, as it involves many different techniques and procedures and comprises many individual steps. Thus, the explicit identification of a specific bias in certain selection procedures would be very time-consuming and labour-intensive and may not even be achievable. Therefore, the failure of selections against synthetic sweeteners and bisphenols cannot be attributed to precise factors.

3.2.3 Suitability of small compounds as target molecules for Capture-SELEX

Selections against small molecules involve various difficulties. In the classical SELEX method, the target molecules are immobilised on a solid surface. Especially with very small ligands, this is only partially applicable or not possible at all. Furthermore, the use of a specific functional group for the immobilisation of the ligands excludes a possible interaction site with the RNA. The Capture-SELEX used in this study had the great advantage of immobilising the RNA sequences so that small compounds could be freely present in solution. Therefore, all functional groups of the ligand could interact with the aptamers without restriction during the specific elution.

Interactions between nucleic acids and small molecules determine binding

However, small molecules often only have a limited number of functional groups that are available for interaction with RNA. In addition, they lack epitopes such as those found in proteins, which play a crucial role in binding to RNA. In the interaction between small compounds and nucleic acids, the most important interactions are the formation of hydrogen bonds and stacking.¹⁹⁰ As soon as the RNA is larger than the target molecule, the tendency arises to integrate the target into its structure. This is facilitated if stacking interactions are possible.¹⁹¹ Especially ligands with extended aromatic ring systems can intercalate during stacking and place themselves between stacked base pairs. This intensifies the existing π -interactions and in turn favours binding.¹⁹⁰ Hydrogen bonds can occur between residues of the nucleic acid and certain functional groups of the ligand, such as hydroxyl or amine moieties.¹⁶⁸ The different groups serve as hydrogen donor and acceptor in a matching manner. In addition to these possible ways of forming a bond between RNA and a small molecule, electrostatic interactions are also possible through positively charged ligands and the negatively charged backbone of the RNA.¹⁶⁸

Solubility of target molecules and conditions of selection are decisive factors

In addition to the potential binding opportunities, the solubility of the target in aqueous solution is also crucial. The buffers used in the Capture-SELEX conducted in this work were all water-based and had a pH value close to neutral. Thus, the ligands to be used should have adequate solubility in the prevailing buffer conditions and the adjusted pH value.

Furthermore, attention should be paid to the context from which the target molecules originate and what application a developed aptamer should have.¹⁵⁹ If possible, both can be incorporated directly into the selection process. Disregarding certain circumstances can lead to the obtained aptamer no longer binding to the ligand in the actual application under changed conditions.¹⁵⁹

Evaluation of the small compounds used as targets for *in vitro* selections

The ligands chosen for this work were evaluated for their suitability as target molecules in the Capture-SELEX before they were used. In theory, the **synthetic sweeteners** were suitable ligands, as interactions with nucleic acids were possible via various functional groups such as hydroxyl, amine and oxo/carbonyl moieties. Furthermore, they are highly water-soluble and thus theoretically suitable ligands for *in vitro* selection. However, there are currently no known aptamers against the sweeteners that have been tested. Only in 2002 Hiroshi Saitoh and his colleagues were able to develop a DNA aptamer against the sweetener aspartame.¹⁹²

Antibiotics are frequently applied ligands for the *in vitro* selection of aptamers. The following table shows examples of DNA or RNA aptamers that have been successfully selected against different antibiotics (Table 3).

Table 3 Summary of examples of antibiotic-binding aptamers

Antibiotics class	Ligand	Nucleic acid ¹	K _D range ²	Reference
β-lactam	ampicillin	DNA	nM	193
	penicillin G	DNA	nM	194
aminoglycosides	neomycin	RNA	nM	166
	tobramycin	RNA	μM	152
	kanamycin	RNA/DNA	μM/nM	56, 150
	paromomycin	RNA	nM	151
fluoroquinolones	danofloxacin	RNA	nM	195
	ofloxacin	DNA	nM	196
	ciprofloxacin	RNA	nM	197
tetracyclines	oxytetracycline	DNA	nM	198, 199
	tetracycline	RNA	μM	165
	chloramphenicol	DNA	μM	200

¹ Indication of whether the aptamer is DNA or RNA

² Concentration range of the dissociation constant; micromolar range (μM) or nanomolar range (nM)

This represents only a very small collection of aptamers against antibiotics. Nevertheless, it reveals that DNA or RNA aptamers have already been selected for many different classes of antibiotics and their individual members. Especially within the class of aminoglycosides, numerous aptamers have already been found. Since aptamers had already been developed for the structurally very similar ciprofloxacin^{201, 202} and other fluoroquinolone antibiotics (see Table 3), it was speculated that a selection against levofloxacin could also be successful. The aromatic ring system of the fluoroquinolone has the potential to intercalate into the RNA by participating in the stacking of base pairs.¹⁹⁰ The results obtained showed that levofloxacin could be successfully applied as a ligand in an *in vitro* selection.

The **bisphenols** have some properties that probably make them suitable ligands. In addition to functional groups for hydrogen bonding, they have aromatic rings for stacking interactions. However, they are not as soluble in water as the previous ligands. In particular, bisphenol A had to be mixed with 10% (v/v) ethanol at a lower concentration than the 1 mM usually used to be soluble in aqueous solution. None of the selections carried out yielded an enrichment of target-binding RNA aptamers. An enrichment was only obtained in the bisphenol A selection. Unfortunately, this was specific to ethanol. However, literature indicates that bisphenol A-binding aptamers are already used in biosensors.^{203, 204} These biosensors use the DNA aptamers selected by Jo *et al.* in 2011. One of these aptamers exhibits an affinity in the nanomolar range as well as a high specificity, since it can bind structurally similar molecules such as bisphenol B or 4,4'-bisphenol, only with a significantly lower affinity.²⁰⁵ Consequently, a successful selection against this target is possible.

3.2.4 Assessing the elution of RNA molecules by monohydric alcohols

The enrichment achieved in the bisphenol A selection was caused by ethanol present in the ligand solution. Subsequent selections with methanol, ethanol and isopropanol yielded different results for the monohydric alcohols (see Figure 10). In the case of methanol, there was no increased elution with the alcohol (see Figure 10A). This might be attributed to the very small molecular size of the ligand. Methanol is the simplest organic alcohol and consists only of an alkyl residue with one carbon atom and one hydroxyl group. It is assumed that the RNA with the layout of the used library cannot interact sufficiently with such a small molecule to be eluted effectively. In contrast, ethanol and isopropanol are larger by one and two carbon atoms, respectively. Both alcohols led to better elutions of RNA (see Figure 10B and C). Thus, the efficiency of elution was assumed to depend on the length of the carbon chain of the alcohols. The longer the alkyl residue, the better the elution of RNA aptamers.

Precipitating and denaturing effects on nucleic acids by ethanol and isopropanol

The results obtained lead to the question of whether elution by binding of the RNA to the monohydric alcohols was actually achieved. Both alcohols can be used for the precipitation of nucleic acids. This is based on the very polar nucleic acids being highly soluble in water. Their negative charge of the backbone is shielded against positively charged ions in solution by water molecules. However, if a less polar solvent such as ethanol or isopropanol is added, this shielding is disturbed. The negatively charged nucleic acid and positively charged ions can then interact more easily and stable ionic bonds are formed. Consequently, the nucleic acid molecules become less polar and their hydrophilicity decreases. This leads to their precipitation from an aqueous solution with the addition of ethanol or isopropanol. In the case of ethanol, at least 64% (v/v) must

be present in the solution, otherwise precipitation cannot occur.²⁰⁶ However, in the selection against bisphenol A performed in this study, a maximum of 10% (v/v) was used and no precipitation of the RNA could ever be noticed.

Possible denaturation effects due to the alcohol at this low concentration are difficult to assess in terms of their influence on the immobilisation of the RNA molecules. The testing for non-specific elution with 10 % (v/v) ethanol using an enriched pool from a kanamycin A selection did not show an increased value of the elution fraction. Thus, it can be assumed that such denaturing effects do not occur with a single use of the alcohol in the elution. However, the effect of repeated use of ethanol as a ligand cannot be estimated with this experiment.

Repeated exposure of RNA aptamers to ethanol has no effect on the specific elution by this alcohol

The consideration of whether the repeated treatment of the RNA with ethanol in the specific elution could have led to detachment can be rather negated by the precipitation methods used in the Capture-SELEX protocol. For each conducted round, precipitation of the RNA with ethanol was performed after the elution and *in vitro* transcription. Both precipitations were carried out with much higher alcohol concentrations than in the specific elution. This treatment is applied to the pools of all Capture-SELEX experiments. The RNA is thus repeatedly exposed to ethanol in each selection. If repeated ethanol exposure of the RNA would lead to non-specific elution as soon as the alcohol is also present in the ligand solution, this should also have led to increased elution by 10% (v/v) ethanol with the kanamycin A pool. Therefore, it is assumed that there is indeed a kind of binding interaction between ethanol or isopropanol and RNA molecules, which causes them to be released from immobilisation.

The conducted specificity tests suggest a binding between RNA and the monohydric alcohols

This assumption of a actually binding event is additionally supported by the specificity tests carried out for potential aptamers and the truncations of one candidate (see 2.3.3.3). In this context, it is considered that if the elutions by monohydric alcohols were exclusively non-specific, there should not be any discrepancies for different RNA sequences. However, such discrepancies were evident in the specificity test of the six aptamer candidates I to VI. Besides the generally different elution rates caused by the alcohols (cf. Figure 11, candidates V and VI), some sequences showed a striking difference between ethanol and isopropanol-based elution (candidate I).

Moreover, another specificity test for truncations of aptamer I showed that various truncations of the sequence also yielded differing results (see Figure 14). This led to the assumption that different shortenings, which also resulted in strong changes in the predicted secondary structure (cf. Figure 13), also seem to influence the binding ability of the RNA to the monohydric alcohols. However, this was not the case for all truncations with significantly deviating secondary structures. For example, the truncations 5.5 and 5.10 as well as 3.15 and 3.20 only showed a difference in the folding of the closing stem. Nevertheless, they yielded significantly worse results in the elution assay than the original aptamer. Maybe the formation of the closing stem is decisive for the binding between RNA and ligand. In the parent aptamer I, besides a small stem loop, the closing stem also contains an internal loop. In contrast, the truncations 5.5, 5.10, 3.15 and 3.20 do not have this internal loop. They only exhibit stem loops at the 3' or 5' end. Thus, even the changing of a relatively small part such as the internal loop could influence the binding ability of the entire aptamer. This assumption is also supported by the results of the shortenings A, 3.5 and 3.10. All of them had an internal loop in the closing stem of the predicted secondary structure and produced comparable or even better results than aptamer I. In contrast, shortening B showed slightly poorer

results in the elution assay, which may also be due to the lack of an internal loop in the predicted structure. These results suggest that the elution behaviour of aptamer I may correlate with its secondary structure. Therefore, the assumption that actual RNA-ligand binding was responsible and that no unspecific effects were causing the elution was even more supported. However, no aptamers are known in literature that bind the monohydric alcohols used here and could therefore serve as a comparison.

A verification of the binding between an RNA aptamer and a monohydric alcohol is necessary

Whether this interaction between the aptamers and the monohydric alcohols ethanol or isopropanol really are 'classical' ligand-aptamer binding events should be assessed with further investigations. For example, ITC could be used to determine a K_D value or in-line probing to investigate the secondary structure and the binding to the ligand. However, the possible negative effects of these alcohols on nucleic acids (see above) and their physical properties have to be considered. Alcohols are more volatile than water, and isopropanol in particular changes very quickly from the liquid to the gaseous state.²⁰⁷ In addition, the dilution of ethanol or isopropanol in aqueous solutions leads to a change in temperature.²⁰⁸ These circumstances could lead to problems in the application or execution of methods like ITC or in-line probing.

The investigation of aptamer-ligand binding will therefore probably have to be carried out with many optimisation processes in the individual methods to be used. This could be very labour-intensive and time-consuming. However, it would be quite interesting if the binding between RNA and ethanol or isopropanol could be successfully proven. The benefit of such aptamers lies not only necessarily in their application in biosensor systems for the detection of alcohols, but also in their contribution to research on aptamers against small compounds. It is known that aptamers can bind small molecules, but also even smaller ligands such as heavy metal ions.^{39, 209} In the size range of molecules, only a few aptamers are known that can bind such tiny ligands, which have a similar size like isopropanol. One example would be the aptamers against ethanolamine.²¹⁰ Ethanolamine consists only of an amine and hydroxyl group linked by an aliphatic carbon chain of two carbon atoms. Ethanol as a ligand would therefore be an even smaller molecule that can be bound. This would be an interesting discovery in the field of aptamers against small molecules.

Despite the possibility of further research on an aptamer that can bind monohydric alcohols, the project was stopped at this point. The characterisation of the aptamer I was considered to be very time-consuming and labour-intensive due to the possible negative influences of alcohols as ligands in various methods. Furthermore, the project of developing a levofloxacin-binding aptamer was already at an advanced stage. Due to time constraints, a decision would have to be made in favour of one project.

3.3 Development of the levofloxacin-binding aptamer trLXC

3.3.1 The method of selection monitoring can be based on the pool affinity or its enrichment

Various methods are available for tracking and assessing the selection process. These can be based on two different aspects. First, there is the possibility of monitoring the affinity of the pool across the selection. This can be done by measuring the amount of DNA/RNA molecules that exhibit ligand binding. Examples of such monitoring methods are fluorescence labelling^{56, 211}, qPCR²¹² or, like the method used in this study, radioactive labelling of nucleic acids. Using these methods, selection is terminated when the number of eluted aptamers no longer increases¹⁵⁹, or an enrichment could be obtained by comparison to a reference value (here the last washing step). A similar approach is based on the measurement of the dissociation constant of an entire pool. This can be determined, for example, with the enzyme-linked oligonucleotide assay (ELONA)²¹³, the surface plasmon resonance (SPR) method^{214, 215} or the fluorescent dye-linked aptamer assay (FLAAS)²¹⁶. The selection is stopped as soon as the bulk K_D of the pool no longer improves or a desired value is reached.¹⁵⁹

In addition to determining the affinity of a selection pool, estimating the enrichment itself is also a possible monitoring tool. The diversity of the sequence library is assessed and selection is terminated as soon as it ceases to change.¹⁵⁹ These changes in diversity can be determined using NMR²¹⁷ or HPLC-based²¹⁸ methods, melting and remelting curve analyses²¹⁹⁻²²¹ and high-throughput sequencing (HITS)^{217, 222, 223}.

Would it have been useful to change the applied monitoring method?

All these monitoring methods would probably have no significant advantage if they had been used for the Capture-SELEX experiments carried out in this work. All of them only allow estimations of the affinity or the enrichment state of the selection pools. This is also provided by the radioactive labelling of the RNA molecules and measurement of the counts per minute for different elution fractions. Furthermore, it would be necessary to adapt the selection protocol to a new tracking method. This would require adjustments as well as re-optimisation and would therefore be time-consuming and labour-intensive.

However, the HITS method has the advantage that potential aptamer candidates could be identified at a very early stage, thus reducing the number of selection rounds.¹⁵⁹ This would not necessarily be very effective, with the procedure used here, which involves the introduction of stringency increases. Nevertheless, it is possible to influence the number of rounds of a selection with different monitoring techniques.¹⁵⁹ But there is no predictable control of the affinity of the selected aptamers¹⁵⁹, which would be more useful.

Therefore, the literature suggests that a combination of different monitoring methods should be used.²²⁴ However, this should also be reasonable for the aim of the selection, as it depends greatly on the available equipment and monetary resources.¹⁵⁹ Since the method of monitoring the selection used in this study has already achieved success and there is a well-established and published protocol^{58, 57, 59, 151}, it is assumed that a change in the method would not be necessary.

3.3.2 Evaluating the selection process and identify potential aptamers using Next Generation Sequencing

Comparison of cloning-based Sanger sequencing and Next Generation Sequencing

In the course of this work, enriched pools were analysed in two different ways. On the one hand, cloning and Sanger sequencing were used for individual enriched pools of the selections against ethanol and isopropanol (see 2.3.3.2). On the other hand, the entire selection process with the target molecule levofloxacin was evaluated using the high-throughput sequencing method of Next Generation Sequencing (NGS) (see 2.4.2.1). The former is described in literature as a traditional method of rapid and simple aptamer candidate identification, with 30-100 different cloned sequences.¹⁵⁹ This was also done in this study with 48 different clones for the pools of selections against ethanol and isopropanol respectively.

A comparison of both sequencing methods during a selection by Civit and colleagues revealed a major disadvantage of single-pool Sanger sequencing. The best binders could not be found with the Sanger sequencing approach. It was assumed that their very low abundance in the pool was responsible for this.²²⁵ Contrary results were obtained by Stoltenburg *et al.* After analysing the same enriched pool from a DNA SELEX, it was found that both methods were able to identify the best binder.²²⁶ Thus, it can be considered that the use of cloning a single pool and sequencing a limited number of clones is a kind of 'hit or miss' method. However, the Sanger sequencing has the advantages of being relatively inexpensive, fast and straightforward compared to high-throughput sequencing methods.¹⁵⁹

NGS analyses provided insights into the selection process on sequence level

Despite the higher costs, the NGS used for the development of a levofloxacin-binding aptamer was of great benefit. It enabled the analysis of the entire selection process as well as the assessment of the enrichment and diversity of each individual round (see 2.4.2.1). However, due to the large amount of information obtained by NGS, it was only possible to analyse the data with the help of bioinformatics. This could not be done by myself and was therefore accomplished by Philipp Fröhlich (Department of Electrical Engineering and Information Technology, TU Darmstadt, Self-Organizing Systems, 64283 Darmstadt, Germany). Therefore, the method of NGS-based evaluation of an entire selection and identification of potential aptamers requires extensive bioinformatics expertise.¹⁵⁹ The analyses of the sequencing data prepared by Philipp Fröhlich were based on various evaluation approaches. Some of them revealed that the results of the chosen method of selection monitoring was in line with the processes in the RNA pool and the enrichment starting in the 5th round. Thus, the monitoring can be considered to be quite suitable for this selection against levofloxacin.

Tracking the 25 most abundant sequences from the last round over the entire selection process showed that these sequences could be found already at a very early stage (Figure 17B). From the 9th round onwards, they accounted for almost half of the sequences found. This is consistent with the results of Schütze *et al.* In their study, the best binders from later rounds were tracked across the entire selection. This revealed that these sequences could be found in early rounds. However, they showed only a low abundance at that moment.²²³

NGS examination of the initial sequence library revealed reduced diversity

Based on the sequencing of the start RNA library used here and the inclusion of this in certain bioinformatic evaluations (as round '0'), it became apparent that this library did not have the desired diversity. In particular, the graphs of the percentage of total sequence amount and the absolute number of orphans (Figure 17C and D) as well as the cumulative distribution function of the reads per million (CDF RPM, Figure 17E) showed that the sequence composition of the start library was not perfectly distributed. The ideal condition for the library is considered to be an equal frequency of all sequences. However, all three graphs indicate with the round '0' that not all sequences had the same abundance. On the one hand, this could be due to the preparation of the start library. A bias could have been introduced by the PCR-based amplification of the DNA template pool and the subsequent *in vitro* transcription. This has already been discussed in detail in section 3.2.2 and could also apply to the preparation of the RNA library used to start the selection. Furthermore, the chosen method of NGS and the reads carried out for each round also limit the precise analysis. For each sample submitted, only a maximum of 50,000 reads was guaranteed by the service provider for the NGS (GENEWIZ, Leipzig: Amplicon EZ Service). Furthermore, a quality control has to be carried out on the sequences obtained. This excludes sequences that are sequenced with errors and those that are too long or too short. This also leads to a reduction in the possible number of reads.

With the 50 randomised positions (N40 + N10) of the library used for the selections in this work, theoretically more than 10^{30} different sequences are possible. On the one hand, this is not completely covered by the use of only 10^{15} sequences for the first selection round (see 3.1), and on the other hand, the existence of all possible sequences cannot be proven with the sequencing reads of a maximum of 50,000 carried out in NGS. It is quite likely that, despite an ideal composition of a library, all sequences occur more than once. Therefore, even taking a small portion of the library for selection or NGS can lead to an imbalance. However, the probability that all sequences have the same frequency is relatively low due to the bias introduced by library preparation. Moreover, if only a small fraction of the total library volume is taken, the probability of a perfect distribution decreases even further. Thus, the investigation of the entire levofloxacin selection also enabled the discovery of a possible bias in the starting library.

Nevertheless, the enrichment process and the associated reduction in diversity could be successfully tracked by determining the entropy (Figure 17F) and compared with the previously documented course of selection (Figure 17G). In addition, the NGS enabled the identification of various potential sequences, which led to the preliminary levofloxacin-binding aptamer LXC by testing their specificity.

3.3.3 Characterising the aptamer trLXC enabled secondary structure elucidation and provided insights into aptamer-ligand binding

Not all established methods are applicable for the characterisation of an RNA aptamer

The chosen characterisation methods for the aptamers LXC and trLXC included isothermal titration calorimetry (ITC), a web tool driven secondary structure prediction, a newly established ITC-based mutation study as well as in-line probing. After testing the specificity of eight potential aptamers, fluorescence titration was performed prior to the investigations presented in the results section (data not shown). The fluorescence of levofloxacin²²⁷ was to be exploited. It was expected that the fluorescence emission spectrum of the ligand would be attenuated or enhanced by binding

with one of the potential aptamers. This has already been done successfully for other antibiotic ligands^{202, 228}. However, these expectations were not fulfilled. For example, this can be attributed to changed experimental conditions. Under these new conditions, binding between RNA and the target molecule may no longer occur.¹⁵⁹ However, the same conditions as in the Capture-SELEX were used in the fluorescence titration experiments carried out, which excludes this explanation. Furthermore, it is also possible that two different sequences have to work together for binding to the ligand.¹⁵⁹ In the case of the ligand levofloxacin, which is very small compared to an RNA aptamer, this is considered unlikely. It seemed more plausible that the binding of the aptamer candidates to the antibiotic did not measurably influence its fluorescence emissions spectrum. This demonstrated that not every characterisation method is suitable for the investigation of an aptamer. Supporting this, the study by Maureen McKeague and her colleagues showed that a correct investigation of aptamer-target binding should be based on several different methods of characterisation.²²⁹ Thus, misleading conclusions due to inappropriate binding studies can be avoided.

The choice of a candidate from several potential aptamers can be based on affinity or specificity

In addition to this first unsuccessful attempt to investigate the binding between potential aptamers and the ligand, further characterisation studies were subsequently carried out. This included a traditional determination of the dissociation constant (K_D) for the aptamer candidate LXC using ITC. This candidate was chosen for further evaluation due to its ability to distinguish very well between the target molecule and the structurally very similar ciprofloxacin. This choice of the most specific candidate already considered the later desired application as a receptor in a biosensor, for which a high specificity is advantageous. Furthermore, this intended use of the aptamer caused the truncation of the sequence and the development of the final trLXC aptamer. This shortening of the full-length LXC aptamer was again achieved by using ITC experiments to determine the minimum sequence length necessary to allow binding to the ligand. The subsequent mutation study, which also relied on ITC, was designed and established to rapidly investigate a variety of different mutations of the aptamer sequence. This allowed initial information on the aptamer-ligand binding to be collected through the preservation or loss of the binding ability due to the mutation applied. The determination of a K_D value, which was also possible with this method, allows the conclusion that the final aptamer trLXC also showed a binding affinity in the low micromolar range. A direct comparison with other levofloxacin-binding DNA or RNA is not possible due to the lack of such aptamers in the literature. However, aptamers against other fluoroquinolones show lower K_D values in the nanomolar range.^{230, 197, 196} However, since the choice of a suitable candidate was not based on the best affinity, but on the best ability to distinguish between the ligand and a structurally similar molecule, it was not unexpected that there was not such low K_D value. However, it would still be an option to re-examine potential candidates and then use their affinity as a measure of evaluation. Furthermore, it would also be possible to consider both affinity and specificity and identify an aptamer with the best compromise between the two parameters.

The characteristics of an aptamer should be verified by different methods

In order to validate the first indications of important areas of the aptamer for binding to the ligand, a further characterisation method aimed at this was necessary. This was consistent with McKeague's research and recommendation to use multiple methods with the same outcome.²²⁹ The method of in-line probing chosen for this purpose additionally allowed the confirmation of the secondary structure that had initially only been predicted. However, by using a concentration

gradient of levofloxacin, the desired investigation of sequence regions that change due to ligand binding was also possible. Therefore, different in-line probing experiments confirmed the secondary structure as well as the regions of the RNA aptamer that are likely to be involved in or change due to ligand binding.

Comparing the secondary structure and ligand binding sites of trLXC with two other fluoroquinolone-binding RNA aptamers, different observations can be made. Initially, it is evident that the levofloxacin-binding aptamer exhibits a significantly shorter sequence than the ciprofloxacin-binding aptamer R10K6¹⁹⁷ or the CFX riboswitch²⁰¹. Both ciprofloxacin-binding RNA molecules comprise more than 100 nt^{197, 201}, whereas trLXC is only 73 nt long (see Figure 24). Furthermore, the secondary structure of the aptamer against levofloxacin is considerably simpler than that of the CFX riboswitch, which features a pseudoknot.²⁰¹ Consequently, the binding sites for their ligands also differ significantly from each other. In the riboswitch, the nucleotides that mediate binding with ciprofloxacin are mainly located within the pseudoknot structure.²⁰¹ In contrast, some common features can be discovered with the aptamer R10K6 against ciprofloxacin. In addition to a relatively similar structure consisting primarily of stems, loops and junctions, the binding sites are at comparable locations. In both aptamers, several nucleotides involved in ligand binding are located centrally in the aptamer at the base of a small stem loop (see Figure 24).¹⁹⁷ Therefore, considerably more parallels in the structure and binding sites of the trLXC aptamer against levofloxacin can be identified for an aptamer than for a riboswitch binding to ciprofloxacin.

Further investigations of the structure of the aptamer trLXC developed would be possible and necessary. The tertiary structure would have to be elucidated using biophysical methods or chemical probing. A region of the aptamer that is altered by the binding of levofloxacin cannot be clearly attributed to participate in the binding to the ligand. An analysis of the tertiary structure could provide further information.

3.3.4 Using the levofloxacin-binding aptamer as a receptor in a biosensor

The RNA aptamer trLXC developed in this study is suitable for the application as a receptor in a biosensor due to its high specificity. Furthermore, the presence of the capture sequence enables the integration of the aptamer into a modular biosensor system. This modularity is made possible by using the same capture sequence in different aptamers. A system like this has already been developed in the form of a lateral flow assay (LFA) by Leon Kraus and colleagues (Department of Biology, TU Darmstadt, Synthetic RNA biology, 64287 Darmstadt, Germany). The implementation of the trLXC aptamer as a bioreceptor in the LFA was successfully accomplished and is to be published soon with the publication of the levofloxacin aptamer developed here. The specificity of the aptamer was tested and could also be demonstrated in the biosensor system. However, the use of trLXC as a bioreceptor in a LFA can only serve as a proof of concept, as the binding affinity achieved by the aptamer in the low micromolar range would not be sufficient to detect traces of levofloxacin in environmental samples. The concentrations of the fluoroquinolone are mostly in the picomolar to nanomolar range for surface water or wastewater.⁶ However, it would be possible to perform a new screening for potential aptamer candidates using affinity rather than specificity as a criterion. Since aptamers that bind other representatives of this antibiotic class have already shown better K_D values in the low nanomolar range^{230, 197, 196}, it is assumed that the selection against levofloxacin conducted in this study could also include aptamers with better affinity.

4 Material

Table 4 Summary of used chemicals as well as purchased solutions and their sources of supply

Chemicals and purchased solutions	Source
4-Hydroxyacetophenone	Sigma-Aldrich (Merck, Darmstadt)
Acesulfame K	Sigma-Aldrich (Merck, Darmstadt)
Acetic acid	Carl Roth, Karlsruhe
Agar	Thermo Fisher Scientific, USA
Agarose	VWR, Darmstadt
Ampicillin	Carl Roth, Karlsruhe
APS	Carl Roth, Karlsruhe
ATP	Sigma-Aldrich (Merck, Darmstadt)
Bisphenol A	Sigma-Aldrich (Merck, Darmstadt)
Bisphenol F	Sigma-Aldrich (Merck, Darmstadt)
Bisphenol S	Sigma-Aldrich (Merck, Darmstadt)
Boric acid	Carl Roth, Karlsruhe
Bromophenol blue (sodium salt)	Carl Roth, Karlsruhe
Chloroform	Carl Roth, Karlsruhe
Ciprofloxacin	Sigma-Aldrich (Merck, Darmstadt)
Cyclamate	Sigma-Aldrich (Merck, Darmstadt)
Deionised formamide	Carl Roth, Karlsruhe
DMSO	Carl Roth, Karlsruhe
DTT	Carl Roth, Karlsruhe
EDTA	Carl Roth, Karlsruhe
Ethanol	VWR, Darmstadt
Glycerine	Carl Roth, Karlsruhe
GlycoBlue™ Coprecipitant	Thermo Fisher Scientific, USA
HCl	Carl Roth, Karlsruhe
HEPES	Carl Roth, Karlsruhe
Hydrophilic Streptavidin Magnetic Beads	New England Biolabs, Frankfurt am Main
Isoamyl alcohol	Carl Roth, Karlsruhe
Isopropanol	Sigma-Aldrich (Merck, Darmstadt)
K ₂ HPO ₄	Carl Roth, Karlsruhe
Kanamycin A	Carl Roth, Karlsruhe
KCl	Carl Roth, Karlsruhe
KH ₂ PO ₄	Carl Roth, Karlsruhe
Levofloxacin	Sigma-Aldrich (Merck, Darmstadt)
Methanol	Carl Roth, Karlsruhe
Mg(Ac) ₂ · 4 H ₂ O	Carl Roth, Karlsruhe
MgCl ₂ · 6 H ₂ O	Carl Roth, Karlsruhe

MATERIAL

Na ₂ CO ₃	Carl Roth, Karlsruhe
NaAc	Carl Roth, Karlsruhe
NaCl	Carl Roth, Karlsruhe
Na-EDTA (disodium salt dihydrate)	Carl Roth, Karlsruhe
ROTI®Aqua-P/C/I for RNA extraction	Carl Roth, Karlsruhe
ROTI®Phenol for extraction of nucleic acids	Carl Roth, Karlsruhe
ROTIPHORESE®Gel 40 (19:1)	Carl Roth, Karlsruhe
ROTISZINT®Filter (scintillation solution)	Carl Roth, Karlsruhe
Saccharin	Sigma-Aldrich (Merck, Darmstadt)
Spermidine	Carl Roth, Karlsruhe
Sucralose	Sigma-Aldrich (Merck, Darmstadt)
TEMED	Carl Roth, Karlsruhe
Tobramycin	Sigma-Aldrich (Merck, Darmstadt)
Tris	Carl Roth, Karlsruhe
Trisodium citrate dihydrat	Carl Roth, Karlsruhe
Triton X-100	Carl Roth, Karlsruhe
Tryptone	Thermo Fisher Scientific, USA
Tween-20	Carl Roth, Karlsruhe
Ultrapure water	self-made
Urea	Carl Roth, Karlsruhe
Yeast extract	Thermo Fisher Scientific, USA

Table 5 Summary of used enzymes as well as commercial buffers and their sources of supply

Enzymes and commercial buffers	Source
10X Kination buffer	Roche, CH
10X T4 ligase buffer	New England Biolabs, Frankfurt am Main
10X Taq Thermopol buffer	New England Biolabs, Frankfurt am Main
5X Q5 reaction buffer	New England Biolabs, Frankfurt am Main
AP buffer	Roche, CH
CIP (alkaline phosphatase, calf intestine)	Roche, CH
EcoRI-HF	New England Biolabs, Frankfurt am Main
HindIII-HF	New England Biolabs, Frankfurt am Main
NcoI-HF	New England Biolabs, Frankfurt am Main
Polynucleotide kinase	Roche, CH
Q5 DNA polymerase	New England Biolabs, Frankfurt am Main
rCutSmart buffer	New England Biolabs, Frankfurt am Main
RNase inhibitor	Molox, Berlin
RNase T1	Thermo Fisher Scientific, USA
Superscript II reverse transcriptase	Thermo Fisher Scientific, USA
T4 ligase	New England Biolabs, Frankfurt am Main

T7 RNA polymerase	self-made
Taq DNA polymerase	self-made
TURBO™ DNase	Thermo Fisher Scientific, USA

Table 6 Summary of used Nucleotides as well as size standard and their sources of supply

Nucleotides and Ladders	Source
α - ³² P-ATP (6000 Ci/mmol, 10 mCi/mL)	HARTMANN ANALYTIC, Braunschweig
α - ³² P-UTP (6000 Ci/mmol, 10 mCi/mL)	HARTMANN ANALYTIC, Braunschweig
γ - ³² P-ATP (6000 Ci/mmol, 10 mCi/mL)	HARTMANN ANALYTIC, Braunschweig
1 kb DNA ladder	Thermo Fisher Scientific, USA
dNTP	Thermo Fisher Scientific, USA
NTP	Sigma-Aldrich (Merck, Darmstadt)
RNA ladder	self-made
Ultra low range DNA ladder	Thermo Fisher Scientific, USA

Table 7 List of all used DNA oligonucleotides purchased desalted from Sigma-Aldrich (Merck, Darmstadt)

Primer	
pool_template	5'-AGTGAAAAGTTCTTCTCCTTTGCTAGCCATTTTNNNNNNNNNNNTAG AAGCCAGTAGNN NNNNNACCGGTAGATCTAGCTTGGAGTTG CCC-3'
pool_fwd	5'-CCAAGTAATACGACTCACTATAGGGCAACTCCAAGCTAGATCTAC CGGT-3'
pool_rev	5'-AGTGAAAAGTTCTTCTCCTTTGCTAGCCATTTT-3'
biotinylated capture- oligonucleotide	5'-TAGAAGCCAGTAG-biotin TEG linker-3'
pHDV_Preprep_fwd	5'-CGATACGAATTCTAATACGACTCACTATAGGGCAAC-3'
pHDV_Preprep_rev	5'-ACATTGCCATGGCCGGCAGTGAAAAGTTCTTCTCCT-3'
hdv_seq	5'-CACTTTATGCTTCCGGCTCG-3'
DNA templates	
I	5'-GGGCAACTCCAAGCTAGATCTACCGGTGATTTAGTAAGCACACG GTAATGCGACTGGGCAAGTCTTCTACTGGCTTCTACAGCGCCCTTAA AATGGCTAGCAAAGGAGAAGAAGTCTTTC-3'
II	5'-GGGCAACTCCAAGCTAGATCTACCGGTACCAAATGCATCGTGGT GCCGGTACCTTTTACGGGAGTCTTCTACTGGCTTCTACTGGACTGGAA AATGGCTAGCAAAGGAGAAGAAGTCTTTC-3'
III	5'-GGGCAACTCCAAGCTAGATCTACCGGTAGAAATCAATAACTCCCG GTACCAACCGACAAGTCTTCTACTACTGGCTTCTAGGCAATGGTTAA AATGGCTAGCAAAGGAGAAGAAGTCTTTC-3'
IV	5'-GGGCAACTCCAAGCTAGATCTACCGGTGACAAATGCTTGCACA ACCCCGCTGCCAGAGCAGTCTTCTACTGGCTTCTACTGGGGCGGCA AATGGCTAGCAAAGGAGAAGAAGTCTTTC-3'
V	5'-GGGCAACTCCAAGCTAGATCTACCGGTAACGGTCCTTCGTAGGA TACCTACGTGCATGTGACGTCTTCTACTGGCTTCTATGACACGAGCA AATGGCTAGCAAAGGAGAAGAAGTCTTTC-3'

MATERIAL

VI	5'-GGGCAACTCCAAGCTAGATCTACCGGTACGTGAACGATAGTACA GTGTAGATAAACGTCGAGGTCTTCTACTGGCTTCTACCATTGTGACA AAATGGCTAGCAAAGGAGAAGAACTTTTC-3'
LXA1	5'-GGGCAACTCCAAGCTAGATCTACCGGTCTTTTTCAGGCGGCTTAA AAACCAGGAAAGGTGGAGACTTCTACTGGCTTCTATCCAGCCGGTA AAATGGCTAGCAAAGGAGAAGAACTTTTC-3'
LXA2	5'-GGGCAACTCCAAGCTAGATCTACCGGTCTTTTTCTGGCGGCTTAA AAACCAGGAAAGGTGGAGACTTCTACTGGCTTCTATCCAGCCGGTA AAATGGCTAGCAAAGGAGAAGAACTTTTC-3'
LXB1	5'-GGGCAACTCCAAGCTAGATCTACCGGTGTGTAACGGAAGCACAA AGGTGCCTCCTACAGCAGGTCTTCTACTGGCTTCTACTGATACACTA AAATGGCTAGCAAAGGAGAAGAACTTTTC-3'
LXB2	5'-GGGCAACTCCAAGCTAGATCTACCGGTGTGTAACGGAAGCACAA AGGTGCCTCCTACAGCAGGTCTTCTACTGGCTTCTACTGATACGCTA AAATGGCTAGCAAAGGAGAAGAACTTTTC-3'
LXC	5'-GGGCAACTCCAAGCTAGATCTACCGGTTTGGGTAGTGCGATTTCG CACTGAATGCCGCGTAGGCTTCGCTACTGGCTTCTACTACGTACCC AAAATGGCTAGCAAAGGAGAAGAACTTTTC-3'
LXD	5'-GGGCAACTCCAAGCTAGATCTACCGGTCGTAGTGGACCTGTTTA GGTTTGCATACGTTAGATGTCTTCTACTGGCTTCTAAATCGAACCGA AAATGGCTAGCAAAGGAGAAGAACTTTTC-3'
LXE	5'-GGGCAACTCCAAGCTAGATCTACCGGTCGTAGTGGACCTGTTTA GGTTTGCATACGTTAGATGTCTTCTACTGGCTTCTAAATCGAACCGA AAATGGCTAGCAAAGGAGAAGAACTTTTC-3'
LXF	5'-GGGCAACTCCAAGCTAGATCTACCGGTGCAGGTCTGGGAACCTCG TTCCCGGCTCCAGCTGGATTCTTCTACTGGCTTCTAGCCCGACCGG AAAATGGCTAGCAAAGGAGAAGAACTTTTC-3'
DNA template LXC for pHDV insert preparation	5'-CCAAGTAATACGACTCACTATAGGGCAACTCCAAGCTAGATCTAC CGGTTTGGGTAGTGCGATTTCGCACTGAATGCCGCGTAGGCTTCGCT ACTGGCTTCTACTACGTACCCAAAATGGCTAGCAAAGGAGAAGAAC TTTTC-3'
I_A_fwd	5'-CCAAGTAATACGACTCACTATAGGGCTCCAAGCTAGATCTACCGG TGTATTTAGTAAGCACACGGTAATGCGAC-3'
I_A_rev	5'-CTCCTTTGCTAGCCATTTTAAGGGCGCTGTAGAAGCCAGTAGAAG ACTTGCCAGTCGCATTACCGTGTGCTTA-3'
I_B_fwd	5'-CCAAGTAATACGACTCACTATAGGGCTAGATCTACCGGTGATTT AGTAAGCACACGGTAATGCGAC-3'
I_B_rev	5'-GCTAGCCATTTTAAGGGCGCTGTAGAAGCCAGTAGAAGACTTGC CCAGTCGCATTACCGTGTGCTTA-3'
I_C_fwd	5'-CCAAGTAATACGACTCACTATAGGGTACCGGTGATTTAGTAAGC ACACGGTAATGCGACT-3'
I_C_rev	5'-CCATTTTAAGGGCGCTGTAGAAGCCAGTAGAAGACTTGCCAGTC GCATTACCGTGTGCTT-3'
I_3_fwd	5'-CCAAGTAATACGACTCACTATAGGGCAACTCCAAGCTAGAT CTA-3'
I_3.5_rev	5'-AAAGTTCTTCTCCTTTGCTAGCCATTTTAAGGGCGCTGTAGAAGCC AGTAGAAGACTTGCCAGTCGCATTACCGTGTGCTTACTAAATACAC CGGTAGATCTAGCTTGGAGTTGC-3'
I_3.10_rev	5'-TCTTCTCCTTTGCTAGCCATTTTAAGGGCGCTGTAGAAGCCAGTA GAAGACTTGCCAGTCGCATTACCGTGTGCTTACTAAATACACCGGT AGATCTAGCTTGGAGTTGC-3'

I_3.15_rev	5'-TCCTTTGCTAGCCATTTTAAGGGCGCTGTAGAAGCCAGTAGAAGA CTTGCCCAGTCGCATTACCGTGTGCTTACTAAATACACCCGGTAGATC TAGCTTGGAGTTGC-3'
I_3.20_rev	5'-TGCTAGCCATTTTAAGGGCGCTGTAGAAGCCAGTAGAAGACTTGC CCAGTCGCATTACCGTGTGCTTACTAAATACACCCGGTAGATCTAGCT TGGAGTTGC-3'
I_3.25_rev	5'-GCCATTTTAAGGGCGCTGTAGAAGCCAGTAGAAGACTTGCCCAG TCGCATTACCGTGTGCTTACTAAATACACCCGGTAGATCTAGCTTGGGA GTTGC-3'
I_5_rev	5'-AGTGAAAAGTTCTTCTCCTTTGCTAGCCATTTTAAGGGCGCTGTAG AAGC-3'
I_5.5_fwd	5'-CCAAGTAATACGACTCACTATAGGGCCAAGCTAGATCTACCGGT GTATTTAGTAAGCACACGGTAATGCGACTGGGCAAGTCTTCTACTGG CTTCTACAGCGCCCTTAAA-3'
I_5.10_fwd	5'-CCAAGTAATACGACTCACTATAGGGCTAGATCTACCGGTGATTT AGTAAGCACACGGTAATGCGACTGGGCAAGTCTTCTACTGGCTTCTA CAGCGCCCTTAAA-3'
I_5.15_fwd	5'-CCAAGTAATACGACTCACTATAGGGTCTACCGGTGATTTAGTAA GCACACGGTAATGCGACTGGGCAAGTCTTCTACTGGCTTCTACAGC GCCCTTAAA-3'
I_5.20_fwd	5'-CCAAGTAATACGACTCACTATAGGGCGGTGATTTAGTAAGCACA CGGTAATGCGACTGGGCAAGTCTTCTACTGGCTTCTACAGCGCCCT TAAA-3'
I_5.25_fwd	5'-CCAAGTAATACGACTCACTATAGGGTATTTAGTAAGCACACGGTA ATGCGACTGGGCAAGTCTTCTACTGGCTTCTACAGCGCCCTT AAA-3'
LXC_76_fwd	5'-CCAAGTAATACGACTCACTATAGGGCGGTTTGGGTAGTGC-3'
LXC_76_rev	5'-CATTTTGGGTACGTAGTAGAAGCCAGTAGCGAAGCCTACGCGGC ATTCAGTGCGAATCGCACTACCCAACCCCTA-3'
LXC_68_fwd	5'-CCAAGTAATACGACTCACTATAGGGTTGGGTAGTGCGATT-3'
LXC_68_rev	5'-TTGGGTACGTAGTAGAAGCCAGTAGCGAAGCCTACGCGGCATTC AGTGCGAATCGCACTACCCAACCCCTA-3'
trLXC_fwd	5'-CCAAGTAATACGACTCACTATAGGGTTTGGGTAGTGCGAT-3'
trLXC_rev	5'-GGGTTTGGGTACGTAGTAGAAGCCAGTAGCGAAGCCTACGCGGC ATTCAGTGCGAATCGCACTACCCAACCCCTA-3'
trLXC_M1_fwd	5'-CCAAGTAATACGACTCACTATAGGGTATGGGTAGTGCGAT-3'
trLXC_M1_rev	5'-GGGTATGGGTACGTAGTAGAAGCCAGTAGCGAAGCCTACGCGGC ATTCAGTGCGAATCGCACTACCCATACCCTA-3'
trLXC_M2_fwd	5'-CCAAGTAATACGACTCACTATAGGGTTTGCGTAGTGCGAT-3'
trLXC_M2_rev	5'-GGGTTTGCGTACGTAGTAGAAGCCAGTAGCGAAGCCTACGCGGC ATTCAGTGCGAATCGCACTACGCAAACCCCTA-3'
trLXC_M3_fwd	5'-CCAAGTAATACGACTCACTATAGGGTTTGGGTAGTGCGAT-3'
trLXC_M3_rev	5'-GGGTTTGGGTACGTAGTAGAAGCCAGTAGCGAAGCCTACGCGGC TTCAGTGCGAATCGCACTACCCAACCCCTA-3'
trLXC_M4_fwd	5'-CCAAGTAATACGACTCACTATAGGGTTTGGGTAGTGCGAT-3'
trLXC_M4_rev	5'-GGGTTTGGGTACGTAGTAGAAGCCAGTAGCGAAGCCTACCGGCA TTCAGTGCGAATCGCACTACCCAACCCCTA-3'
trLXC_M5_fwd	5'-CCAAGTAATACGACTCACTATAGGGTTTGGGTAGTTTGCCTGAA TGCCGCGTAGGCTTCGCTACTGGCTTCTACTACGTACCCAACCC-3'

MATERIAL

trLXC_M5_rev	5'-GGGTTTGGGTACGTAGTAGAAGCCAGTAGCGAAGCCTACGCGGC ATTCAGTGCAAACCTACCCAAACCCTATAGTGAGTCGTATTACTTGG-3'
trLXC_M6_fwd	5'-CCAAGTAATACGACTCACTATAGGGTTTGGGTAGCGATT-3'
trLXC_M6_rev	5'-GGGTTTGGGTACGTAGTAGAAGCCAGTAGCGAAGCCTACGCGGC ATTCAGCGAATCGCTACCCAAACCCTA-3'
trLXC_M7_fwd	5'-CCAAGTAATACGACTCACTATAGGGTTTGGGTATGAATGCCGCGT AGGCTTCGCTACTGGCTTCTACTACGTACCCAAACCC-3'
trLXC_M7_rev	5'-GGGTTTGGGTACGTAGTAGAAGCCAGTAGCGAAGCCTACGCGGC ATTCATACCCAAACCCTATAGTGAGTCGTATTACTTGG-3'
trLXC_M8_fwd	5'-CCAAGTAATACGACTCACTATAGGGTTTGGGTAGTCGATT-3'
trLXC_M8_rev	5'-GGGTTTGGGTACGTAGTAGAAGCCAGTAGCGAAGCCTACGCGGC ATTCAGTCGAATCGACTACCCAAACCCTA-3'
trLXC_M9_fwd	5'-CCAAGTAATACGACTCACTATAGGGTTTGGGTAGTCGTTTCG-3'
trLXC_M9_rev	5'-GGGTTTGGGTACGTAGTAGAAGCCAGTAGCGAAGCCTACGCGGC ATTCAGTCGCGAACGACTACCCAAACCCTA-3'
trLXC_M10_fwd	5'-CCAAGTAATACGACTCACTATAGGGTTTGGGTAGTGCGATTTCGCA CTGAATGCCGCGTAGTTCGCTACTGGCTTCTACTACGTACCCAAAC CC-3'
trLXC_M10_rev	5'-GGGTTTGGGTACGTAGTAGAAGCCAGTAGCGAACTACGCGGCAT TCAGTGCGAATCGCACTACCCAAACCCTATAGTGAGTCGTATTACTT GG-3'
trLXC_M11_fwd	5'-CCAAGTAATACGACTCACTATAGGGTTTGGGTAGTGCGATTTCGCA CTGAATGCTTCGGCTTCTACTACGTACCCAAACCC-3'
trLXC_M11_rev	5'-GGGTTTGGGTACGTAGTAGAAGCCGAAGCATTTCAGTGCGAATCG CACTACCCAAACCCTATAGTGAGTCGTATTACTTGG-3'
trLXC_M12_fwd	5'-CCAAGTAATACGACTCACTATAGGGTTTGGGTGAATGCCG-3'
trLXC_M12_rev	5'-GGGTTTGGGTACGTAGTAGAAGCCAGTAGCGAAGCCTACGCGGC ATTCACCCAAACCCTA-3'
trLXC_M13_fwd	5'-CCAAGTAATACGACTCACTATAGGGTTTGGGTAGAATGCC-3'
trLXC_M13_rev	5'-GGGTTTGGGTACGTAGTAGAAGCCAGTAGCGAAGCCTACGCGGC ATTCTACCCAAACCCTA-3'
trLXC_M14_fwd	5'-CCAAGTAATACGACTCACTATAGGGCGCACTGAATGCCGC-3'
trLXC_M14_rev	5'-GGGCGCACTATACGTAGTAGAAGCCAGTAGCGAAGCCTACGCG GCATTTCAGTGCGCCCTA-3'
trLXC_inline_fwd	5'-CCAAGTAATACGACTCACTATAGGGCAACAACAACAACAAG GGTTTGGGTAGTGCGATTTCGCACTGAATGCCGCGTAGGCTTCGCTA CTGGCTTCTACTACGTACCCAAACCC-3'
trLXC_inline_rev	5'-GGGTTTGGGTACGTAGTAGAAGCCAGTAGCGAAGCCTACGCGGC ATTCAGTGCGAATCGCACTACCCAAACCCTTGTGTTGTTGTTGTTG CCCTATAGTGAGTCGTATTACTTGG-3'

Table 8 Summary of used bacterial strains and their sources of supply

Bacterial strains	Source
Competent <i>E. coli</i> DH5 α hsdR17(rK-, mK-), recA1, endA1, gyrA96, supE44, thi	self-made, Sambrook <i>et al.</i> 1989
Competent <i>E. coli</i> Top10 F- mcrA Δ (mrr-hsdRMS-mcrBC) ϕ 80lacZ Δ M15 Δ lacX74 nupG recA1 araD139 Δ (ara-leu)7697 galE15 galK16 rpsL(StrR) endA1 λ -	self-made

Table 9 Summary of used plasmids and their plasmid map

Plasmids	Plasmid map
<p>pUC19</p> <p>self-made</p>	<p>pUC19 2686 bp</p>
<p>pHDV</p> <p>self-made</p>	<p>pHDV 3112 bp</p>
<p>pJET1.2</p> <p>Thermo Fisher Scientific, USA</p>	<p>pJET1.2_blunt 2974 bp</p>

Table 10 Summary of used kits and their sources of supply

Kits	Source
CloneJET PCR Cloning Kit	Thermo Fisher Scientific, USA
QIAGEN, Hilden GmbH Plasmid Mega Kit	QIAGEN, Hilden
Qubit™ RNA BR Assay Kit	Thermo Fisher Scientific, USA
Wizard® SV Gel and PCR Clean-Up System	Promega, Walldorf

Table 11 Summary of used consumables as well as auxiliaries and their sources of supply

Consumables and Auxiliaries	Source
1.5 ml MaXtract High Density Tubes	QIAGEN, Hilden
15 ml MaXtract High Density Tubes	QIAGEN, Hilden
4X Optical cuvettes (disposable)	Sarstedt, Nümbrecht
Disposable gloves (nitrile)	Starlab, Hamburg
Disposable pipette (5/10/25 ml)	Greiner Bio-One, Frickenhausen
Disposable syringe (50 ml)	B. Braun, Melsungen
Glass bottles (100/250/500/1000 ml)	VWR, Darmstadt Schott AG, Mainz SIMAX Glass, CZ
Micropipette (P2, P20, P200, P1000)	Gilson, USA
Micropipette filter tips (2/20/200/1000 µl)	Starlab, Hamburg
Micropipette tips (20/200/1000 µl)	Greiner Bio-One, Frickenhausen, Gilson, USA
Plastic beakers (10/25/50/250/500/1000/2000 ml)	VWR, Darmstadt VITLAB, Grossostheim
Plastic graduated cylinders (10/50/250/500/1000/2000 ml)	VITLAB, Grossostheim
Reaction tube (1.5/2 ml)	Greiner Bio-One, Frickenhausen
Reaction tube (15/50 ml)	Greiner Bio-One, Frickenhausen Sarstedt, Nümbrecht
Scintillation tube	Zinsser Analytic, Eschborn
Sephadex G-25 column	Cytiva, Freiburg im Breisgau
Vivaspin® 2, membrane 5,000 MWCO PES	Sartorius, Göttingen

Table 12 Summary of used instruments and their manufacturers

Instruments	Source
Gel documentation system	Intas Science Imaging, Göttingen
Gel dryer	Bio-Rad, USA
Hand-held UV lamp	Benda, Wiesloch
Horizontal electrophoresis chamber (agarose)	VWR, Darmstadt
MicroCal PEAQ-ITC Instrument	Malvern Pananalytical, Kassel
NanoPhotometer® N60/N50	IMPLEN, München
Phosphorimager (Amersham, Typhoon)	Cytiva, Freiburg im Breisgau

Pipette controller (PIPETBOY acu 2)	INTEGRA Biosciences GmbH, Biebertal
Power supply	Consort, BE
Qubit 4 Fluorometer	Thermo Fisher Scientific, USA
Scintillation detector	Perkin Elmer, USA
Thermocycler	PEQLAB, Erlangen
Ultrapure water system (PURELAB® flex 2)	ELGA VEOLIA, Celle
Vacuum pump	Vacuubrand, Wertheim
Vertical electrophoresis chamber (PAA)	CBS Scientific, USA

Table 13 Summary of used software and their developers

Software	Source
ImageJ	Wayne Rasband, National Institutes of Health
MicroCal PEAQ-ITC Analysis Software	Malvern Pananalytical, Kassel
Microsoft Office 365	Microsoft®, USA
SnapGene	Dotmatics, USA
Citavi 6	Swiss Academic Software GmbH, CH
Inkscape	Inkscape Community
RNAfold web server	Gruber AR, Lorenz R, Bernhart SH, Neuböck R, Hofacker IL. The Vienna RNA websuite. <i>Nucleic Acids Res.</i> 2008 Jul 1;36
Forna web tool	Kerpedjiev P, Hammer S, Hofacker IL (2015) Forna (force-directed RNA): Simple and effective online RNA secondary structure diagrams. <i>Bioinformatics</i> 31(20):3377-9

5 Methods

Formulations of solutions and buffers are tabulated below each section. Sometimes the same solutions or buffers were used in different methods; these are not listed repeatedly. Everything was prepared with ultrapure water unless otherwise stated and, if possible, autoclaved. If sterilisation by autoclaving was not applicable, sterile filtration was done. Procedures were carried out at room temperature unless otherwise indicated.

5.1 Capture-SELEX

In addition to the selection process itself, Capture-SELEX also includes the preparation of an RNA pool. Furthermore, the selection method can be used in a shortened format for testing the elution behaviour of individual sequences of potential aptamers.

5.1.1 Pool preparation

The RNA library used to start a Capture-SELEX was specifically designed for this selection method. The 27 nt long 5' and the 33 nt long 3' region are maintained constant throughout the entire selection process. They are required for primer binding in polymerase chain reaction (PCR) amplification. An additional constant region (docking/capture sequence) consists of 13 nucleotides. It is sided by a 40 nt (5') and a 10 nt (3') long randomised region (N40/N10). Thus, the RNA library could be described by the following sequence:

5'-GGGCACUCCAAGCUAGAUCUACCGGU N40 CUACUGGCUUCUA N10 AAAAUGGCUAGC AAAGGAGAAGAACUUCACU-3'

The RNA pool was prepared using a DNA template pool (purchased from Sigma-Aldrich (Merck, Darmstadt); PAGE purified). Initially, the DNA pool was amplified by PCR. This amplification was carried out on a large scale with the following reaction set-up and programme:

Table 14 Reaction set-up and PCR programme for amplification of DNA template pool

Reaction Set-Up		PCR Programme	
50 mM	KCl	3 min	95°C
10 mM	Tris-HCl pH 9.0	1 min	95°C
0.1% (v/v)	Triton X-100	1 min	54°C
0.2 mM	dNTP (each)	2 min	72°C
1.5 mM	MgCl ₂	3 min	72°C
24 nM	pool_template	X5	
2.4 µM	pool_fwd		
2.4 µM	pool_rev		
50 U/mL	Taq DNA polymerase		
filled to 50 mL	ultrapure water		

The subsequent precipitation was performed by adding 1/10 volume of 3 M NaAc pH 6.5 as well as 2.5 volumes of absolute EtOH and incubating at -20°C for 30 min. Centrifugation at 17,000xg and 4°C for 30 min and discard of the supernatant was followed by washing with 20 ml fresh 70%

(v/v) EtOH. The centrifugation was repeated at 17,000xg and 4°C for 10 min. The supernatant was discarded again. The pellet was dried and resuspended in 2 ml ultrapure water. Verification using a 3% agarose gel ensured that the correct PCR product with good quality was obtained. To produce the RNA pool, large-scale *in vitro* transcription was performed:

Table 15 Reaction set-up for *in vitro* transcription of RNA start pool for Capture-SELEX

Reaction Set-Up	
200 mM	Tris-HCl pH 8.0
20 mM	MgAc ₂
20 mM	DTT
2 mM	spermidine
4 mM	NTP (each)
1/10	DNA template pool from previous step
250 U/mL	T7 RNA polymerase
filled to 10 mL	ultrapure water

After incubation at 37°C for 16 hours, the resulting RNA was purified using polyacrylamide gel electrophoresis (see 5.4.1).

5.1.2 *In vitro* selection

The volumes and incubation times used in the first selection round differed from those used in the following rounds. The varying volumes and times are indicated in square brackets. In addition, the initial selection round was carried out with a ready-to-use RNA pool of high diversity. The preparation of this pool was done on a large scale and by gel purification (see 5.4). Therefore, and due to the radioactive decay over time, it was carried out without radioactive labelling. This enabled the RNA pool to be stored ready to be used at -20°C. However, this prevented quantification via radioactive measurement and consequently round 1 is never included in the evaluations of the Capture-SELEX experiments.

Each selection round started with the hybridisation of the RNA pool to a biotinylated capture oligonucleotide (CO). This was done by mixing 10 µl [40 µl] 5X Capture-SELEX buffer (CSB), 1.5 µl [15 µl] biotinylated CO, 5 µl [volume corresponding to 1 nmol] RNA pool with ultrapure water to a final volume of 50 µl [200 µl]. After 5 min at 65°C, incubation for 1 h at 21°C followed. Meanwhile, the magnetic beads were prepared for later immobilisation. Therefore, 150 µl [1000 µl] hydrophilic streptavidin magnetic beads were washed three times with 500 µl [1000 µl] binding and wash buffer (B&W buffer) respectively. The resulting supernatants could be discarded using a magnetic rack. Afterwards, the washed beads were resuspended in 150 µl [200 µl] 1X CSB. The addition of the entire hybridisation reaction allowed the subsequent immobilisation of the RNA-DNA hybrids onto the beads. This was done by incubation for 30 min at 21°C on a revolver rotator. Finally, the supernatant was discarded.

The selection process consisted of three washing steps, a specific elution with the target molecule and an optional elution with a counter target molecule. After each step, the resulting supernatant was separated from the beads using a magnetic rack and collected for later measurement (not applicable for the first round). The first washing step was performed with 200 µl [400 µl] 1X CSB

and incubation in a revolver rotator for 5 min at 21°C. For the next wash, the same volume of 1X CSB was used, but incubation was carried out at 30°C for 5 minutes in a thermoblock. The sample was briefly vortexed after 2.5 min. The last washing step was identical to the initial one. If a counter selection was performed, the beads were resuspended in 200 µl [400 µl] counter target solution and incubated for 5 min at 21°C in a revolver rotator. The following elution with the target molecule was carried out by adding 200 µl [400 µl] target solution. The sample was incubated for 5 min at 21°C in a revolver rotator. The remaining beads were resuspended with 200 µl [not necessary] 1X CSB for subsequent measurement.

Quantification of the collected supernatants of the individual selection steps by measuring their radioactivity was carried out using a scintillation counter. Therefore, 4 µl of each sample was mixed with 2 ml of scintillation solution and measured each. The evaluation of the measurement results was done by summing all analysed samples, which represents the total amount of radioactively labelled RNA in this selection round. This was followed by calculation the percentage share of total amount from the last washing step, the specific elution and, if necessary, the counter elution. Plotting these percentages as 'input eluted' over the entire selection resulted in the bar graphs shown for Capture-SELEX experiments.

To start a new selection round, it was necessary to extract and amplify the eluted RNA from the target molecule elution. Thus, the RNA was first precipitated with 20 µl [40 µl] 3 M NaAc pH 6.5, 500 µl [1000 µl] absolute EtOH and 1 µl GlycoBlue™ Coprecipitant at -20°C for 15 min [30 min]. After centrifugation for 15 min [30 min] at 17,000xg and 4°C, the supernatant was discarded and 800 µl of fresh 70% (v/v) EtOH was added to the pellet. The supernatant was discarded by centrifugation again at 17,000xg and 4°C for 10 min. After drying for 5 min, the RNA pellet was resuspended in 50 µl of ultrapure water. The addition of 47 µl RT-PCR mix, 1 µl Superscript II reverse transcriptase and 1 µl Taq DNA polymerase then enabled RT-PCR according to the following scheme:

Table 16 Programme for reverse transcription of precipitated RNA and PCR amplification of cDNA

Reverse Transcription	
10 min	54°C
1 min	95°C
→ Addition of 1 µl 100 µM pool_fwd	
PCR Programme	
10 s [1 min]	95°C
10 s [1 min]	58°C
20 s [1 min]	72°C
cycles varied overamplification avoided	

The amplification was checked on a 3% (w/v) agarose gel.

Subsequently, the obtained DNA had to be transcribed into RNA again. This was prepared by mixing 10 µl RT-PCR product, 87 µl transcription mix, 1 µl α -³²P-ATP or α -³²P-UTP (depending on availability), 100 U T7 RNA polymerase, 40 U RNase inhibitor with ultrapure water (final volume 100 µl). After incubation for 6 h at 37°C, the resulting pyrophosphate could be separated by centrifugation for 1 min at 17,000xg and 4°C. The RNA was precipitated with 50 µl 7.5 M NH₄Ac and 250 µl absolute EtOH for 10 min at -20°C. The supernatant was discarded after centrifugation at 17,000xg and 4°C for 15 minutes. The resulting pellet was washed with 200 µl of fresh 70%

(v/v) EtOH and centrifugation for 10 min at 17,000xg and 4°C. The supernatant was discarded and the RNA dried for 5 min. Finally, resuspension of the pellet in 50 µl ultrapure water provided an RNA pool for the next round of selection.

Table 17 Formulations of solutions and buffers used for *in vitro* selection

Solution/Buffer	Components
50X TAE pH 8.3	2 M Tris
	1 M Acetic acid
	50 mM Na-EDTA
6X DNA Loading Buffer	25 vol. Glycerine
	1 vol. 50X TAE
	some Bromophenol blue
5X CSB	200 mM HEPES
	1.25 mM KCl
	100 mM NaCl
	25 mM MgCl ₂
	pH 7.4 with HCl
1X CSB	1 vol. 5X CSB
	4 vol. Ultrapure water
	0.01% (v/v) Tween-20
B&W Buffer	5 mM Tris-HCl
	0.5 mM EDTA
	1 M NaCl
	0.01% (v/v) Tween-20
	pH 7.5 with HCl
RT-PCR Mix (stored as 47 µl aliquots)	40 mM Tris-HCl pH 9.0
	130 mM KCl
	4.2 mM MgCl ₂
	4 mM DTT
	0.2% (v/v) Triton X-100
	2 µM pool_rev
	0.6 mM dNTP (each)
Transcription Mix (stored as 87 µl aliquots)	40 mM Tris-HCl pH 8.0
	5 mM DTT
	2.5 mM NTP (each)
	15 mM MgCl ₂

5.1.3 Evaluation of the elution of potential aptamers (specificity assay)

The elution behaviour of potential aptamers was analysed in a shortened version of the Capture-SELEX. It was necessary to prepare an RNA pool containing only copies of the identical sequence which should be examined. Therefore, DNA templates were prepared by PCR and overhang filling PCR (see 5.3.1). Subsequently, 10 µl of the resulting PCR products were used for *in vitro* transcription according to Capture-SELEX (see 5.1.2). All further steps were identical to the *in vitro* selection procedure starting in the second round. However, the method was only carried out until quantification of the collected samples. Precipitation, amplification and further *in vitro* transcription were not necessary.

Elution was always performed with 1 mM or 10% (v/v) target solution and there was no counter elution. If the Capture-SELEX counter target was used, a separate elution test was performed for it. The test was done at least 2 times for each sample and the applied target molecule. The evaluation was carried out according to Capture-SELEX. It was based on the total amount of radioactively labelled RNA and the percentage share of the elution with the target. The results of the eluted input by the different targets were graphically plotted side by side and their ratio was calculated.

5.2 Analysis of enriched RNA pools or complete selection processes

5.2.1 Cloning and Sanger sequencing

This method was used for rapid but not comprehensive sequence analysis of individual selection rounds of Capture-SELEX. The RT-PCR products of these rounds were cloned using the CloneJET PCR Cloning Kit (Thermo Fisher Scientific, USA) and subsequently sequenced using Sanger sequencing service from Microsynth Seqlab GmbH.

Therefore, 8 μ l of RT-PCR product were used as a template for PCR amplification and purified (see 5.3.1). The following ligation was carried out according to the blunt-end cloning protocol from manufacturer, but the ligation mixture was incubated for 30 min instead of 5 min. Transformation was then carried out using prepared competent *E. coli* Top10. After the addition of 100 μ l thawed cells to ligation mixture, incubation on ice for 1 h followed. A short heat shock was carried out at 42° for 90 s and the sample was left on ice for 10 minutes. The cells were regenerated by adding 1 ml of sterile LB medium and incubating for 1 h at 37°C and 1,000 rpm in a thermoshaker. Finally, the cells were plated on LB plates containing ampicillin and incubated at 37°C overnight. Sequencing was done using the Ecoli NightSeq service by Microsynth Seqlab GmbH. The results were analysed with SnapGene software and individual abundant sequences were determined.

Table 18 Formulations of solutions and buffers used for cloning and sequencing of individual selection rounds

Solution/Buffer	Components	
Ampicillin Stock Solution	100 mg/ml in 70% (v/v) EtOH	Ampicillin
		1% (w/v) Tryptone
LB Medium		1% (w/v) NaCl
		0.5% (w/v) Yeast extract
		1.5% (w/v) Agar
LB Plate with Ampicillin		0.1 mg/ml Ampicillin

5.2.2 Next Generation Sequencing

For deep sequencing of the entire selection process using Next Generation Sequencing (NGS), each individual SELEX round had to be prepared. Therefore, the respective RT-PCR products were amplified with PCR and then purified (see 5.3.1). For amplification, 8 μ l RT-PCR product of each individual round were used. In order to adjust samples to a concentration of 20 ng/ μ l with ultrapure water, their concentrations were determined by spectrophotometric measurement. NGS was performed with 500 ng of each selection round using GENEWIZ (Leipzig) and their application Amplicon-EZ.

The bioinformatic evaluation was carried out by Philipp Fröhlich (Department of Electrical Engineering and Information Technology, TU Darmstadt, Self-Organizing Systems, 64283 Darmstadt, Germany). More detailed information can be found soon in the publication about the LX-binding aptamer. This publication is currently in preparation.

5.3 Preparation of DNA templates for *in vitro* transcription

DNA templates for *in vitro* transcription were generated using various methods. In addition to the classical PCR, an overhang filling PCR, the cloning of an aptamer sequence into a pHDV vector and simple hybridisation of two complementary DNA oligonucleotides could be used to produce templates.

5.3.1 PCR and overhang filling PCR

Polymerase chain reaction (PCR) with template and primers was used for *in vitro* amplification of DNA and carried out with the following reaction set-up and PCR programme:

Table 19 Reaction set-up and PCR programme for PCR

Reaction Set-Up		PCR Programme	
1/5 vol.	5X Q5 reaction buffer	30 s	98°C
200 µM	dNTP (each)	10 s	98°C
0.5 µM	pool_fwd	20 s	55°C
0.5 µM	pool_rev	20 s	72°C
10 nM*	DNA template	2 min	72°C
2 U	Q5 DNA polymerase		
filled to 100 µl	Ultrapure water		

*unless otherwise indicated

Another method for generating DNA templates was the overhang filling PCR with two single stranded DNA oligonucleotides sharing a complementary region. The ability to anneal DNA oligonucleotides made it unnecessary to use a template with matching forward and reverse primer. During PCR, the single stranded overhangs of the DNA hybrids were filled and double stranded DNA was produced. The reaction set-up and the PCR programme used for this are listed below:

Table 20 Reaction set-up and PCR programme for overhang filling PCR

Reaction Set-Up		PCR Programme	
1/5 vol.	5X Q5 reaction buffer	2 min	98°C
200 µM	dNTP (each)	10 s	98°C
0.5 µM	DNA oligonucleotide forward	20 s	55°C
0.5 µM	DNA oligonucleotide reverse	20 s	72°C
2 U	Q5 DNA polymerase	2 min	72°C
filled to 100 µl	Ultrapure water		

All PCR products obtained were checked for overamplification in a 3% agarose gel. This was followed by purification with the Wizard® SV Gel and PCR Clean-Up System (Promega, Walldorf), if necessary, and concentration determination by spectrophotometric measurement.

5.3.2 Cloning with pHDV

The cloning of an aptamer sequence into a pHDV vector carrying hepatitis delta virus ribozyme has a major advantage. The use of this vector as a DNA template in an *in vitro* transcription and the possibility of the self-cleavage reaction of the ribozyme result in homogeneous 3' ends of the synthesised RNA. Transcription with T7 RNA polymerase using a DNA oligonucleotide could lead to heterogeneous 3' ends as well as undesired 3' extensions.

In preparation of cloning, the aptamer sequence of LXC which should be incorporated has to be modified to be a suitable insert. Initially, a PCR is used to introduce additional restriction sites for the enzymes EcoRI and NcoI with the corresponding primers. This PCR follows the procedure described in 5.3.1. Purification of PCR product was done out by phenolisation. The PCR products were mixed with 1 volume of phenol, vortexed and transferred to a MaXtract High Density Tube (QIAGEN, Hilden). This was followed by centrifugation for 5 min at 16,000xg and 4°C. The supernatant was transferred to a new MaXtract High Density Tube (QIAGEN, Hilden), mixed with 1 volume of chloroform-isoamyl alcohol (24:1) and shaken well. After centrifugation under same conditions as before, the DNA contained in the supernatant was precipitated with 1 volume of isopropanol, 1/10 volume of 3 M NaAc and 1 µl of GlycoBlue™ Coprecipitant for 30 min at -20°C. Subsequent centrifugation was performed for 30 min at 16,000xg and 4°C. The supernatant was discarded and 500 µl of fresh 70% (v/v) EtOH was added to the pellet. After centrifugation at 16,000xg and 4°C for 15 min, the supernatant was discarded and the pellet dried for 10 min. The resulting DNA was resuspended in ultrapure water. Finally, the sample was analysed in 3% agarose gel and the concentration was determined by spectrophotometric measurement.

This was followed by the restriction of the insert as well as the vector with EcoRI and NcoI according to the manufacturer's instructions. Thus, suitable ends for ligation could be obtained. The purification of the restricted insert and vector was carried out using the Wizard® SV Gel and PCR Clean-Up System (Promega, Walldorf). The restricted vector was loaded onto a 1% agarose gel and the relevant band was cut out. Controls were carried out in corresponding agarose gels and concentrations were determined spectrophotometrically. The following reaction mixture and controls were used for the subsequent ligation:

Table 21 Reaction set-up and controls for ligation of aptamer insert and pHDV vector

Reaction Set-Up	
25 ng	pHDV restricted with EcoRI and NcoI
5X molar quantity of vector	Insert restricted with EcoRI and NcoI
1/10 vol.	10X T4 ligase buffer
1 mM	ATP
400 U	T4 ligase
filled to 20 µl	ultrapure water
Controls	
without insert	substituted by ultrapure water
without T4 ligase	substituted by ultrapure water

The ligation mixtures were incubated for 45 min and then used directly for transformation into competent *E. coli* DH5 α . The transformation followed the same procedure as already described in 5.2.1. Verification of the success of the cloning was performed using colony PCR with the following reaction set-up and PCR programme:

Table 22 Reaction set-up and PCR programme of colony PCR

Reaction Set-Up for One Transformant		PCR Programme	
1/10 vol.	10X Taq Thermopol buffer	4 min	95°C
200 μ M	dNTP (each)	30 s	95°C
0.3 μ M	hdv_seq (forward primer)	30 s	53°C
0.3 μ M	pool_rev	30 s	72°C
0.25 μ l	Taq DNA polymerase	5 min	72°C
filled to 25 μ l	Ultrapure water		

A selection of transformants was transferred to a new LB plate containing ampicillin as well as into PCR reaction mix. Positive transformants containing the insert showed a band in 3% agarose control gel. The negative transformants did not show amplification of DNA, since the pool_rev primer could not bind to their pHDV vector due to the absence of the insert.

Large quantities of pHDV vector were produced using the QIAGEN, Hilden GmbH Plasmid Mega Kit according to the manufacturer's protocol. The pHDV vector had to be restricted with the HindIII enzyme following the manufacturer's instructions before using it as a DNA template for *in vitro* transcription. Purification was carried out using phenolisation (see above). The concentration was determined by spectrophotometric measurement. Finally, sequencing (Microsynth Seqlab GmbH) was carried out to verify accuracy of the sequence of the inserted aptamer and HDV ribozyme.

5.3.3 Hybridisation

For the preparation of DNA templates smaller or equal to 120 bp, fully complementary single stranded DNA oligonucleotides could be used. Due to their complete complementarity, a simple hybridisation to a double stranded DNA could be carried out. This was done by mixing 100 μ l of 100 μ M forward DNA oligonucleotide with 100 μ l of 100 μ M reverse DNA oligonucleotide and incubating at 95°C for 5 minutes. The thermoblock used to incubate was switched off and samples were allowed to cool to room temperature. The success of the hybridisation was checked in a 3% agarose gel. The concentration was measured spectrophotometrically.

5.4 *In vitro* transcription and purification

The production of RNA was performed using *in vitro* transcription. The reaction set-ups to produce large amounts of RNA and for *in vitro* transcription in Capture-SELEX differed in their composition:

Table 23 Reaction set-ups for large-scale and Capture-SELEX *in vitro* transcription

Large-Scale	
200 mM	Tris-HCl pH 8.0
20 mM	MgAc ₂
20 mM	DTT
2 mM	spermidine
if needed: 15% (v/v)	DMSO
4 mM	NTP (each)
3 µg/ml	no plasmid DNA template
	or
100 µg/ml	plasmid DNA template
250 U/ml	T7 RNA polymerase
filled to 100 µl - 10 ml	ultrapure water
Capture-SELEX	
40 mM	Tris-HCl pH 8.0
15 mM	MgCl ₂
5 mM	DTT
2,5 mM	NTP (each)
1/10	RT-PCR product
40 U	RNase inhibitor
250 U/ml	T7 RNA polymerase
filled to 100 µl	ultrapure water

Incubation always carried out at 37°C for a minimum of 6 h and a maximum of 16 h. The purification of the obtained RNA was done using polyacrylamide gel electrophoresis (PAGE) or molecular weight cut-off columns.

5.4.1 Gel purification

The pyrophosphate formed during the transcription was separated by centrifugation at 8,400xg and 4°C for 1 min. RNA precipitation was achieved with 100 mM EDTA pH 8.0, 400 µM NaAc and 2.5 volumes of -20°C cold absolute EtOH. After incubation for 1 h at -20°C and centrifugation at 8,400xg and 4°C for 1 h, the supernatant was discarded. This was followed by washing with 10 ml fresh 70% (v/v) EtOH and centrifugation at 8,400xg and 4°C for 15 min to discard the supernatant again. The pellet was dried for 5 min and finally resuspended in a suitable volume of 2X RNA loading buffer.

A maximum of 2 ml RNA solution was loaded onto a 20x20 cm gel for denaturing polyacrylamide gel electrophoresis (PAGE) with 8% polyacrylamide (PAA), 8 M urea and 1X TBE buffer

(sometimes more than one gel). The gel ran until the bromophenol blue front almost leaked out. UV shadowing was used to visualise the RNA for cutting out the corresponding band. The gel was sliced into 0.5 cm small pieces. The slices of each cut gel band were transferred into a 50 ml tube and topped with 300 mM NaAc pH 6.5. The RNA was eluted by incubation for 16 h at 4°C in an overhead shaker. Subsequently, gel residues were removed from the supernatant using a syringe filter. RNA was precipitated with 2.5 volumes -20°C cold absolute EtOH for 1 h at -20°C. After centrifugation at 8,400xg and 4°C for 1 h, the supernatants could be discarded. The resulting pellet was washed with 10 ml fresh 70% (v/v) EtOH each and centrifuged at 8,400xg and 4°C for 15 min. Once dried for 5 min, the RNA was dissolved in a suitable volume of ultrapure water. Finally, the concentration was determined spectrophotometrically and a denaturing PAGE was performed with 8% PAA, 8 M urea and 1X TBE as a control.

Table 24 Formulations of solutions and buffers used for gel purification of RNA

Solution/Buffer	Components	
2X RNA Loading Buffer	10 ml	Deionized formamide
	25 mM	EDTA
	some	Bromophenol blue
PAA Gel	8% (v/v)	Polyacrylamide
	1/10 vol.	10X TBE
	8 M	Urea
	1% (v/v)	10% (w/v) APS solution
	0.1% (v/v)	TEMED
10X TBE pH 8.3	0.89 M	Tris
	0.89 M	Boric acid
	10 mM	Na-EDTA

5.4.2 Purification using molecular weight cut-off columns

Purification of an *in vitro* transcript using molecular weight cut-off (MWCO) columns yielded less clean RNA but was much faster than PAGE-based purification. This method was only used to purify large-scale *in vitro* transcriptions.

The pyrophosphate formed was separated in the same way as in gel-based purification. Besides the synthesised RNA, the resulting sample also contained the template DNA. This was eliminated by treating the sample with TURBO™ DNase according to the manufacturer's instructions in an incubation for 1 h at 37°C. Subsequently, it was necessary to remove enzymes such as T7 RNA polymerase and DNase using phenolisation. Therefore, the sample was mixed with 1 volume of phenol-chloroform-isoamyl alcohol solution, vortexed and transferred into a 15 ml MaXtract High Density Tube (QIAGEN, Hilden). After centrifugation for 5 min at 1,500xg and 4°C, the supernatant was transferred to a fresh 15 ml MaXtract High Density Tube (QIAGEN, Hilden), mixed with 1 volume of 24:1 chloroform-isoamyl alcohol solution and shaken well. Centrifugation was repeated under the same conditions. The resulting supernatant was collected in a 50 ml tube and the RNA was precipitated with 2.5 volumes of absolute EtOH and 1/10 volume of 3 M NaAc pH 6.5 for 1 h at -20°C. The supernatant was discarded after centrifugation for 1 h at 8,400xg and 4°C. The remaining pellet was washed with 10 ml fresh 70% (v/v) EtOH and a centrifugation at 8,400xg and

4°C for 15 min. After drying the RNA for 5 min, it was resuspended in an appropriate volume (1-2 ml) of ultrapure water.

Subsequently, the RNA was purified using MWCO columns. Attention had to be paid to the filter size and the molecular weight of the desired RNA. These columns have a filter with a specific size exclusion, which only allows smaller molecules than specified to pass through. Larger molecules, such as the required RNA, remain above the filter. This allows the RNA to be separated from unwanted residues of phenolisation and precipitation as well as very small by-products of transcription. In addition, it was possible to concentrate the RNA solution.

Preparation of the MWCO columns was done by washing with 2 ml ultrapure water and centrifugation for 40 min at 12,000xg. Filtrate and residues above the filter were discarded. The entire sample volume was loaded onto the columns and centrifuged at 12,000xg until only 100-200 µl remained above the filter. The filtrate was discarded. This was followed by washing the sample three times. The sample was filled up to a volume of 1 ml with ultrapure water each time and centrifuged at 12,000xg until a residue of 100-200 µl remained. The resulting filtrates were discarded. After the last wash, the remaining, clean and concentrated RNA solution above the filter was transferred to a 1.5 ml tube. Subsequently, the concentration was determined using a fluorometer with Qubit™ RNA BR Assay Kit according to the manufacturer's instructions. Finally, a denaturing PAGE with 8% PAA, 8 M urea and 1X TBE was performed as control.

5.5 Isothermal titration calorimetry

Isothermal titration calorimetry (ITC) served both to determine a dissociation constant (K_D) precisely and to provide a basis for straightforward mutation experiments. The latter was not designed to determine an exact K_D , but rather to identify whether a particular mutation in an aptamer leads to a loss of its binding ability.

5.5.1 Determination of the dissociation constant

For the ITC measurements, 5X Capture-SELEX buffer was used for the preparation of 1X CSB as well as ligand and RNA in 1X CSB. The measurements were performed with 500 μM freshly prepared LX solution and 50 μM RNA. To ensure correct folding of the aptamer, the RNA, which was stored in ultrapure water only, was heated to 98°C for 5 min and then immediately placed on ice. After adding cold 5X CSB to a final concentration of 1X, the RNA was incubated on ice. This incubation was carried out for at least 20 min, after which the RNA could be used for measurement. Care was taken to ensure that all of the solutions required for the measurements were at room temperature. The experiments were conducted using a MicroCal PEAQ-ITC from Malvern Panalytical. The cell was filled with 200 μl of RNA sample and the syringe was loaded with 40 μl of LX solution. The measurement started with a delay of 60 s after setting the temperature to 25°C and equilibrating the system. The first test injection was made with 0.2 μl in 0.4 s. The following 19 injections were carried out with 2 μl in 4 s each. Between the individual injections there was a delay of 180 s. The even distribution of the injected LX solution was maintained by continuous stirring at 750 rpm. The measurement results were recorded in a graph of the change in differential power (DP; μW) over time (min). By integrating the heat ΔQ (μJ ; area of each peak) and relating it to the molar ratio of ligand and RNA, the molar enthalpy ΔH (kJ/mol) could be calculated. Plotting ΔH against the molar ratio resulted in a binding curve. Finally, based on the one-site binding model available with the MicroCal PEAQ-ITC Analysis Software (version 1.41), the K_D could be determined from the data of the fitted binding curve. All measurements were performed at least twice.

5.5.2 Mutation and truncation study

The ITC-based mutation experiments with the aptamers LXC and trLXC followed the same parameters and procedures as described in 5.5.1. Variations included the use of only 30 μM RNA in combination with 500 μM LX, the application of only 13 injections and a delay of 150 s between injections. The recording and analysis of the results was done according to the same method as described above. The determination of whether a mutation led to the preservation or loss of binding ability of the aptamer was based on the yield of a valid binding curve. Furthermore, if a reliable binding curve was obtained, attention was paid to how great the K_D differences of the mutated aptamers were compared to the K_D of the original LXC or trLXC aptamer.

5.6 In-line probing

In-line probing was performed with an already gel purified RNA (see 5.4/5.4.1). To improve the resolution of the sample in in-line probing PAGE, a 21 nt long linker (5'-GGGCAACAACAACAA-3') was added to the aptamer at the 5' end by DNA template preparation via PCR (see 5.3.1). The design of this linker allows no interaction with the aptamer sequence. The removal of the 5' phosphate by dephosphorylation reaction was carried out with an alkaline phosphatase according to the manufacturer's instructions at 50°C for 30 minutes. This was followed by heat inactivation at 95°C for 3 min. Thus, the RNA could be used directly for the 5'-labelling. The labelling was done with a polynucleotide kinase and γ -³²P-ATP, according to manufacturer's instructions. After incubation at 37°C for 40 min, the remaining γ -³²P-ATP molecules were separated using a Sephadex G25 column following the manufacturer's protocol. The radioactivity of the labelled RNA was measured in counts per minute (CPM) as in Capture-SELEX (see 5.2.1).

Before an analysable in-line probing could be carried out, a number of parameters had to be determined. These included the concentration range of the aptamer target molecule and incubation time of the in-line reaction. Furthermore, incubation times had to be determined for the required ladders. The determination of these parameters was conducted in accordance with the actual procedure for in-line probing (described below). However, additional reactions were prepared and incubation times were tested.

Table 25 Compositions of in-line probing samples

Sample	Compositions	
In-Line Probing Reaction	1 pmol	Native RNA
	50,000 CPM	Labelled RNA
	1X	2X in-line buffer
	1X	10X LX solution
	filled to 10 μ l	Ultrapure water
Non-Reacted RNA	1 pmol	Native RNA
	50,000 CPM	Labelled RNA
	1X	2X RNA loading buffer
	filled to 10 μ l	Ultrapure water
G Ladder	1 pmol	Native RNA
	50,000 CPM	Labelled RNA
	1X	10X sodium citrate buffer
	1 U	T1 RNase
	1X	2X RNA loading buffer
OH Ladder	filled to 10 μ l	Ultrapure water
	1 pmol	Native RNA
	50,000 CPM	Labelled RNA
	1X	10X Na ₂ CO ₃ buffer
	1X	2X RNA loading buffer
	filled to 10 μ l	Ultrapure water

In-line probing reactions consisted of native RNA, labelled RNA, 2X in-line buffer and 10X LX stock solution. The reactions were stopped after incubation for 4 days by adding 2X RNA loading buffer and frozen at -20°C . In order to obtain the first ladder for guanine residues (G ladder) native and labelled RNA were digested by T1 RNase at 55°C for 5 min. The second ladder served as a size standard for single nucleotides (OH ladder). Based on alkaline hydroxylation, native and labelled RNA were mixed and treated with 10X Na_2CO_3 buffer for 6 min at 98°C . In addition, a non-reacted RNA sample was prepared. The exact compositions for these in-line probing samples are listed in Table 25.

All samples were separated by denaturing polyacrylamide gel electrophoresis using a 0.75 mm thick and 50x20 cm 10% or 8% PAA gel with 8 M urea and 1X TBE. The resulting gel was dried at 80°C with a gel dryer. Finally, the gel was scanned using phosphorimager following the manufacturer's guidelines. The gel image was analysed using ImageJ software. Thereby, the intensity of single or whole signal regions was analysed for each applied ligand concentration. The results were then normalised to the most intense signal with a value of 1 and plotted against the logarithmically scaled LX concentration.

Table 26 Formulations of solutions and buffers used for in-line probing

Solution/Buffer	Components	
2X In-Line Buffer pH 8.3	40 mM	MgCl_2
	100 mM	Tris-HCl
	200 mM	KCl
10X Sodium Citrate Buffer pH 5.0	0.25 M	Trisodium citrate
10X Na_2CO_3 Buffer pH 9.0	0.5 M	Na_2CO_3
	10 mM	EDTA
PAA Gel	10% (v/v)	Polyacrylamide
	1/10 vol.	10X TBE
	8 M	Urea
	0.5% (v/v)	10% (w/v) APS solution
	0.05% (v/v)	TEMED

6 Bibliography

- 1 Fath A (2016) Rheines Wasser: 1231 Kilometer mit dem Strom, 1. Aufl. Hanser eLibrary. Hanser, Carl, München
- 2 Buerge IJ, Keller M, Buser H-R *et al.* (2011) Saccharin and other artificial sweeteners in soils: estimated inputs from agriculture and households, degradation, and leaching to groundwater. *Environ Sci Technol* 45:615–621. <https://doi.org/10.1021/es1031272>
- 3 Soh L, Connors KA, Brooks BW *et al.* (2011) Fate of sucralose through environmental and water treatment processes and impact on plant indicator species. *Environ Sci Technol* 45:1363–1369. <https://doi.org/10.1021/es102719d>
- 4 Chiriac FL, Paun I, Pirvu F *et al.* (2021) Occurrence and Fate of Bisphenol A and its Congeners in Two Wastewater Treatment Plants and Receiving Surface Waters in Romania. *Environ Toxicol Chem* 40:435–446. <https://doi.org/10.1002/etc.4929>
- 5 Zhou J, Chen X-H, Pan S-D *et al.* (2019) Contamination status of bisphenol A and its analogues (bisphenol S, F and B) in foodstuffs and the implications for dietary exposure on adult residents in Zhejiang Province. *Food Chem* 294:160–170. <https://doi.org/10.1016/j.foodchem.2019.05.022>
- 6 Hanna N, Sun P, Sun Q *et al.* (2018) Presence of antibiotic residues in various environmental compartments of Shandong province in eastern China: Its potential for resistance development and ecological and human risk. *Environ Int* 114:131–142. <https://doi.org/10.1016/j.envint.2018.02.003>
- 7 Rochester JR (2013) Bisphenol A and human health: a review of the literature. *Reprod Toxicol* 42:132–155. <https://doi.org/10.1016/j.reprotox.2013.08.008>
- 8 Rochester JR, Bolden AL (2015) Bisphenol S and F: A Systematic Review and Comparison of the Hormonal Activity of Bisphenol A Substitutes. *Environ Health Perspect* 123:643–650. <https://doi.org/10.1289/ehp.1408989>
- 9 Rosenmai AK, Dybdahl M, Pedersen M *et al.* (2014) Are structural analogues to bisphenol a safe alternatives? *Toxicol Sci* 139:35–47. <https://doi.org/10.1093/toxsci/kfu030>
- 10 Zhou Z, Zhang Z, Feng L *et al.* (2020) Adverse effects of levofloxacin and oxytetracycline on aquatic microbial communities. *Sci Total Environ* 734:139499. <https://doi.org/10.1016/j.scitotenv.2020.139499>
- 11 He K, Blaney L (2015) Systematic optimization of an SPE with HPLC-FLD method for fluoroquinolone detection in wastewater. *J Hazard Mater* 282:96–105. <https://doi.org/10.1016/j.jhazmat.2014.08.027>
- 12 Ribbers K, Breuer L, Düring R-A (2019) Detection of artificial sweeteners and iodinated X-ray contrast media in wastewater via LC-MS/MS and their potential use as anthropogenic tracers in flowing waters. *Chemosphere* 218:189–196. <https://doi.org/10.1016/j.chemosphere.2018.10.193>
- 13 Honeychurch KC, Piano M (2022) Sensors for Environmental Monitoring and Food Safety. *Biosensors (Basel)* 12. <https://doi.org/10.3390/bios12060366>
- 14 Cai Y, Zhu K, Shen L *et al.* (2022) Evolved Biosensor with High Sensitivity and Specificity for Measuring Cadmium in Actual Environmental Samples. *Environ Sci Technol* 56:10062–10071. <https://doi.org/10.1021/acs.est.2c00627>

- 15 Cheng Y, Wang H, Zhuo Y *et al.* (2022) Reusable smartphone-facilitated mobile fluorescence biosensor for rapid and sensitive on-site quantitative detection of trace pollutants. *Biosens Bioelectron* 199:113863. <https://doi.org/10.1016/j.bios.2021.113863>
- 16 Florinel-Gabriel B (2012) *Chemical sensors and biosensors: Fundamentals and applications*. Wiley, Chichester
- 17 Turner APF, Karube I, Wilson GS (eds) (1989) *Biosensors: Fundamentals and applications*, [Nouv. tirage]. Oxford university press, Oxford, New York, Tokyo
- 18 Cammann K (1977) Bio-sensors based on ion-selective electrodes. *Z Anal Chem* 287:1–9. <https://doi.org/10.1007/BF00539519>
- 19 Vo-Dinh T, Cullum B (2000) Biosensors and biochips: advances in biological and medical diagnostics. *Fresenius Journal of Analytical Chemistry* 366:540–551. <https://doi.org/10.1007/s002160051549>
- 20 Ziegler C, Göpel W (1998) Biosensor development. *Current Opinion in Chemical Biology* 2:585–591. [https://doi.org/10.1016/s1367-5931\(98\)80087-2](https://doi.org/10.1016/s1367-5931(98)80087-2)
- 21 Borisov SM, Wolfbeis OS (2008) Optical biosensors. *Chem Rev* 108:423–461. <https://doi.org/10.1021/cr068105t>
- 22 Cesewski E, Johnson BN (2020) Electrochemical biosensors for pathogen detection. *Biosens Bioelectron* 159:112214. <https://doi.org/10.1016/j.bios.2020.112214>
- 23 Walton PW, O'Flaherty MR, Butler ME *et al.* (1993) Gravimetric biosensors based on acoustic waves in thin polymer films. *Biosens Bioelectron* 8:401–407. [https://doi.org/10.1016/0956-5663\(93\)80024-J](https://doi.org/10.1016/0956-5663(93)80024-J)
- 24 Berg JM, Stryer L, Tymoczko JL (2013) *Stryer Biochemie*, 7. Auflage. Springer Berlin Heidelberg, Berlin, Heidelberg
- 25 Purves WK, Purves WK, Markl J *et al.* (2011) *Purves Biologie*, 9. Aufl. Spektrum Akademischer Verl., Heidelberg
- 26 Varani G, McClain WH (2000) The G x U wobble base pair. A fundamental building block of RNA structure crucial to RNA function in diverse biological systems. *EMBO Rep* 1:18–23. <https://doi.org/10.1093/embo-reports/kvd001>
- 27 Crick FH (1966) Codon--anticodon pairing: the wobble hypothesis. *J Mol Biol* 19:548–555. [https://doi.org/10.1016/s0022-2836\(66\)80022-0](https://doi.org/10.1016/s0022-2836(66)80022-0)
- 28 Svoboda P, Di Cara A (2006) Hairpin RNA: a secondary structure of primary importance. *Cell Mol Life Sci* 63:901–908. <https://doi.org/10.1007/s00018-005-5558-5>
- 29 Lehmann J, Jossinet F, Gautheret D (2013) A universal RNA structural motif docking the elbow of tRNA in the ribosome, RNase P and T-box leaders. *Nucleic Acids Res* 41:5494–5502. <https://doi.org/10.1093/nar/gkt219>
- 30 Klein DJ, Schmeing TM, Moore PB *et al.* (2001) The kink-turn: a new RNA secondary structure motif. *EMBO J* 20:4214–4221. <https://doi.org/10.1093/emboj/20.15.4214>
- 31 Staple DW, Butcher SE (2005) Pseudoknots: RNA structures with diverse functions. *PLoS Biol* 3:e213. <https://doi.org/10.1371/journal.pbio.0030213>
- 32 Kruger K, Grabowski PJ, Zaugg AJ *et al.* (1982) Self-splicing RNA: autoexcision and autocyclization of the ribosomal RNA intervening sequence of *Tetrahymena*. *Cell* 31:147–157. [https://doi.org/10.1016/0092-8674\(82\)90414-7](https://doi.org/10.1016/0092-8674(82)90414-7)

- 33 Saberi F, Kamali M, Najafi A *et al.* (2016) Natural antisense RNAs as mRNA regulatory elements in bacteria: a review on function and applications. *Cell Mol Biol Lett* 21:6. <https://doi.org/10.1186/s11658-016-0007-z>
- 34 Tucker BJ, Breaker RR (2005) Riboswitches as versatile gene control elements. *Curr Opin Struct Biol* 15:342–348. <https://doi.org/10.1016/j.sbi.2005.05.003>
- 35 Sashital DG, Butcher SE (2006) Flipping off the riboswitch: RNA structures that control gene expression. *ACS Chem Biol* 1:341–345. <https://doi.org/10.1021/cb6002465>
- 36 Ellington AD, Szostak JW (1990) *In vitro* selection of RNA molecules that bind specific ligands. *Nature* 346:818–822. <https://doi.org/10.1038/346818a0>
- 37 Long SB, Long MB, White RR *et al.* (2008) Crystal structure of an RNA aptamer bound to thrombin. *RNA* 14:2504–2512. <https://doi.org/10.1261/rna.1239308>
- 38 Jung J in, Han SR, Lee S-W (2018) Development of RNA aptamer that inhibits methyltransferase activity of dengue virus. *Biotechnol Lett* 40:315–324. <https://doi.org/10.1007/s10529-017-2462-7>
- 39 DasGupta S, Shelke SA, Li N *et al.* (2015) Spinach RNA aptamer detects lead(II) with high selectivity. *Chem Commun (Camb)* 51:9034–9037. <https://doi.org/10.1039/c5cc01526j>
- 40 Hanson S, Berthelot K, Fink B *et al.* (2003) Tetracycline-aptamer-mediated translational regulation in yeast. *Mol Microbiol* 49:1627–1637. <https://doi.org/10.1046/j.1365-2958.2003.03656.x>
- 41 Wrist A, Sun W, Summers RM (2020) The Theophylline Aptamer: 25 Years as an Important Tool in Cellular Engineering Research. *ACS Synth Biol* 9:682–697. <https://doi.org/10.1021/acssynbio.9b00475>
- 42 Vorobyeva MA, Dymova MA, Novopashina DS *et al.* (2021) Tumor Cell-Specific 2'-Fluoro RNA Aptamer Conjugated with Closo-Dodecaborate as A Potential Agent for Boron Neutron Capture Therapy. *Int J Mol Sci* 22. <https://doi.org/10.3390/ijms22147326>
- 43 Han SR, Lee S-W (2014) *In vitro* selection of RNA aptamer specific to *Staphylococcus aureus*. *Ann Microbiol* 64:883–885. <https://doi.org/10.1007/s13213-013-0720-z>
- 44 Padroni G, Patwardhan NN, Schapira M *et al.* (2020) Systematic analysis of the interactions driving small molecule-RNA recognition. *RSC Med Chem* 11:802–813. <https://doi.org/10.1039/d0md00167h>
- 45 Tsuji S, Tanaka T, Hirabayashi N *et al.* (2009) RNA aptamer binding to polyhistidine-tag. *Biochem Biophys Res Commun* 386:227–231. <https://doi.org/10.1016/j.bbrc.2009.06.014>
- 46 Hunsicker A, Steber M, Mayer G *et al.* (2009) An RNA aptamer that induces transcription. *Chem Biol* 16:173–180. <https://doi.org/10.1016/j.chembiol.2008.12.008>
- 47 Dwidar M, Yokobayashi Y (2019) Development of a histamine aptasensor for food safety monitoring. *Sci Rep* 9:16659. <https://doi.org/10.1038/s41598-019-52876-1>
- 48 Conroy PJ, Hearty S, Leonard P *et al.* (2009) Antibody production, design and use for biosensor-based applications. *Semin Cell Dev Biol* 20:10–26. <https://doi.org/10.1016/j.semcdb.2009.01.010>
- 49 Park KS (2018) Nucleic acid aptamer-based methods for diagnosis of infections. *Biosens Bioelectron* 102:179–188. <https://doi.org/10.1016/j.bios.2017.11.028>

- 50 Ng EWM, Shima DT, Calias P *et al.* (2006) Pegaptanib, a targeted anti-VEGF aptamer for ocular vascular disease. *Nat Rev Drug Discov* 5:123–132. <https://doi.org/10.1038/nrd1955>
- 51 Zhou G, Wilson G, Hebbard L *et al.* (2016) Aptamers: A promising chemical antibody for cancer therapy. *Oncotarget* 7:13446–13463. <https://doi.org/10.18632/oncotarget.7178>
- 52 Flamme M, McKenzie LK, Sarac I *et al.* (2019) Chemical methods for the modification of RNA. *Methods* 161:64–82. <https://doi.org/10.1016/j.ymeth.2019.03.018>
- 53 Tuerk C, Gold L (1990) Systematic evolution of ligands by exponential enrichment: RNA ligands to bacteriophage T4 DNA polymerase. *Science* 249:505–510. <https://doi.org/10.1126/science.2200121>
- 54 Zhang Y, Lai BS, Juhas M (2019) Recent Advances in Aptamer Discovery and Applications. *Molecules* 24. <https://doi.org/10.3390/molecules24050941>
- 55 Nutiu R, Li Y (2005) *In vitro* selection of structure-switching signaling aptamers. *Angew Chem Int Ed Engl* 44:1061–1065. <https://doi.org/10.1002/anie.200461848>
- 56 Stoltenburg R, Nikolaus N, Strehlitz B (2012) Capture-SELEX: Selection of DNA Aptamers for Aminoglycoside Antibiotics. *J Anal Methods Chem* 2012:415697. <https://doi.org/10.1155/2012/415697>
- 57 Kramat J, Suess B (2022) Efficient Method to Identify Synthetic Riboswitches Using RNA-Based Capture-SELEX Combined with In Vivo Screening. *Methods Mol Biol* 2518:157–177. https://doi.org/10.1007/978-1-0716-2421-0_10
- 58 Boussebayle A, Groher F, Suess B (2019) RNA-based Capture-SELEX for the selection of small molecule-binding aptamers. *Methods* 161:10–15. <https://doi.org/10.1016/j.ymeth.2019.04.004>
- 59 Kraus L, Suess B (2023) RNA Capture-SELEX on Streptavidin Magnetic Beads. *Methods Mol Biol* 2570:63–71. https://doi.org/10.1007/978-1-0716-2695-5_5
- 60 Moreno M (2015) Aptasensor. In: Gargaud M, Irvine WM, Amils R (eds) *Encyclopedia of astrobiology*, Second edition. Springer, Heidelberg, pp 114–115
- 61 Farjami E, Campos R, Nielsen JS *et al.* (2013) RNA aptamer-based electrochemical biosensor for selective and label-free analysis of dopamine. *Anal Chem* 85:121–128. <https://doi.org/10.1021/ac302134s>
- 62 Hosseinzadeh L, Mazloum-Ardakani M (2020) Advances in aptasensor technology. *Adv Clin Chem* 99:237–279. <https://doi.org/10.1016/bs.acc.2020.02.010>
- 63 Ma X, Guo Z, Mao Z *et al.* (2017) Colorimetric theophylline aggregation assay using an RNA aptamer and non-crosslinking gold nanoparticles. *Mikrochim Acta* 185:33. <https://doi.org/10.1007/s00604-017-2606-4>
- 64 Rankin CJ, Fuller EN, Hamor KH *et al.* (2006) A simple fluorescent biosensor for theophylline based on its RNA aptamer. *Nucleosides Nucleotides Nucleic Acids* 25:1407–1424. <https://doi.org/10.1080/15257770600919084>
- 65 Lei S, Xu L, Liu Z *et al.* (2019) An enzyme-free and label-free signal-on aptasensor based on DNAzyme-driven DNA walker strategy. *Anal Chim Acta* 1081:59–64. <https://doi.org/10.1016/j.aca.2019.07.005>

- 66 Yang L, Zhong X, Huang L *et al.* (2019) C60@C3N4 nanocomposites as quencher for signal-off photoelectrochemical aptasensor with Au nanoparticle decorated perylene tetracarboxylic acid as platform. *Anal Chim Acta* 1077:281–287. <https://doi.org/10.1016/j.aca.2019.05.058>
- 67 Cheng AKH, Sen D, Yu H-Z (2009) Design and testing of aptamer-based electrochemical biosensors for proteins and small molecules. *Bioelectrochemistry* 77:1–12. <https://doi.org/10.1016/j.bioelechem.2009.04.007>
- 68 Wang H-M, Fang Y, Yuan P-X *et al.* (2019) Construction of ultrasensitive label-free aptasensor for thrombin detection using palladium nanocones boosted electrochemiluminescence system. *Electrochimica Acta* 310:195–202. <https://doi.org/10.1016/j.electacta.2019.04.093>
- 69 Aktas GB, Skouridou V, Masip L (2019) Sandwich-type aptasensor employing modified aptamers and enzyme-DNA binding protein conjugates. *Anal Bioanal Chem* 411:3581–3589. <https://doi.org/10.1007/s00216-019-01839-6>
- 70 Shafiei F, McAuliffe K, Bagheri Y *et al.* (2020) Paper-based fluorogenic RNA aptamer sensors for label-free detection of small molecules. *Anal Methods* 12:2674–2681. <https://doi.org/10.1039/d0ay00588f>
- 71 Cho EJ, Lee J-W, Ellington AD (2009) Applications of aptamers as sensors. *Annu Rev Anal Chem (Palo Alto Calif)* 2:241–264. <https://doi.org/10.1146/annurev.anchem.1.031207.112851>
- 72 Fischer NO, Tarasow TM, Tok JB-H (2007) Aptasensors for biosecurity applications. *Current Opinion in Chemical Biology* 11:316–328. <https://doi.org/10.1016/j.cbpa.2007.05.017>
- 73 Suez J, Korem T, Zeevi D *et al.* (2014) Artificial sweeteners induce glucose intolerance by altering the gut microbiota. *Nature* 514:181–186. <https://doi.org/10.1038/nature13793>
- 74 Schödl I, Hilliges F (2021) Vorkommen künstlicher Süßstoffe in deutschen Grundwässern. *Grundwasser - Zeitschrift der Fachsektion Hydrogeologie* 26:357–365. <https://doi.org/10.1007/s00767-021-00489-9>
- 75 Scheurer M, Brauch H-J, Lange FT (2009) Analysis and occurrence of seven artificial sweeteners in German waste water and surface water and in soil aquifer treatment (SAT). *Anal Bioanal Chem* 394:1585–1594. <https://doi.org/10.1007/s00216-009-2881-y>
- 76 Clauß K, Jensen H (1973) Oxathiazinondioxide, eine neue Gruppe von Süßstoffen. *Angew Chem* 85:965–973. <https://doi.org/10.1002/ange.19730852202>
- 77 Whitehouse CR, Boullata J, McCauley LA (2008) The potential toxicity of artificial sweeteners. *AAOHN J* 56:251-9; quiz 260-1. <https://doi.org/10.3928/08910162-20080601-02>
- 78 Renwick AG (1986) The metabolism of intense sweeteners. *Xenobiotica* 16:1057–1071. <https://doi.org/10.3109/00498258609038983>
- 79 Castronovo S, Wick A, Scheurer M *et al.* (2017) Biodegradation of the artificial sweetener acesulfame in biological wastewater treatment and sandfilters. *Water Res* 110:342–353. <https://doi.org/10.1016/j.watres.2016.11.041>

- 80 Loos R, Carvalho R, António DC *et al.* (2013) EU-wide monitoring survey on emerging polar organic contaminants in wastewater treatment plant effluents. *Water Res* 47:6475–6487. <https://doi.org/10.1016/j.watres.2013.08.024>
- 81 Packard VS (1978, 1976) *Processed foods and the consumer: Additives, labeling, standards, and nutrition.* University of Minnesota Press, Minneapolis
- 82 Kojima S, Ichibagase H (1966) Studies on synthetic sweetening agents. 8. Cyclohexylamine, a metabolite of sodium cyclamate. *Chem Pharm Bull (Tokyo)* 14:971–974. <https://doi.org/10.1248/cpb.14.971>
- 83 van Stempvoort DR, Robertson WD, Brown SJ (2011) Artificial Sweeteners in a Large Septic Plume. *Ground Water Monitoring & Remediation* 31:95–102. <https://doi.org/10.1111/j.1745-6592.2011.01353.x>
- 84 van Stempvoort DR, Roy JW, Brown SJ *et al.* (2011) Artificial sweeteners as potential tracers in groundwater in urban environments. *Journal of Hydrology* 401:126–133. <https://doi.org/10.1016/j.jhydrol.2011.02.013>
- 85 Fahlberg C, Remsen I (1879) Ueber die Oxydation des Orthotoluolsulfamids. *Ber Dtsch Chem Ges* 12:469–473. <https://doi.org/10.1002/cber.187901201135>
- 86 Pantarotto C, Salmona M, Garattini S (1981) Plasma kinetics and urinary elimination of saccharin in man. *Toxicol Lett* 9:367–371. [https://doi.org/10.1016/0378-4274\(81\)90012-6](https://doi.org/10.1016/0378-4274(81)90012-6)
- 87 Li S, Ren Y, Fu Y *et al.* (2018) Fate of artificial sweeteners through wastewater treatment plants and water treatment processes. *PLoS One* 13:e0189867. <https://doi.org/10.1371/journal.pone.0189867>
- 88 Gan Z, Sun H, Feng B *et al.* (2013) Occurrence of seven artificial sweeteners in the aquatic environment and precipitation of Tianjin, China. *Water Res* 47:4928–4937. <https://doi.org/10.1016/j.watres.2013.05.038>
- 89 Lapworth DJ, Baran N, Stuart ME *et al.* (2012) Emerging organic contaminants in groundwater: A review of sources, fate and occurrence. *Environ Pollut* 163:287–303. <https://doi.org/10.1016/j.envpol.2011.12.034>
- 90 Knight I (1994) The development and applications of sucralose, a new high-intensity sweetener. *Can J Physiol Pharmacol* 72:435–439. <https://doi.org/10.1139/y94-063>
- 91 Roberts A, Renwick AG, Sims J *et al.* (2000) Sucralose metabolism and pharmacokinetics in man. *Food and Chemical Toxicology* 38 Suppl 2:S31-41. [https://doi.org/10.1016/s0278-6915\(00\)00026-0](https://doi.org/10.1016/s0278-6915(00)00026-0)
- 92 Tollefsen KE, Nizzetto L, Huggett DB (2012) Presence, fate and effects of the intense sweetener sucralose in the aquatic environment. *Sci Total Environ* 438:510–516. <https://doi.org/10.1016/j.scitotenv.2012.08.060>
- 93 Torres CI, Ramakrishna S, Chiu C-A *et al.* (2011) Fate of Sucralose During Wastewater Treatment. *Environmental Engineering Science* 28:325–331. <https://doi.org/10.1089/ees.2010.0227>
- 94 Spoelstra J, Schiff SL, Brown SJ (2013) Artificial sweeteners in a large Canadian river reflect human consumption in the watershed. *PLoS One* 8:e82706. <https://doi.org/10.1371/journal.pone.0082706>

- 95 Zincke T (1905) Ueber die Einwirkung von Brom und von Chlor auf Phenole: Substitutionsproducte, Pseudobromide und Pseudochloride. *Justus Liebigs Ann Chem* 343:75–99. <https://doi.org/10.1002/jlac.19053430106>
- 96 Hoekstra EJ, Simoneau C (2013) Release of bisphenol A from polycarbonate: a review. *Crit Rev Food Sci Nutr* 53:386–402. <https://doi.org/10.1080/10408398.2010.536919>
- 97 Kang J-H, Asai D, Katayama Y (2007) Bisphenol A in the aquatic environment and its endocrine-disruptive effects on aquatic organisms. *Crit Rev Toxicol* 37:607–625. <https://doi.org/10.1080/10408440701493103>
- 98 Torres-García JL, Ahuactzin-Pérez M, Fernández FJ *et al.* (2022) Bisphenol A in the environment and recent advances in biodegradation by fungi. *Chemosphere* 303:134940. <https://doi.org/10.1016/j.chemosphere.2022.134940>
- 99 Vélez MP, Arbuckle TE, Fraser WD (2015) Female exposure to phenols and phthalates and time to pregnancy: the Maternal-Infant Research on Environmental Chemicals (MIREC) Study. *Fertil Steril* 103:1011-1020.e2. <https://doi.org/10.1016/j.fertnstert.2015.01.005>
- 100 Porta M, Lee D-H (2012) Review Of The Science Linking Chemical Exposures To The Human Risk Of Obesity And Diabetes. <https://chemtrust.org/obesity-and-diabetes/>
- 101 Umweltbundesamt (2010) Bisphenol A – Massenchemikalie mit unerwünschten Nebenwirkungen. <https://www.umweltbundesamt.de/publikationen/bisphenol-a?anfrage=Kennnummer&Suchwort=3782>
- 102 Lobos JH, Leib TK, Su TM (1992) Biodegradation of bisphenol A and other bisphenols by a gram-negative aerobic bacterium. *Appl Environ Microbiol* 58:1823–1831. <https://doi.org/10.1128/aem.58.6.1823-1831.1992>
- 103 Yu X, Xue J, Yao H *et al.* (2015) Occurrence and estrogenic potency of eight bisphenol analogs in sewage sludge from the U.S. EPA targeted national sewage sludge survey. *J Hazard Mater* 299:733–739. <https://doi.org/10.1016/j.jhazmat.2015.07.012>
- 104 Stachel B, Ehrhorn U, Heemken OP *et al.* (2003) Xenoestrogens in the River Elbe and its tributaries. *Environ Pollut* 124:497–507. [https://doi.org/10.1016/s0269-7491\(02\)00483-9](https://doi.org/10.1016/s0269-7491(02)00483-9)
- 105 Liao C, Liu F, Guo Y *et al.* (2012a) Occurrence of eight bisphenol analogues in indoor dust from the United States and several Asian countries: implications for human exposure. *Environ Sci Technol* 46:9138–9145. <https://doi.org/10.1021/es302004w>
- 106 Liao C, Liu F, Moon H-B *et al.* (2012b) Bisphenol analogues in sediments from industrialized areas in the United States, Japan, and Korea: spatial and temporal distributions. *Environ Sci Technol* 46:11558–11565. <https://doi.org/10.1021/es303191g>
- 107 Rastkari N, Ahmadkhaniha R, Yunesian M *et al.* (2010) Sensitive determination of bisphenol A and bisphenol F in canned food using a solid-phase microextraction fibre coated with single-walled carbon nanotubes before GC/MS. *Food Additives & Contaminants: Part A* 27:1460–1468. <https://doi.org/10.1080/19440049.2010.495730>
- 108 Xue J, Wu Q, Sakthivel S *et al.* (2015) Urinary levels of endocrine-disrupting chemicals, including bisphenols, bisphenol A diglycidyl ethers, benzophenones, parabens, and triclosan in obese and non-obese Indian children. *Environ Res* 137:120–128. <https://doi.org/10.1016/j.envres.2014.12.007>

- 109 Chen D, Kannan K, Tan H, Zheng Z, Feng YL, Wu Y, Widelka M (2016) Bisphenol Analogues Other Than BPA: Environmental Occurrence, Human Exposure, and Toxicity-A Review. *Environ Sci Technol* 50:5438–5453. <https://doi.org/10.1021/acs.est.5b05387>
- 110 Higashihara N, Shiraishi K, Miyata K *et al.* (2007) Subacute oral toxicity study of bisphenol F based on the draft protocol for the "Enhanced OECD Test Guideline no. 407". *Arch Toxicol* 81:825–832. <https://doi.org/10.1007/s00204-007-0223-4>
- 111 Eladak S, Grisin T, Moison D *et al.* (2015) A new chapter in the bisphenol A story: bisphenol S and bisphenol F are not safe alternatives to this compound. *Fertil Steril* 103:11–21. <https://doi.org/10.1016/j.fertnstert.2014.11.005>
- 112 Danzl E, Sei K, Soda S *et al.* (2009) Biodegradation of bisphenol A, bisphenol F and bisphenol S in seawater. *Int J Environ Res Public Health* 6:1472–1484. <https://doi.org/10.3390/ijerph6041472>
- 113 Ike M, Chen MY, Danzl E *et al.* (2006) Biodegradation of a variety of bisphenols under aerobic and anaerobic conditions. *Water Sci Technol* 53:153–159. <https://doi.org/10.2166/wst.2006.189>
- 114 Liao C, Liu F, Kannan K (2012) Bisphenol s, a new bisphenol analogue, in paper products and currency bills and its association with bisphenol a residues. *Environ Sci Technol* 46:6515–6522. <https://doi.org/10.1021/es300876n>
- 115 Xu Z, Tian L, Liu L *et al.* (2023) Food Thermal Labels are a Source of Dietary Exposure to Bisphenol S and Other Color Developers. *Environ Sci Technol* 57:4984–4991. <https://doi.org/10.1021/acs.est.2c09390>
- 116 Thayer KA, Taylor KW, Garantziotis S *et al.* (2016) Bisphenol A, Bisphenol S, and 4-Hydroxyphenyl 4-Isopropoxyphenylsulfone (BPSIP) in Urine and Blood of Cashiers. *Environ Health Perspect* 124:437–444. <https://doi.org/10.1289/ehp.1409427>
- 117 Pivnenko K, Pedersen GA, Eriksson E *et al.* (2015) Bisphenol A and its structural analogues in household waste paper. *Waste Manag* 44:39–47. <https://doi.org/10.1016/j.wasman.2015.07.017>
- 118 Naderi M, Kwong RWM (2020) A comprehensive review of the neurobehavioral effects of bisphenol S and the mechanisms of action: New insights from *in vitro* and *in vivo* models. *Environ Int* 145:106078. <https://doi.org/10.1016/j.envint.2020.106078>
- 119 Thoene M, Dzika E, Gonkowski S *et al.* (2020) Bisphenol S in Food Causes Hormonal and Obesogenic Effects Comparable to or Worse than Bisphenol A: A Literature Review. *Nutrients* 12. <https://doi.org/10.3390/nu12020532>
- 120 Žalmanová T, Hošková K, Nevoral J *et al.* (2016) Bisphenol S instead of bisphenol A: a story of reproductive disruption by regrettable substitution - a review. *Czech J Anim Sci* 61:433–449. <https://doi.org/10.17221/81/2015-CJAS>
- 121 Hoffmann-La Roche AG (2003) Roche-Lexikon Medizin: [62.000 Stichwörter, Tabellen, 40.000 englische Übersetzungen], 5., neu bearb. und erw. Aufl., [Neuausg.]. Elsevier, Urban & Fischer, München
- 122 Mutschler E (ed) (2008) Arzneimittelwirkungen: Lehrbuch der Pharmakologie und Toxikologie ; mit einführenden Kapiteln in die Anatomie, Physiologie und Pathophysiologie ; 264 Tabellen und 1357 Strukturformeln, 9., vollst. neu bearb. und erw. Aufl. Wiss. Verl.-Ges, Stuttgart

- 123 Martindale W, Reynolds JEF, Parfitt K (eds) (1989) *The extra pharmacopoeia*: Martindale, 29th ed. The Pharmaceutical Press, London
- 124 Zinner SH (2007) Antibiotic use: present and future. *New Microbiol* 30:321–325
- 125 Davies J, Davies D (2010) Origins and evolution of antibiotic resistance. *Microbiol Mol Biol Rev* 74:417–433. <https://doi.org/10.1128/MMBR.00016-10>
- 126 WHO (2021) Antimicrobial resistance. <https://www.who.int/en/news-room/fact-sheets/detail/antimicrobial-resistance>
- 127 Machowska A, Stålsby Lundborg C (2018) Drivers of Irrational Use of Antibiotics in Europe. *Int J Environ Res Public Health* 16. <https://doi.org/10.3390/ijerph16010027>
- 128 Kovalakova P, Cizmas L, McDonald TJ *et al.* (2020) Occurrence and toxicity of antibiotics in the aquatic environment: A review. *Chemosphere* 251:126351. <https://doi.org/10.1016/j.chemosphere.2020.126351>
- 129 Aminov RI (2009) The role of antibiotics and antibiotic resistance in nature. *Environ Microbiol* 11:2970–2988. <https://doi.org/10.1111/j.1462-2920.2009.01972.x>
- 130 Pan M, Chu LM (2018) Occurrence of antibiotics and antibiotic resistance genes in soils from wastewater irrigation areas in the Pearl River Delta region, southern China. *Sci Total Environ* 624:145–152. <https://doi.org/10.1016/j.scitotenv.2017.12.008>
- 131 Wu S, Hua P, Gui D *et al.* (2022) Occurrences, transport drivers, and risk assessments of antibiotics in typical oasis surface and groundwater. *Water Res* 225:119138. <https://doi.org/10.1016/j.watres.2022.119138>
- 132 Meng T, Cheng W, Wan T *et al.* (2021) Occurrence of antibiotics in rural drinking water and related human health risk assessment. *Environ Technol* 42:671–681. <https://doi.org/10.1080/09593330.2019.1642390>
- 133 Sneader W (2005) *Drug discovery: A history*. Wiley, Chichester, England
- 134 Suzuki J, Kunitomo T, Hori M (1970) Effects of kanamycin on protein synthesis: inhibition of elongation of peptide chains. *J Antibiot (Tokyo)* 23:99–101. <https://doi.org/10.7164/antibiotics.23.99>
- 135 Elsevier Ltd. (2008) Kanamycin. *Tuberculosis (Edinb)* 88:117–118. [https://doi.org/10.1016/S1472-9792\(08\)70012-X](https://doi.org/10.1016/S1472-9792(08)70012-X)
- 136 Carrer H, Hockenberry TN, Svab Z *et al.* (1993) Kanamycin resistance as a selectable marker for plastid transformation in tobacco. *Mol Gen Genet* 241:49–56. <https://doi.org/10.1007/BF00280200>
- 137 Woegerbauer M, Zeinzinger J, Gottsberger RA *et al.* (2015) Antibiotic resistance marker genes as environmental pollutants in GMO-pristine agricultural soils in Austria. *Environ Pollut* 206:342–351. <https://doi.org/10.1016/j.envpol.2015.07.028>
- 138 Atarashi S (2018) Research and Development of Quinolones in Daiichi Sankyo Co., Ltd. <https://infectweb.com/articles/400.html>
- 139 Drlica K, Zhao X (1997) DNA gyrase, topoisomerase IV, and the 4-quinolones. *Microbiol Mol Biol Rev* 61:377–392. <https://doi.org/10.1128/membr.61.3.377-392.1997>
- 140 Hooper DC (2001) Mechanisms of action of antimicrobials: focus on fluoroquinolones. *Clin Infect Dis* 32 Suppl 1:S9–S15. <https://doi.org/10.1086/319370>

- 141 Drlica K, Malik M, Kerns RJ *et al.* (2008) Quinolone-mediated bacterial death. *Antimicrob Agents Chemother* 52:385–392. <https://doi.org/10.1128/AAC.01617-06>
- 142 Mutschler E (ed) (2001) *Arzneimittelwirkungen: Lehrbuch der Pharmakologie und Toxikologie ; mit einführenden Kapiteln in die Anatomie, Physiologie und Pathophysiologie*, 8., völlig neu bearb. und erw. Aufl. Wiss. Verl.-Ges, Stuttgart
- 143 North DS, Fish DN, Redington JJ (1998) Levofloxacin, a second-generation fluoroquinolone. *Pharmacotherapy* 18:915–935
- 144 Sitovs A, Sartini I, Giorgi M (2021) Levofloxacin in veterinary medicine: a literature review. *Res Vet Sci* 137:111–126. <https://doi.org/10.1016/j.rvsc.2021.04.031>
- 145 Papich MG (2021) Antimicrobial agent use in small animals what are the prescribing practices, use of PK-PD principles, and extralabel use in the United States? *J Vet Pharmacol Ther* 44:238–249. <https://doi.org/10.1111/jvp.12921>
- 146 Vercelli C, Łebkowska-Wieruszewska B, Barbero R *et al.* (2020) Pharmacokinetics of levofloxacin in non-lactating goats and evaluation of drug effects on resistance in coliform rectal flora. *Res Vet Sci* 133:283–288. <https://doi.org/10.1016/j.rvsc.2020.09.028>
- 147 Sartini I, Łebkowska-Wieruszewska B, Kim TW *et al.* (2020) Pharmacokinetic and tissue analyses of levofloxacin in sheep (*Ovis aries* Linnaeus) after multiple-dose administration. *Res Vet Sci* 128:124–128. <https://doi.org/10.1016/j.rvsc.2019.11.008>
- 148 Wang C, Deng L, Zhu Y *et al.* (2021) Pharmacokinetics of levofloxacin mesylate in healthy adult giant panda after single-dose administration via different routes. *J Vet Pharmacol Ther* 44:644–649. <https://doi.org/10.1111/jvp.12945>
- 149 Fish DN, Chow AT (1997) The clinical pharmacokinetics of levofloxacin. *Clin Pharmacokinet* 32:101–119. <https://doi.org/10.2165/00003088-199732020-00002>
- 150 Lato SM, Boles AR, Ellington AD (1995) *In vitro* selection of RNA lectins: using combinatorial chemistry to interpret ribozyme evolution. *Chem Biol* 2:291–303. [https://doi.org/10.1016/1074-5521\(95\)90048-9](https://doi.org/10.1016/1074-5521(95)90048-9)
- 151 Boussebayle A, Torka D, Ollivaud S *et al.* (2019) Next-level riboswitch development-implementation of Capture-SELEX facilitates identification of a new synthetic riboswitch. *Nucleic Acids Res* 47:4883–4895. <https://doi.org/10.1093/nar/gkz216>
- 152 Wang Y, Rando RR (1995) Specific binding of aminoglycoside antibiotics to RNA. *Chem Biol* 2:281–290. [https://doi.org/10.1016/1074-5521\(95\)90047-0](https://doi.org/10.1016/1074-5521(95)90047-0)
- 153 Dhiman A, Anand A, Malhotra A *et al.* (2018) Rational truncation of aptamer for cross-species application to detect krait envenomation. *Sci Rep* 8:17795. <https://doi.org/10.1038/s41598-018-35985-1>
- 154 Hassan EM, Dixon BR, Sattar SA *et al.* (2021) Highly sensitive magnetic-microparticle-based aptasensor for *Cryptosporidium parvum* oocyst detection in river water and wastewater: Effect of truncation on aptamer affinity. *Talanta* 222:121618. <https://doi.org/10.1016/j.talanta.2020.121618>
- 155 Macdonald J, Houghton P, Xiang D *et al.* (2016) Truncation and Mutation of a Transferrin Receptor Aptamer Enhances Binding Affinity. *Nucleic Acid Ther* 26:348–354. <https://doi.org/10.1089/nat.2015.0585>
- 156 Gruber AR, Lorenz R, Bernhart SH *et al.* (2008) The Vienna RNA websuite. *Nucleic Acids Res* 36:W70-4. <https://doi.org/10.1093/nar/gkn188>

- 157 Kerpedjiev P, Hammer S, Hofacker IL (2015) Forna (force-directed RNA): Simple and effective online RNA secondary structure diagrams. *Bioinformatics* 31:3377–3379. <https://doi.org/10.1093/bioinformatics/btv372>
- 158 Soukup GA, Breaker RR (1999) Relationship between internucleotide linkage geometry and the stability of RNA. *RNA* 5:1308–1325. <https://doi.org/10.1017/s1355838299990891>
- 159 Komarova N, Kuznetsov A (2019) Inside the Black Box: What Makes SELEX Better? *Molecules* 24. <https://doi.org/10.3390/molecules24193598>
- 160 Hall B, Micheletti JM, Satya P *et al.* (2009) Design, synthesis, and amplification of DNA pools for *in vitro* selection. *Curr Protoc Nucleic Acid Chem* Chapter 9:Unit 9.2. <https://doi.org/10.1002/0471142700.nc0902s39>
- 161 Sampson T (2003) Aptamers and SELEX: the technology. *World Patent Information* 25:123–129. [https://doi.org/10.1016/S0172-2190\(03\)00035-8](https://doi.org/10.1016/S0172-2190(03)00035-8)
- 162 Stoltenburg R, Reinemann C, Strehlitz B (2007) SELEX--a (r)evolutionary method to generate high-affinity nucleic acid ligands. *Biomol Eng* 24:381–403. <https://doi.org/10.1016/j.bioeng.2007.06.001>
- 163 Salehi-Ashtiani K, Szostak JW (2001) *In vitro* evolution suggests multiple origins for the hammerhead ribozyme. *Nature* 414:82–84. <https://doi.org/10.1038/35102081>
- 164 Jenison RD, Gill SC, Pardi A *et al.* (1994) High-resolution molecular discrimination by RNA. *Science* 263:1425–1429. <https://doi.org/10.1126/science.7510417>
- 165 Berens C, Thain A, Schroeder R (2001) A tetracycline-binding RNA aptamer. *Bioorg Med Chem* 9:2549–2556. [https://doi.org/10.1016/s0968-0896\(01\)00063-3](https://doi.org/10.1016/s0968-0896(01)00063-3)
- 166 Wallis MG, Ahsen U von, Schroeder R *et al.* (1995) A novel RNA motif for neomycin recognition. *Chem Biol* 2:543–552. [https://doi.org/10.1016/1074-5521\(95\)90188-4](https://doi.org/10.1016/1074-5521(95)90188-4)
- 167 Breaker RR (2012) Riboswitches and the RNA world. *Cold Spring Harb Perspect Biol* 4. <https://doi.org/10.1101/cshperspect.a003566>
- 168 Kirsebom LA, Virtanen A, Mikkelsen NE (2006) Aminoglycoside interactions with RNAs and nucleases. *Handb Exp Pharmacol* 173:73–96. https://doi.org/10.1007/3-540-27262-3_4
- 169 Yan R, Li X, Liu Y *et al.* (2022) Design, Synthesis, and Bioassay of 2'-Modified Kanamycin A. *Molecules* 27. <https://doi.org/10.3390/molecules27217482>
- 170 Nikolaus N, Strehlitz B (2014) DNA-aptamers binding aminoglycoside antibiotics. *Sensors (Basel)* 14:3737–3755. <https://doi.org/10.3390/s140203737>
- 171 Weigand JE, Sanchez M, Gunnesch E-B *et al.* (2008) Screening for engineered neomycin riboswitches that control translation initiation. *RNA* 14:89–97. <https://doi.org/10.1261/rna.772408>
- 172 Jiang L, Majumdar A, Hu W *et al.* (1999) Saccharide-RNA recognition in a complex formed between neomycin B and an RNA aptamer. *Structure* 7:817–827. [https://doi.org/10.1016/s0969-2126\(99\)80105-1](https://doi.org/10.1016/s0969-2126(99)80105-1)
- 173 Patel DJ, Suri AK, Jiang F *et al.* (1997) Structure, recognition and adaptive binding in RNA aptamer complexes. *J Mol Biol* 272:645–664. <https://doi.org/10.1006/jmbi.1997.1281>
- 174 Jiang L, Patel DJ (1998) Solution structure of the tobramycin-RNA aptamer complex. *Nat Struct Biol* 5:769–774. <https://doi.org/10.1038/1804>

- 175 Hermann T, Westhof E (1998) Aminoglycoside binding to the hammerhead ribozyme: a general model for the interaction of cationic antibiotics with RNA. *J Mol Biol* 276:903–912. <https://doi.org/10.1006/jmbi.1997.1590>
- 176 Tor Y, Hermann T, Westhof E (1998) Deciphering RNA recognition: aminoglycoside binding to the hammerhead ribozyme. *Chem Biol* 5:R277-83. [https://doi.org/10.1016/s1074-5521\(98\)90286-1](https://doi.org/10.1016/s1074-5521(98)90286-1)
- 177 Tor Y (2003) Targeting RNA with small molecules. *Chembiochem* 4:998–1007. <https://doi.org/10.1002/cbic.200300680>
- 178 Walter F, Vicens Q, Westhof E (1999) Aminoglycoside-RNA interactions. *Current Opinion in Chemical Biology* 3:694–704. [https://doi.org/10.1016/s1367-5931\(99\)00028-9](https://doi.org/10.1016/s1367-5931(99)00028-9)
- 179 Levine HA, Seo Y-J (2015) Discrete Dynamical Systems in Multiple Target and Alternate SELEX. *SIAM J Appl Dyn Syst* 14:1048–1101. <https://doi.org/10.1137/130946368>
- 180 Levine HA, Nilsen-Hamilton M (2007) A mathematical analysis of SELEX. *Comput Biol Chem* 31:11–35. <https://doi.org/10.1016/j.compbiolchem.2006.10.002>
- 181 Sun F, Galas D, Waterman MS (1996) A mathematical analysis of *in vitro* molecular selection-amplification. *J Mol Biol* 258:650–660. <https://doi.org/10.1006/jmbi.1996.0276>
- 182 Srinivasan J, Cload ST, Hamaguchi N *et al.* (2004) ADP-specific sensors enable universal assay of protein kinase activity. *Chem Biol* 11:499–508. <https://doi.org/10.1016/j.chembiol.2004.03.014>
- 183 Irvine D, Tuerk C, Gold L (1991) SELEXION. Systematic evolution of ligands by exponential enrichment with integrated optimization by non-linear analysis. *J Mol Biol* 222:739–761. [https://doi.org/10.1016/0022-2836\(91\)90509-5](https://doi.org/10.1016/0022-2836(91)90509-5)
- 184 Aita T, Nishigaki K, Husimi Y (2012) Theoretical consideration of selective enrichment in *in vitro* selection: optimal concentration of target molecules. *Math Biosci* 240:201–211. <https://doi.org/10.1016/j.mbs.2012.07.006>
- 185 Wang J, Rudzinski JF, Gong Q *et al.* (2012) Influence of target concentration and background binding on *in vitro* selection of affinity reagents. *PLoS One* 7:e43940. <https://doi.org/10.1371/journal.pone.0043940>
- 186 Tsuji S, Hirabayashi N, Kato S *et al.* (2009) Effective isolation of RNA aptamer through suppression of PCR bias. *Biochem Biophys Res Commun* 386:223–226. <https://doi.org/10.1016/j.bbrc.2009.06.013>
- 187 Coleman TM, Huang F (2002) RNA-catalyzed thioester synthesis. *Chem Biol* 9:1227–1236. [https://doi.org/10.1016/s1074-5521\(02\)00264-8](https://doi.org/10.1016/s1074-5521(02)00264-8)
- 188 Coleman TM, Huang F (2005) Optimal random libraries for the isolation of catalytic RNA. *RNA Biol* 2:129–136. <https://doi.org/10.4161/rna.2.4.2285>
- 189 Thiel WH, Bair T, Wyatt Thiel K *et al.* (2011) Nucleotide bias observed with a short SELEX RNA aptamer library. *Nucleic Acid Ther* 21:253–263. <https://doi.org/10.1089/nat.2011.0288>
- 190 Falese JP, Donlic A, Hargrove AE (2021) Targeting RNA with small molecules: from fundamental principles towards the clinic. *Chem Soc Rev* 50:2224–2243. <https://doi.org/10.1039/d0cs01261k>

- 191 Kohlberger M, Gadermaier G (2022) SELEX: Critical factors and optimization strategies for successful aptamer selection. *Biotechnol Appl Biochem* 69:1771–1792. <https://doi.org/10.1002/bab.2244>
- 192 Saitoh H, Nakamura A, Kuwahara M *et al.* (2002) Modified DNA aptamers against sweet agent aspartame. *Nucleic Acids Res Suppl*:215–216. <https://doi.org/10.1093/nass/2.1.215>
- 193 Song K-M, Jeong E, Jeon W *et al.* (2012) Aptasensor for ampicillin using gold nanoparticle based dual fluorescence-colorimetric methods. *Anal Bioanal Chem* 402:2153–2161. <https://doi.org/10.1007/s00216-011-5662-3>
- 194 Lee A-Y, Ha N-R, Jung I-P *et al.* (2017) Development of a ssDNA aptamer for detection of residual benzylpenicillin. *Anal Biochem* 531:1–7. <https://doi.org/10.1016/j.ab.2017.05.013>
- 195 Han SR, Yu J, Lee S-W (2014) *In vitro* selection of RNA aptamers that selectively bind danofloxacin. *Biochem Biophys Res Commun* 448:397–402. <https://doi.org/10.1016/j.bbrc.2014.04.103>
- 196 Reinemann C, Freiin von Fritsch U, Rudolph S *et al.* (2016) Generation and characterization of quinolone-specific DNA aptamers suitable for water monitoring. *Biosens Bioelectron* 77:1039–1047. <https://doi.org/10.1016/j.bios.2015.10.069>
- 197 Jaeger J, Groher F, Stamm J *et al.* (2019) Characterization and Inkjet Printing of an RNA Aptamer for Paper-Based Biosensing of Ciprofloxacin. *Biosensors (Basel)* 9. <https://doi.org/10.3390/bios9010007>
- 198 Niazi JH, Lee SJ, Gu MB (2008) Single-stranded DNA aptamers specific for antibiotics tetracyclines. *Bioorg Med Chem* 16:7245–7253. <https://doi.org/10.1016/j.bmc.2008.06.033>
- 199 Niazi JH, Lee SJ, Kim YS *et al.* (2008) ssDNA aptamers that selectively bind oxytetracycline. *Bioorg Med Chem* 16:1254–1261. <https://doi.org/10.1016/j.bmc.2007.10.073>
- 200 Mehta J, van Dorst B, Rouah-Martin E *et al.* (2011) *In vitro* selection and characterization of DNA aptamers recognizing chloramphenicol. *J Biotechnol* 155:361–369. <https://doi.org/10.1016/j.jbiotec.2011.06.043>
- 201 Groher F, Bofill-Bosch C, Schneider C *et al.* (2018) Riboswitching with ciprofloxacin-development and characterization of a novel RNA regulator. *Nucleic Acids Res* 46:2121–2132. <https://doi.org/10.1093/nar/gkx1319>
- 202 Kaiser C, Schneider J, Groher F *et al.* (2021) What defines a synthetic riboswitch? - Conformational dynamics of ciprofloxacin aptamers with similar binding affinities but varying regulatory potentials. *Nucleic Acids Res* 49:3661–3671. <https://doi.org/10.1093/nar/gkab166>
- 203 Caglayan MO, Şahin S, Üstündağ Z (2022) An Overview of Aptamer-Based Sensor Platforms for the Detection of Bisphenol-A. *Crit Rev Anal Chem*:1–22. <https://doi.org/10.1080/10408347.2022.2113359>
- 204 Liu L, Yu H, Zhao Q (2022) The Characterization of Binding between Aptamer and Bisphenol A and Developing Electrochemical Aptasensors for Bisphenol A with Rationally Engineered Aptamers. *Biosensors (Basel)* 12. <https://doi.org/10.3390/bios12110913>

- 205 Jo M, Ahn J-Y, Lee J *et al.* (2011) Development of single-stranded DNA aptamers for specific Bisphenol a detection. *Oligonucleotides* 21:85–91. <https://doi.org/10.1089/oli.2010.0267>
- 206 Sambrook J, Russell DW (2001) *Molecular cloning: A laboratory manual*, 3rd ed. Cold Spring Harbor Laboratory Press, Cold Spring Harbor, N.Y
- 207 Smallwood IM (1996) *Handbook of organic solvent properties*. Halsted Pr. (Wiley); Arnold, New York, London
- 208 Lama RF, Lu BC-Y (1965) Excess Thermodynamic Properties of Aqueous Alcohol Solutions. *J Chem Eng Data* 10:216–219. <https://doi.org/10.1021/je60026a003>
- 209 Guo W, Zhang C, Ma T *et al.* (2021) Advances in aptamer screening and aptasensors' detection of heavy metal ions. *J Nanobiotechnology* 19:166. <https://doi.org/10.1186/s12951-021-00914-4>
- 210 Mann D, Reinemann C, Stoltenburg R *et al.* (2005) *In vitro* selection of DNA aptamers binding ethanolamine. *Biochem Biophys Res Commun* 338:1928–1934. <https://doi.org/10.1016/j.bbrc.2005.10.172>
- 211 Stoltenburg R, Reinemann C, Strehlitz B (2005) FluMag-SELEX as an advantageous method for DNA aptamer selection. *Anal Bioanal Chem* 383:83–91. <https://doi.org/10.1007/s00216-005-3388-9>
- 212 Yang D-K, Chen L-C, Lee M-Y *et al.* (2014) Selection of aptamers for fluorescent detection of alpha-methylacyl-CoA racemase by single-bead SELEX. *Biosens Bioelectron* 62:106–112. <https://doi.org/10.1016/j.bios.2014.06.027>
- 213 Mondal B, Ramlal S, Lavu PSR *et al.* (2015) A combinatorial systematic evolution of ligands by exponential enrichment method for selection of aptamer against protein targets. *Appl Microbiol Biotechnol* 99:9791–9803. <https://doi.org/10.1007/s00253-015-6858-9>
- 214 Jia W, Li H, Wilkop T *et al.* (2018) Silver decahedral nanoparticles empowered SPR imaging-SELEX for high throughput screening of aptamers with real-time assessment. *Biosens Bioelectron* 109:206–213. <https://doi.org/10.1016/j.bios.2018.02.029>
- 215 Spiga FM, Maietta P, Guiducci C (2015) More DNA-Aptamers for Small Drugs: A Capture-SELEX Coupled with Surface Plasmon Resonance and High-Throughput Sequencing. *ACS Comb Sci* 17:326–333. <https://doi.org/10.1021/acscombsci.5b00023>
- 216 Wochner A, Glökler J (2007) Nonradioactive fluorescence microtiter plate assay monitoring aptamer selections. *Biotechniques* 42:578, 580, 582. <https://doi.org/10.2144/000112472>
- 217 Amano R, Aoki K, Miyakawa S *et al.* (2017) NMR monitoring of the SELEX process to confirm enrichment of structured RNA. *Sci Rep* 7:283. <https://doi.org/10.1038/s41598-017-00273-x>
- 218 Müller J, El-Maarri O, Oldenburg J *et al.* (2008) Monitoring the progression of the *in vitro* selection of nucleic acid aptamers by denaturing high-performance liquid chromatography. *Anal Bioanal Chem* 390:1033–1037. <https://doi.org/10.1007/s00216-007-1699-8>
- 219 Vanbrabant J, Leirs K, Vanschoenbeek K *et al.* (2014) reMelting curve analysis as a tool for enrichment monitoring in the SELEX process. *Analyst* 139:589–595. <https://doi.org/10.1039/c3an01884a>

- 220 Luo Z, He L, Wang J *et al.* (2017) Developing a combined strategy for monitoring the progress of aptamer selection. *Analyst* 142:3136–3139. <https://doi.org/10.1039/c7an01131h>
- 221 Charlton J, Smith D (1999) Estimation of SELEX pool size by measurement of DNA renaturation rates. *RNA* 5:1326–1332. <https://doi.org/10.1017/s1355838299991021>
- 222 Gu G, Wang T, Yang Y *et al.* (2013) An improved SELEX-Seq strategy for characterizing DNA-binding specificity of transcription factor: NF- κ B as an example. *PLoS One* 8:e76109. <https://doi.org/10.1371/journal.pone.0076109>
- 223 Schütze T, Wilhelm B, Greiner N *et al.* (2011) Probing the SELEX process with next-generation sequencing. *PLoS One* 6:e29604. <https://doi.org/10.1371/journal.pone.0029604>
- 224 Mencin N, Šmuc T, Vraničar M *et al.* (2014) Optimization of SELEX: comparison of different methods for monitoring the progress of *in vitro* selection of aptamers. *J Pharm Biomed Anal* 91:151–159. <https://doi.org/10.1016/j.jpba.2013.12.031>
- 225 Civit L, Taghdisi SM, Jonczyk A *et al.* (2018) Systematic evaluation of cell-SELEX enriched aptamers binding to breast cancer cells. *Biochimie* 145:53–62. <https://doi.org/10.1016/j.biochi.2017.10.007>
- 226 Stoltenburg R, Strehlitz B (2018) Refining the Results of a Classical SELEX Experiment by Expanding the Sequence Data Set of an Aptamer Pool Selected for Protein A. *Int J Mol Sci* 19. <https://doi.org/10.3390/ijms19020642>
- 227 Djurdjevic P, Jakovljevic I, Joksovic L *et al.* (2014) The effect of some fluoroquinolone family members on biospeciation of copper(II), nickel(II) and zinc(II) ions in human plasma. *Molecules* 19:12194–12223. <https://doi.org/10.3390/molecules190812194>
- 228 Zhao Y, Ong S, Chen Y *et al.* (2022) Label-free and Dye-free Fluorescent Sensing of Tetracyclines Using a Capture-Selected DNA Aptamer. *Anal Chem* 94:10175–10182. <https://doi.org/10.1021/acs.analchem.2c01561>
- 229 McKeague M, Girolamo A de, Valenzano S *et al.* (2015) Comprehensive analytical comparison of strategies used for small molecule aptamer evaluation. *Anal Chem* 87:8608–8612. <https://doi.org/10.1021/acs.analchem.5b02102>
- 230 Dolati S, Ramezani M, Nabavinia MS *et al.* (2018) Selection of specific aptamer against enrofloxacin and fabrication of graphene oxide based label-free fluorescent assay. *Anal Biochem* 549:124–129. <https://doi.org/10.1016/j.ab.2018.03.021>

7 Appendices

7.1 List of figures

Figure 1 The RNA Capture-SELEX method	8
Figure 2 Chemical structural formulae of synthetic sweeteners	11
Figure 3 Chemical structural formulae of bisphenols and a degradation product	13
Figure 4 Chemical structural formulae of antibiotics	16
Figure 5 Test Capture-SELEX against kanamycin A	19
Figure 6 Capture-SELEX against synthetic sweeteners	20
Figure 7 Capture-SELEX against bisphenols A, F, S and the possible bisphenol A degradation product 4-hydroxyacetophenone	22
Figure 8 Capture-SELEX variations for optimising the selection against bisphenol A	25
Figure 9 Analysis of the ethanol-based enrichment of the bisphenol A Capture-SELEX with non-specific elution control using an enriched kanamycin A Capture-SELEX pool	27
Figure 10 Continuation of the former bisphenol A Capture-SELEX against the monohydric alcohols methanol, ethanol and isopropanol	28
Figure 11 Capture-SELEX-based elution assay with potential monohydric alcohol-binding aptamers	32
Figure 12 Predicted secondary structure of the potential isopropanol aptamer I	33
Figure 13 Predicted secondary structure of all truncations of the potential isopropanol aptamer I	34
Figure 14 Capture-SELEX-based elution assay with truncations of potential isopropanol-binding aptamer I	35
Figure 15 Capture-SELEX with the target molecule kanamycin A	37
Figure 16 Capture-SELEX with the target molecule levofloxacin	39
Figure 17 Multiple analyses of the data obtained from Next Generation Sequencing (NGS)	41
Figure 18 Capture-SELEX-based elution assay with potential levofloxacin-binding aptamers	44
Figure 19 ITC measurement and predicted secondary structure of the aptamer LXC	46
Figure 20 ITC-based analysis of truncations and mutation of the aptamer LXC with predicted secondary structures of LXC, shortenings 68 and 76 as well as the mutant trLXC	47
Figure 21 Summary of all mutations applied to the LX-binding aptamer trLXC	48
Figure 22 Summary of the ITC-based analysis of mutations of the aptamer trLXC	50
Figure 23 In-line probing experiment for trLXC	52
Figure 24 Assessment of the localisation of the ligand binding site by signal intensity quantification as a function of LX concentration	53

7.2 List of tables

Table 1 RNA sequences of potential aptamers against the monohydric alcohols EtOH and i-PrOH _____	31
Table 2 RNA sequences of potential aptamers against LX _____	43
Table 3 Summary of examples of antibiotic-binding aptamers _____	63
Table 4 Summary of used chemicals as well as purchased solutions and their sources of supply _____	73
Table 5 Summary of used enzymes as well as commercial buffers and their sources of supply _____	74
Table 6 Summary of used Nucleotides as well as size standard and their sources of supply _____	75
Table 7 List of all used DNA oligonucleotides purchased desalted from Sigma-Aldrich (Merck, Darmstadt) _____	75
Table 8 Summary of used bacterial strains and their sources of supply _____	78
Table 9 Summary of used plasmids and their plasmid map _____	79
Table 10 Summary of used kits and their sources of supply _____	80
Table 11 Summary of used consumables as well as auxiliaries and their sources of supply _____	80
Table 12 Summary of used instruments and their manufacturers _____	80
Table 13 Summary of used software and their developers _____	81
Table 14 Reaction set-up and PCR programme for amplification of DNA template pool _____	83
Table 15 Reaction set-up for <i>in vitro</i> transcription of RNA start pool for Capture-SELEX _____	84
Table 16 Programme for reverse transcription of precipitated RNA and PCR amplification of cDNA _____	85
Table 17 Formulations of solutions and buffers used for <i>in vitro</i> selection _____	86
Table 18 Formulations of solutions and buffers used for cloning and sequencing of individual selection rounds _____	88
Table 19 Reaction set-up and PCR programme for PCR _____	89
Table 20 Reaction set-up and PCR programme for overhang filling PCR _____	89
Table 21 Reaction set-up and controls for ligation of aptamer insert and pHDV vector _____	90
Table 22 Reaction set-up and PCR programme of colony PCR _____	91
Table 23 Reaction set-ups for large-scale and Capture-SELEX <i>in vitro</i> transcription _____	92
Table 24 Formulations of solutions and buffers used for gel purification of RNA _____	93
Table 25 Compositions of in-line probing samples _____	96
Table 26 Formulations of solutions and buffers used for in-line probing _____	97
Table 27 Values of the signal intensity measurement of specific areas of the in-line probing gels _____	118

7.3 Abbreviations

(v/v)	volume per volume	KM	kanamycin A
μM	$\mu\text{mol} \cdot \text{L}^{-1}$	LB	lysogeny broth
A	adenine	LFA	lateral flow assay
approx.	approximately	LX	levofloxacin
APS	ammonium persulfate	M	$\text{mol} \cdot \text{L}^{-1}$
aRNA	antisense ribonucleic acid	$\text{Mg}(\text{Ac})_2$	magnesium acetate
ATP	adenosine triphosphate	MgCl_2	magnesium chloride
AuNP	gold nanoparticle	mM	$\text{mmol} \cdot \text{L}^{-1}$
B&W	binding and wash buffer	mRNA	messenger ribonucleic acid
BPA	bisphenol A	MWCO	molecular weight cut-off columns
BPF	bisphenol F	Na_2CO_3	sodium carbonate
BPS	bisphenol S	NaAc	sodium acetate
C	cytosine	NaCl	sodium chloride
cf.	lat.: <i>confer</i> - compare	Na-EDTA	ethylenediamine tetraacetic acid disodium salt dihydrate
CO	capture oligonucleotide	NGS	Next Generation Sequencing
CPM	counts per minute	NH_4Ac	ammonium acetate
CSB	Capture-SELEX buffer	nM	$\text{nmol} \cdot \text{L}^{-1}$
CX	ciprofloxacin	nt	nucleotide
DMSO	dimethyl sulfoxide	NTP	nucleoside triphosphates
DNA	deoxyribonucleic acid	PAA	polyacrylamide
dNTP	deoxynucleoside triphosphates	PAGE	polyacrylamide gel electrophoresis
DTT	dithiothreitol	PCR	polymerase chain reaction
<i>E. coli</i>	<i>Escherichia coli</i>	RNA	ribonucleic acid
e.g.	lat.: <i>exempli gratia</i> for example	RPM	reads per million
EDTA	ethylenediaminetetraacetic acid	rRNA	ribosomal ribonucleic acid
EtOH	ethanol	RT-PCR	reverse transcription polymerase chain reaction
G	guanine	SELEX	systematic evolution of ligands by exponential enrichment
HAP	4-hydroxyacetophenone	T	thymine
HCl	hydrochloric acid	TAE	Tis/acetic acid/EDTA
HEPES	4-(2-hydroxyethyl)-1-piperazineethanesulfonic acid	TBE	Tris/borate/EDTA
ITC	isothermal titration calorimetry	TEMED	tetramethyl ethylenediamine
K_2HPO_4	dipotassium phosphate	TM	tobramycin
KCl	potassium chloride	Top25	25 most abundant sequences
K_D	dissociation constant	Tris	tris(hydroxymethyl)aminomethane
KH_2PO_4	potassium dihydrogen phosphate	U	uracil
		UTP	uridine triphosphate

7.4 Supplementary data

Table 27 Values of the signal intensity measurement of specific areas of the in-line probing gels

Position	U4		U10-A11		A17-C20	
c(Lx) ¹	Measured ² [e+05]	Normalised ³	Measured ² [e+05]	Normalised ³	Measured ² [e+05]	Normalised ³
0	18.7	0.97	6.9	0.94	12.0	0.89
10 nM	19.3	1.00	7.2	0.97	12.5	0.93
100 nM	19.2	0.99	6.9	0.94	12.9	0.96
500 nM	18.8	0.97	7.4	1.00	13.5	1.00
1 µM	18.5	0.96	7.2	0.98	13.2	0.98
10 µM	18.5	0.96	6.0	0.82	12.4	0.92
100 µM	18.7	0.97	5.2	0.70	11.6	0.86
500 µM	18.9	0.98	4.7	0.64	11.9	0.88
1 mM	19.1	0.99	4.5	0.61	10.9	0.81
Position	U25-U29		U29		G35	
c(Lx) ¹	Measured ² [e+05]	Normalised ³	Measured ² [e+05]	Normalised ³	Measured ² [e+05]	Normalised ³
0	10.5	0.96	13.7	0.94	11.3	0.98
10 nM	11.0	1.00	14.5	1.00	11.4	0.98
100 nM	10.5	0.96	13.8	0.95	11.2	0.97
500 nM	10.7	0.98	14.1	0.97	11.6	1.00
1 µM	10.7	0.97	14.1	0.97	11.4	0.99
10 µM	9.3	0.85	12.0	0.83	11.1	0.96
100 µM	8.5	0.77	9.8	0.67	11.1	0.96
500 µM	8.5	0.77	10.0	0.69	11.0	0.96
1 mM	7.8	0.71	8.2	0.56	11.2	0.97
Position	G39-C43		A47-G50		U54-C58	
c(Lx) ¹	Measured ² [e+05]	Normalised ³	Measured ² [e+05]	Normalised ³	Measured ² [e+05]	Normalised ³
0	16.4	0.96	14.4	0.83	22.2	0.95
10 nM	17.1	1.00	15.0	0.87	23.0	0.99
100 nM	16.6	0.97	14.8	0.86	22.6	0.97
500 nM	16.9	0.99	15.1	0.87	23.3	1.00
1 µM	17.0	0.99	15.3	0.89	23.0	0.99
10 µM	16.2	0.95	15.4	0.89	20.7	0.89
100 µM	15.9	0.93	16.4	0.95	20.2	0.87
500 µM	16.0	0.94	17.3	1.00	20.6	0.89
1 mM	14.5	0.85	15.71	0.91	19.8	0.85

¹ Indication of the concentration of levofloxacin

² Indication of the measured values

³ Indication of the measured values normalised to the highest intensity value

Curriculum Vitae

Name Janice Kramat

Higher education

2020 – 2023 PhD at the Department of Biology, Synthetic RNA biology
Technische Universität Darmstadt, Germany
Dissertation title: Development of RNA aptamers binding
environmental and food contaminants
Intended degree: Dr. rer. nat.

2017 – 2020 Studies in Biochemistry
Universität Greifswald, Germany
Master thesis title: Untersuchungen zur Degradation und Aktivität des
Regulatorproteins MgsR in *Bacillus subtilis*
Degree: Master of Science

2014 – 2017 Studies in Biochemistry
Universität Greifswald, Germany
Bachelor thesis title: Klonierung und Expression eines Potato-Inhibitor-
like Proteins aus den Speicheldrüsenzellen
von *Hirudo verbana*
Degree: Bachelor of Science

School education

2006 – 2014 Lessing-Gymnasium Hoyerswerda, Germany
Degree: Abitur

2002 – 2006 Grundschule Laubusch, Germany

Publication

Kramat J, Suess B. (2022) Efficient Method to Identify Synthetic Riboswitches Using RNA-Based Capture-SELEX Combined with *In vivo* Screening. *Methods Mol Biol.* doi: 10.1007/978-1-0716-2421-0_10

Kramat J, Kraus L *et al.* Publication on the levofloxacin-binding aptamer trLXC and its application as a receptor in a lateral flow assay (in preparation)

Attendance at meetings and conferences

Aptamers 2021 (Virtual), Oxford, UK (attended)

Cold Spring Harbor Asia 2021 (Hybrid meeting), Suzhou, China (poster and flash talk)

German Conference on Synthetic Biology 2021 (Virtual), Darmstadt/Munich, Germany (attended)

Aptamers 2022 (Virtual), Oxford, UK (attended)

International Synthetic Biology Workshop 2023, Darmstadt, Germany (attended)

Supervised thesis and student competitions

Jasmin Sarah Hallstein (Master Thesis 2021/2022)

Selektion und Charakterisierung synthetischer Riboswitche mit RNA-Capture-SELEX und Fluoreszenz-basiertem Screening in *S. cerevisiae*

SensUs international student competition 2022, Team of TU Darmstadt (TUcanSense), contact person for biological topics

Awarded the 'Athene Preis für Gute Lehre - Sonderpreis Interdisziplinäre Lehre' as part of the Carlo and Karin Giersch Foundation's teaching award at TU Darmstadt

SensUs international student competition 2023, Team of TU Darmstadt (TUcanSense), contact person for biological topics

Ehrenwörtliche Erklärung

Ehrenwörtliche Erklärung

Ich erkläre hiermit, dass ich die vorliegende Arbeit entsprechend den Regeln guter wissenschaftlicher Praxis selbstständig und ohne unzulässige Hilfe Dritter angefertigt habe.

Sämtliche aus fremden Quellen direkt oder indirekt übernommenen Gedanken sowie sämtliche von Anderen direkt oder indirekt übernommenen Daten, Techniken und Materialien sind als solche kenntlich gemacht. Die Arbeit wurde bisher bei keiner anderen Hochschule zu Prüfungszwecken eingereicht. Die eingereichte elektronische Version stimmt mit der schriftlichen Version überein.

Darmstadt, den 07.08.2023

Danksagung

Ein besonderer Dank gilt Frau **Prof. Dr. Beatrix Süß**, welche es mir erst ermöglicht hat meine Doktorarbeit unter Bereitstellung des Themas sowie des Arbeitsplatzes in ihrer Arbeitsgruppe durchzuführen. Vielen Dank für die tolle Betreuung sowie Leitung durch über 3 Jahre Forschung mit interessanten Gesprächen, das Teilen von Wissen und Erfahrungen sowie Eröffnung neuer Blickwinkel. Weiterhin bin ich sehr dankbar, dass trotz der Corona-Pandemie und allen damit einhergegangenen Einschränkungen stets darauf geachtet wurde, dass die Forschung weitergeht und man trotz der schwierigen Situation in einem sicheren Umfeld arbeiten konnte.

Prof. Dr. Dominik Niopek möchte ich herzlich für die Übernahme des Zweitgutachtens sowie das sehr hilfreiche Feedback bei Vorträgen über den Stand meiner Arbeit danken.

Prof. Dr. Heinz Koepl und **Philipp Fröhlich** aus der Arbeitsgruppe „Selbstorganisierende Systeme“ des Fachbereichs Elektrotechnik und Informationstechnik danke ich sehr für die gute Zusammenarbeit und die Unterstützung mit der bioinformatischen Auswertung für diese Arbeit.

Weiterhin möchte ich mich bei **Dr. Michael Vockenhuber** sowie **Dr. Marc Vogel** für die viele Geduld als Postdocs, welche mich in verschiedenste Methoden eingearbeitet haben sowie stets bereit waren mir meine zahlreichen Fragen zu beantworten, bedanken.

Mein Dank gilt auch **Dunja Sehn**, welche mir immer bei bürokratischen, organisatorischen oder auch alltäglichen Problemen geholfen hat. Ohne die Starthilfe mit der kurzfristigen Organisation einer Übergangswohnung in Darmstadt, hätte ich niemals einfach so quer durch Deutschland ziehen können.

Mein Dank gilt auch allen **Mitgliedern der AG Süß**, welche ich in meiner Zeit als Doktorandin kennenlernen durfte, da sie die letzten Jahre für mich unvergesslich gemacht haben. Trotz der Pandemie wurde stets die Möglichkeit gefunden den Zusammenhalt in der Gruppe zu vertiefen. Seien es das gemeinsame Schauen von Online-Konferenzen, ein Zoom-Pub-Quiz oder die tollen BBQs - es hat immer viel Spaß gemacht.

Besonderen Dank möchte ich noch **Michelle** und **Daniel** zukommen lassen. Aus euch beiden als Kollegen wurden schnell Freunde, die ich nicht mehr missen möchte. Uns haben besondere Situationen zusammengebracht und auch zusammengeschweißt. Danke für die vielen lustigen Momente sowie schönen Erinnerungen.

Weiterhin möchte ich **Verena** und **Theresa** für die vielen unterhaltsamen Abende, in denen wir uns über das Doktorandinnen-Dasein ausgetauscht haben, bedanken. Ihr hattet immer ein offenes Ohr für meine Probleme oder Sorgen. Auch wenn wir nicht mehr gemeinsam studieren, haben wir oft festgestellt, dass wir vieles sehr ähnlich in der Promotion erleben - das hat so sehr geholfen.

Ein sehr großer Dank gilt **meinen Eltern und meinem Bruder**, welche mir die letzten Jahre immer Mut gemacht haben, wenn ich es brauchte. Allein mit der Unterstützung im Studium habt ihr mir den Weg zur Promotion erst ermöglicht. Eure Hilfe hat mich stets gefördert.

Und dem wichtigsten Menschen in meinem Leben, meinem Mann **Markus**, möchte ich natürlich auch von ganzem Herzen Danke sagen. Wir beide haben die letzten Jahre so viel geschafft, erlebt und durchgemacht - das ging nur als Team. Danke, dass du immer an meiner Seite bist!